European Commission

JRC SCIENCE AND POLICY REPORTS

Feasibility study on the extension of the Real Driving Emissions (RDE) procedure to Particle Number (PN)

Experimental evaluation of portable emission measurement systems (PEMS) with diffusion chargers (DCs) to measure particle number (PN) concentration

Barouch Giechaskiel
Francesco Riccobono
Pierre Bonnel

2014

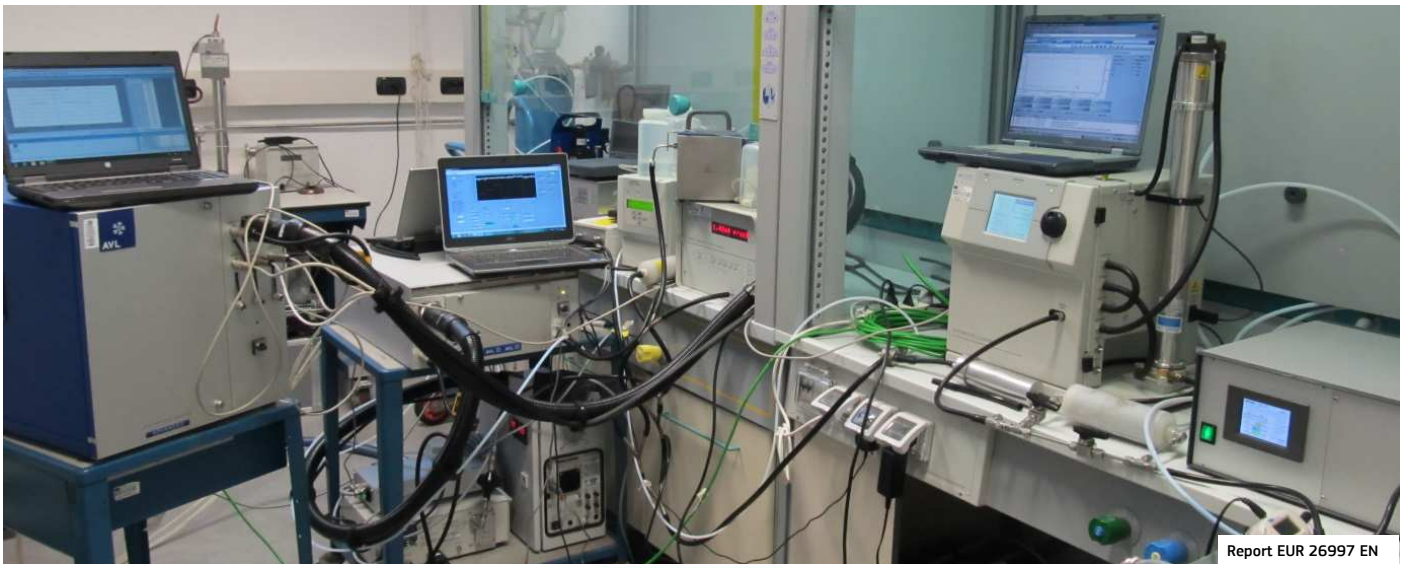

Report EUR 26997 EN

Joint Research Centre

European Commission

Joint Research Centre

Institute for Energy and Transport

Contact information

Barouch Giechaskiel

Address: Joint Research Centre, Via Enrico Fermi 2749, TP 230, 21027 Ispra (VA), Italy

E-mail: barouch.giechaskiel@jrc.ec.europa.eu

Tel.: +39 0332 78 5312

https://ec.europa.eu/jrc

This publication is a Science and Policy Report by the Joint Research Centre of the European Commission.

JRC 93743

EUR 26997 EN

ISBN 978-92-79-44651-1 (PDF)

ISBN 978-92-79-44650-4 (print)

ISSN 1831-9424 (online)

ISSN 1018-5593 (print)

doi:10.2790/326943 (online)

Luxembourg: Publications Office of the European Union, 2014

Printed in Italy

Abstract

The particle number method based on the Particle Measurement Programme (PMP) is part of the light duty legislation and starts to expand to other sectors as well. As a consequence systems for in service conformity and random driving emissions procedures will be necessary. These systems should be small and compact. The commercial systems at the moment are not ready for on-road use because the Particle Number Counters (PNCs) sensors (condensation particle counters, CPC) are sensitive to vibrations. For this reason a different concept has been suggested: Diffusion chargers (DC). The main target of this report was to evaluate theoretically and experimentally in the laboratory various PN-PEMS using diffusion chargers as PNCs as alternative technique to the PMP method for on-road measurements.

It was shown theoretically that DCs introduce an extra 50% uncertainty due to a size dependency since the size is not known during a test; PMP systems should have <15% differences.. Then various prototype PN-PEMS were evaluated in the laboratory. It was shown experimentally that it is feasible to cover a size range of 35-90 nm (for polydisperse aerosol) with differences within -33% and +50% to the PMP system. Based on the experience gained during the evaluations a suitable calibration setup and procedure is recommended. In addition calibration specifications for the next generation of PN-PEMS is given.

Table of contents

Abbreviations

CE	Counting Efficiency
CPC	Condensation Particle Counter
CVS	Constant Volume Sampler
D	Difference from PMP
DC	Diffusion Charger
DF	Dilution Factor
d_p	Particle diameter (usually monodisperse)
E	Efficiency
EU	European Union
GMD	Geometric Mean Diameter
I	Current
JRC	Joint Research Centre
LDSA	Lung Deposited Surface Area
P	Penetrations
PAO	Poly-Alpha-Olefin
PCRF	Particle Number Concentration Reduction Factor
PEMS	Portable Emissions Measurement Systems
PM	Particulate Matter
PMP	Particle Measurement Programme
PN	Particle Number
Pn	Particle x mean charge per particle
PNC	Particle Number Counter
PND	Particle Number Diluter
PTS	Particle Transfer System
Q	Flow rate
R	Reading
RDE	Real Driving Emissions
RT	Residence Time
s	Standard deviations
UNECE	United Nations Economic Commission for Europe
VPR	Volatile Particle Remover
WLTP	World Harmonized Light Duty Test Procedures

1. INTRODUCTION

The Particle Number (PN) was recently introduced in the EU regulation for light duty diesel vehicles (Commission Regulation 715/2007), based on the findings of the PMP (Particle Measurement Programme). A limit of 6×10^{11} p/km applies since September 2011. A limit of 6×10^{11} p/kWh was also introduced for Heavy Duty Engines since 2013 (Commission Regulation 595/2009). A limit of 6×10^{12} was introduced for Gasoline Direct Injection vehicles after September 2014 and 6×10^{11} p/km after September 2017 (Commission Regulation 459/2012).

PMP system

According to UNECE Regulation 83 (Light Duty) and Regulation 49 (Heavy Duty), the Particle Number system should consist of a Volatile Particle Remover (VPR) and a Particle Number Counter (PNC) (**Figure 1.1**) (Giechaskiel et al., 2012). The VPR removes volatile particles and dilutes the sample. The PNC measures the number concentration of particles >23 nm to exclude possible confounding of measurements by low volatility species present as nucleation mode particles, while including the primary soot (spherule) size of 23 nm. A Particle Transfer System is used to connect the PN system to the full dilution tunnel (CVS). The requirements of the main systems are described below.

Particle Transfer System (PTS)

The VPR should be connected to the full dilution tunnel with a tube of inner diameter ≥8 mm (laminar flow). The residence time (RT) to the primary diluter (PND_1) of the VPR should be ≤3 s.

Volatile Particle Remover (VPR)

The primary dilution factor (DF) should be ≥10 and the temperature of the diluted sample ≥150°C. In the VPR, after the PND_1, a heated tube with wall temperature between 300 and 400°C should exist. A secondary diluter (PND_2) is not required but the temperature at the inlet of the particle number counter should be <35°C. The residence time from the VPR to the PNC should be ≤0.8 s and the diameter of the tube ≥4 mm.

Particle Number Counter (PNC)

The PNC should be full flow (no internal splitting) with a response time of <5 s and counting efficiencies (CE) of 50%±12% and >90% at 23 and 41 nm respectively. The slope should be 1±0.1. The total residence time in the VPR and PNC should be ≤20 s.

All commercial systems use Condensation Particle Counters (CPC) as PNCs. Thus from now on the PNC of the PMP systems will be called CPC. The PN systems that fulfill the legislation requirements will be called PMP systems and it will be assumed that they consist of a VPR and a CPC.

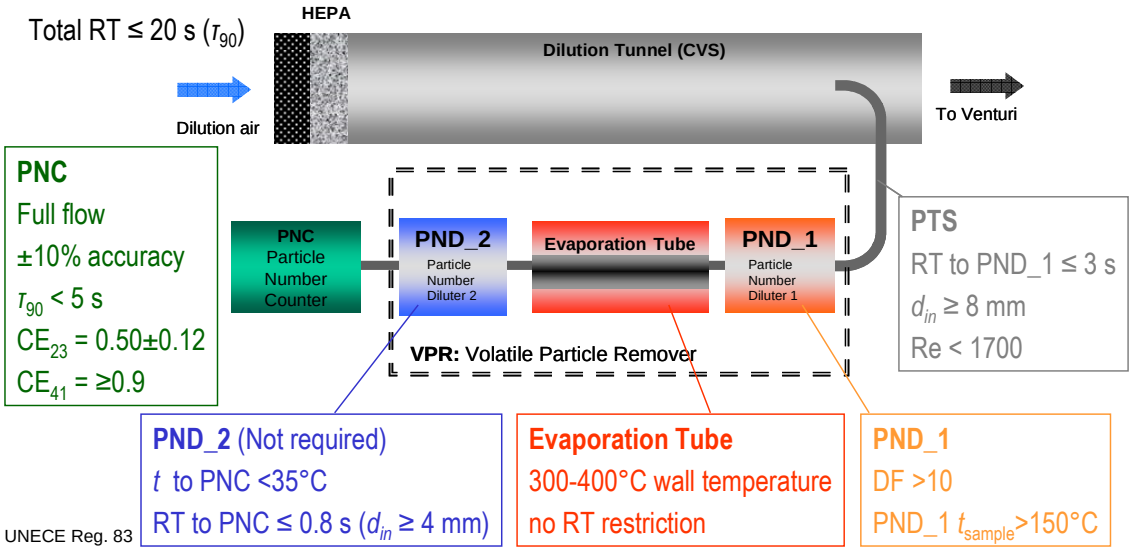

Figure 1.1: *Summary of PN regulation.*

PN-PEMS

At the moment a vehicle is certified in the laboratory with a specific test cycle (e.g. for light duty vehicles NEDC). However, the emissions measured during the certification process do not always represent the emissions in real operation of the vehicle. According to Regulation 715/2007 revisions may be necessary to ensure that real world emissions correspond to those measured at type approval. The use of portable emission measurement systems (PEMS) and the introduction of the 'not-to exceed' regulatory concept should also be considered.

Currently there is no commercially available PN–PEMS equipment using a CPC as PNC. The main reasons are safety issues and the robustness of the CPCs for on-board measurement. Although hand-held CPCs exist and seem quite robust (Matson et al. 2004), more tests are needed to validate their on-board use. Issues related to safety and vibrations need to be resolved. Differential mobility spectrometers have been used for on-board measurements (Barrios et al., 2011) and even hand-held versions are available (Qi & Kulkarni, 2012; Ranjan & Dhaniyala, 2007).

An alternative to PN–PEMS is to use an instrument that measures other properties that correlate with SPN. The most studied method with adequate sensitivity for modern engines is the PN–soot correlation, with a ratio of approximately 2x10^12 particles/mg soot (Giechaskiel et al., 2012; Maricq et al., 2011).

Another promising technique is the diffusion charger (DC), where one can get an estimation of PN (or PM mass) based on theoretical assumptions or by calibration against the regulatory method. Initial comparisons gave differences around ±50%, which could be justified by the different cut-off diameters of the instruments (Meier et al., 2013). Recently it was reported that comparability of DCs is on the order of ±30% (Asbach et al., 2012, Kaminski et al., 2013). However, some exceptions were noted. A DC reported 7 times higher number concentration when challenged with aerosol with a modal diameter of 200 nm (beyond the specified range of the instrument). Another DC underestimated the number concentration of 30 nm soot particles by about 60%.

The on-board robustness of DCs remains to be proved, but preliminary results are promising (Fierz et al., 2008; Ntziachristos et al., 2011). DC also faces issues with long

term stability: Corona tips and wires would age over time and accumulate a coating of silicone dioxide which progressively reduces the corona current for a given corona voltage (Davidson & McKinney, 1998; Fierz et al., 2011). Finally, the DC calibration procedures need to be specified.

Diffusion Charger (DC)

The concept that was recommended to replace number counting was diffusion charging.

Principle of operation

In a Diffusion Charger, shown in **Figure 2.1**, ions usually from a corona discharge attach to particles and an electrometer registers a current proportional to the number of particles times the average charge per particle.

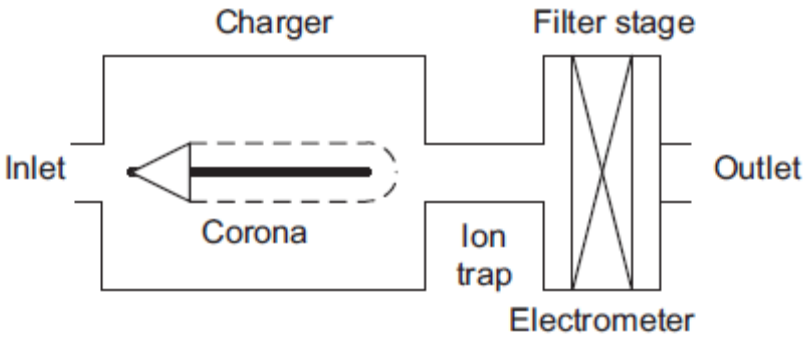

Figure 1.2: *Schematic of a diffusion charger*.

The measured quantity is often called the active surface area to differentiate it from the Fuchs surface area which is used to characterize the attachment of molecules onto particles (Siegmann & Siegmann, 2000). For practical applications to polydisperse diesel exhaust aerosols, with typical diameters of 10–300 nm, there is a small difference between active and Fuchs surface areas, which is caused by electrical forces (Ntziachristos et al., 2004; Jung & Kittelson, 2005). Theoretically, the measured current is proportional to particle diameter squared in the free molecular regime (e.g. Ku and Maynard 2005) and proportional to particle diameter in the continuum regime. Experimentally, for the size range of interest, which lies in the transition regime, an exponent x of 1.1–1.4 to particle mobility diameter d_p is found (response $\sim d_p^x$) (Kulkarni et al. 2013, Bau et al., 2012) (see **Table 1.1** and **Table 1.2**). This varies with the charging area design and with particle losses at and downstream of the charging area. Charging efficiency weakly depends on particle material (dielectric constant) and fractality (Kulkarni et al., 2011, Ouf & Sillon, 2009).

Based on the previous tables, for the size range of interest (30-150 nm) for particles from vehicles, the theoretical and experimental exponent is around 1.3.

Table 1.1: *Responses of DCs based on experimental data (from Kulkarni et al. 2013).*

Charger type	Response	Range	Aerosol	Reference
Direct	1.64	8-23	Ag / DOS	Ntziachristos et al. (2004)
Direct	1.32	23-700	Ag / DOS	Ntziachristos et al. (2004)
Direct	1.41	30-460	Diesel	Ntziachristos et al. (2004)
Direct	1.91	30-112	NaCl / DOS	Park et al. (2007)
Direct	1.27	112-700	NaCl / DOS	Park et al. (2007)
Indirect	1.12	20-700	NaCl / DOP	Liu and Pui (1975)
Indirect	1.11	20-240	NaCl	Fierz et al. (2008)
Indirect	1.36	30-150	NaCl / Diesel	Jung and Kittelson (2005)
Turbulent jet	1.13	30-150	NaCl / Diesel	Jung and Kittelson (2005)
Turbulent jet	1.13	6-100	Ag	Fissan et al. (2007)
Turbulent jet	1.17	30-700	NaCl / DOS	Park et al. (2007)

Table 1.2: *Relationship between active surface area and particle size. From Bau et al. (2012).*

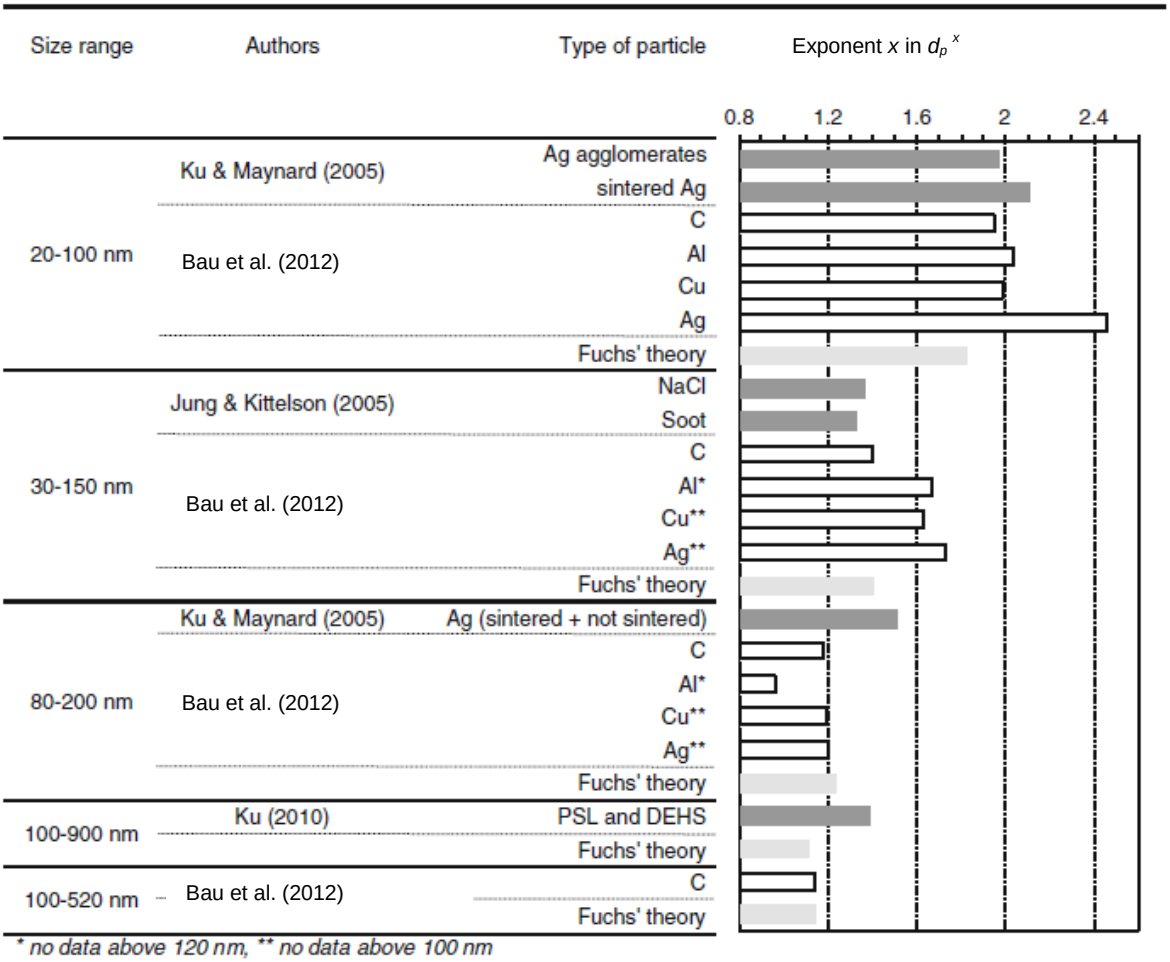

Aerosol detection based on diffusion charging offers fast response (1 s), very good sensitivity, simplicity, repeatability, and a wide dynamic range (Mohr et al., 2005; Ntziachristos et al., 2004). This technique has been used to characterize ambient aerosols (Bukowiecki et al., 2002; Woo et al., 2001) and vehicle exhaust aerosols (Kittelson et al., 2005; Ntziachristos et al., 2004, 2007). Diffusion chargers have a strong potential to be used alone to measure relative changes in particle emissions or in combination with other instruments to provide additional information on particle properties, such as the mean diameter when combined with a CPC (Frank et al., 2008; Ntziachristos & Samaras, 2006).

Recently the conventional diffusion charger concept was augmented by adding a diffusion screen stage upstream of the filter stage (Fierz et al., 2008, 2011). The idea is that smaller particles are more likely to be trapped by the diffusion screens, whereas larger particles penetrate this stage and are collected by the filter. Thus, the ratio of filter to diffusion stage currents relates to mean particle diameter. This measure of size plus an assumed distribution width can then be used to calculate number concentration from the total current. This instrument was designed for ambient ultrafine particle measurement, so its applicability to diluted engine exhaust needs further investigation (Maricq 2013).

A new concept, the aerosol measurement by induced currents, was recently introduced (Fierz et al., 2014). It is based on pulsed unipolar charging followed by non-contact measurement of the rate of aerosol space charge in a Faraday cage. The advantage is that the electrometer zero offset is irrelevant for the measurement, even though there is always a non-zero baseline noise even for particle free air.

There have been efforts to adopt diffusion chargers to measure particles in raw engine exhaust (Rostedt et al., 2009; Ntziachristos et al., 2011, 2013). These are based on the idea of “escaping charge”. The aerosol particles are charged, but instead of collecting them to measure the associated electric current, the particles are allowed to exit the sensor. This loss of charge requires a make-up current to flow into the corona to restore electrical balance, and it is this current that is measured and equated with aerosol active surface. The first version was designed to be mounted directly to the vehicle tailpipe and accept the total exhaust flow (Rostedt et al., 2009). Although it could successfully monitor particulate emissions, the measurements were affected by exhaust temperature and flow variations, and continued exposure to raw exhaust necessitated frequent cleaning and maintenance. A modified version of this approach has recently been introduced (Ntziachristos et al., 2011). This incorporates an integral ejector pump that provides two advantages: First, it mitigates exhaust flow variations and produces a stable flow through the sensor. Second, the design places the corona needle in the clean air portion of the ejector to protect it from contamination. Initial evaluations indicate that this instrument operates well under the harsh environment of raw engine exhaust (Ntziachristos et al., 2011, 2013), but as with other diffusion chargers it requires auxiliary information, e.g., mean particle size, to convert the measured currents to particle number or mass concentration.

Influencing parameters of DC signal

The signal of the DC can be influenced by many parameters (Kulkarni et al. 2013):

- *Ion properties:* E.g. alcohol and water vapor attach to the ions, reduce their mobility and increase their mass. Different properties used in the calculations can give 10% difference on the theoretical average particle charge.

- *Temperature:* At higher temperatures the ion velocity increases and bigger particles can acquire more charge. For example, +10°C can have 2% increase in the average particle charge for 100 nm particles.
- *Pressure:* At lower pressures the ion mobility increases and the average charge acquired by particles increases. At 900 mbar particles can have 3% higher average charge at 100 nm compared to ambient pressure. See also (Biskos et al. 2005).
- *Dielectric constant of particles:* Affects the image force. E.g. PSL particles can have 15% less average charge at 100 nm compared to metal particles.
- *Morphology:* Fractal particles acquire more charge than compact particles of the same mobility (see e.g. Wang et al., 2010; Ouf and Sillon, 2009). Differences of 10-30% can be observed for 100 nm particles.
- *Pre-existing charge:* If particles are already charged with the same polarity, the final charging level can be up to 30% higher (see e.g. Qi et al. 2009).
- *Particle concentration:* The signal of the DC should be linear with the particle concentration. However, if the particle concentration entering the charger is high compared to the ion concentration, ion depletion leads to a lower average charge per particle.
- *Particle size:* The response of DCs is proportional to particle diameter squared in the free molecular regime and proportional to particle diameter in the continuum regime. For the size range of interest (20- 200 nm), which lies in the transition regime, an exponent of 1.1–1.3 to particle mobility diameter is usually found.

Note that the above mentioned parameters that affect the charging efficiency in function of size will also affect the exponent.

Summary & Objectives

The particle number method based on the Particle Measurement Programme (PMP) is part of the light duty legislation and starts to expand to other sectors as well. As a consequence systems for in service conformity and real driving emissions procedures will be necessary. These systems should be small and compact. The commercial systems at the moment are not ready for on-road use because the Particle Number Counters (PNCs) sensors (condensation particle counters, CPC) are sensitive to vibrations. For this reason a different concept has been suggested: Diffusion chargers (DC). The response of the DCs is proportional to the particle size to the power of 1.1-1.3 approximately (the CPCs do not have this size dependency above 23 nm).

The main target of this report is to evaluate theoretically and experimentally in the laboratory various PN-PEMS using diffusion chargers as PNCs as alternative technique to the PMP method for on-road measurements. Initially the theoretical background for estimating the number concentration from the DC signal will be given. Then experimental results of various PN-PEMS units will be given. Based on the finding the (ideal) expected difference between PN-PEMS and PMP systems will be quantified for typical vehicle exhaust size distributions and the (common) calibration procedures will be standardized.

2. THEORETICAL EVALUATION OF DC TO MEASURE PN

Initially the background of the PMP systems will be given, because the response of the DCs will be compared to what the PMP systems measure. Then the DCs will be evaluated theoretically.

PMP system

What the PMP system (VPR+CPC) measures depends on the (size dependent) penetration of the VPR, the (size dependent) counting efficiency of the CPC and the correction factors applied (mean PCRF of the VPR and inverse of the CPC slope). Some other uncertainties like non-linearity of the CPC, not well determined dilutions of the VPR, losses in the PTS, drift of the systems etc. will be assumed small and not taken into account in the following analysis.

CPC

The CPC counting efficiency *CE* can be expressed as (Mordas et al., 2008):

$$CE = s - s\ exp\left(\frac{d_0 - d_p}{d_{50} - d_0} ln2\right) \quad for\ d_p > d_0 \qquad 2.1a$$

$$CE = 0 \quad for\ d_p < d_0 \qquad 2.1b$$

Where s is the counting efficiency at the plateau region. d_0 and d_{50} are constants that represent the diameter that the counting efficiency is 0% and 50% respectively. d_p is the particle diameter. A correction factor k to normalize the plateau efficiency (the maximum counting efficiency) to 1 (k=1/s) is applied to PMP systems. The determination of k is based on the linearity check of the CPC with a reference instrument (electrometer or CPC). In the analysis below it is assumed that the CPC is linear and its response does not depend on the particle concentration.

VPR

The VPR penetration *P* can be expressed as:

$$P = a\ exp\left(\frac{d_p{}^c}{b}\right) \qquad 2.2$$

Where a, b, c, are constants. A minimum 70% penetration is allowed for 100 nm particles (in future WLTP procedures). Note that *DF* usually equals with b (in Eq. 2.2). Legislation requires measurement of the Particle Number Concentration Reduction Factor (*PCRF*) at 30, 50 and 100 nm based on upstream and downstream of the VPR and a correction is applied based on the mean PCRF of the three sizes. The ratios of $PCRF_{30}$ and $PCRF_{50}$ to $PCRF_{100}$ should be <1.3 and <1.2 respectively.

$$PCRF_{30} = \frac{PN_{in,30}}{PN_{out,30}} \qquad PCRF_{50} = \frac{PN_{in,50}}{PN_{out,50}} \qquad PCRF_{100} = \frac{PN_{in,100}}{PN_{out,100}} \tag{2.3}$$

$$PCRF_{mean} = \frac{PCRF_{30} + PCRF_{50} + PCRF_{100}}{3} \tag{2.4}$$

Penetration *P* and *PCRF* are connected as following. Note that the Dilution Factor (*DF*) is constant but both *P* and *PCRF* are size dependent.

$$DF = PCRF\ P \tag{2.5}$$

PMP system

The final penetration after the corrections will be referred as *Efficiency E* (or *response function*).

$$E_{PMP} = CE\ k\ PCRF\ PCRF_{mean} = CE\ k\ P\ PCRF_{mean}\ /\ DF \tag{2.6}$$

CE, PCRF and *P* are size dependent, the rest constants. Note also that the *P* or *DF* are not necessary; one can use the size dependent *PCRF* values. Alternatively, the efficiency of a PMP system can be modeled with the equation (e.g. if someone measures it experimentally):

$$E_{PMP} = a' \exp\left(\frac{d_p^{\ c'}}{b'}\right) \tag{2.7}$$

Note that the efficiency can go to >100% because of the mean *PCRF* correction, which is a mean correction based on 3 sizes. Note also that for PMP systems, basically the CPC determines the efficiency (response). **Figure 2.1** shows the counting efficiency *CE* of a CPC, the penetration *P* of a VPR and the Efficiency *E* of a PMP system. For the evaluation that will follow the following constants of **Table 2.1** were used (based on the experimental results with an AVL PMP system, APC):

Table 2.1: *Constant based on fittings of experimental data.*

CPC		**VPR**		**PCRF**		**PMP (not used)**	
d_0	16	*b*	0.7	30 nm	1.12	*b'*	1.07
d_{50}	27	*a*	-8x10^15	50 nm	1.04	*a'*	-2.15x10^20
slope *b*	0.94	*c*	-2	100 nm	1.00	*c'*	-2.68

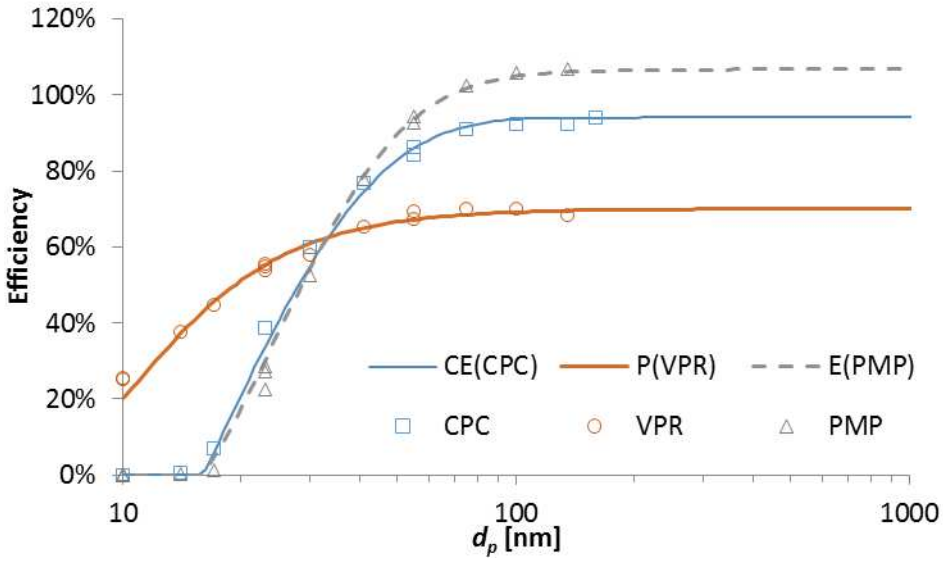

Figure 2.1: *Penetration P of a VPR, counting efficiency CE of a CPC and Efficiency E of a PMP system. Open symbols are measured values. Lines are fits based on the above equations. The PMP fit comes from the multiplication of CPC and the VPR.*

Measurement error with the PMP system

What is at the inlet of the PMP system and what is finally measured do not necessarily match due to the size dependent losses in the PMP system (**Figure 2.2**). Depending on the size distributions, there is an error, which is small (<10%) for size distributions between 50-90 nm. It is much bigger for smaller sizes and becomes extremely high for particles <30 nm because sub23nm particles are not counted. Detail can be found at Giechaskiel et al. (2012).

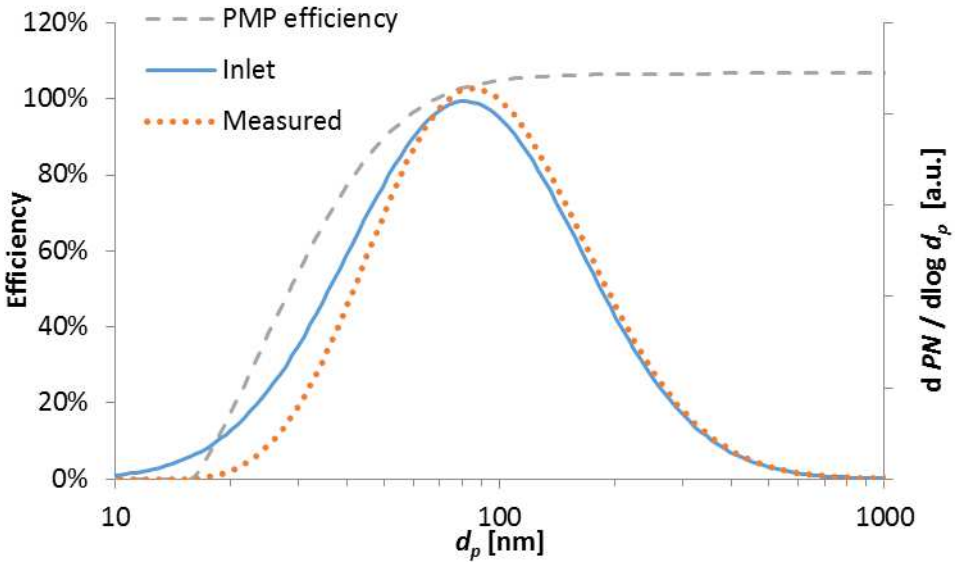

Figure 2.2: *Example of a PMP efficiency curve and inlet and measured 'seen' size distributions.*

DC

DCs have a response that increases as size increases (**Figure 2.3**). The reason is that bigger particles carry more charges, thus they produce higher signal at the electrometer of the DC. The absolute level depends on the instrument and its calibration. Many DCs are almost linear to the particle diameter (d_p^1.1) but higher exponents can also be found (see **Table 1.1**). Due to this strong size dependency, the true inlet size distribution can be distorted. The total concentration can be right or wrong. An example is given in **Figure 2.3**.

Efficiency (or *response function*) is defined as the ratio of the reading *R* of the instrument compared to the true inlet particle number concentration *PN*. Note that the reading is usually the current measured by the DC multiplied by a constant determined after calibration. Sometimes the Efficiency is called Sensitivity (e.g. Shin et al. 2007, a term that will not be used here)

$$E = \frac{R}{PN} \qquad 2.8$$

Where *R* is function of d_p^*x* (with *x* usually between 1 and 1.3).

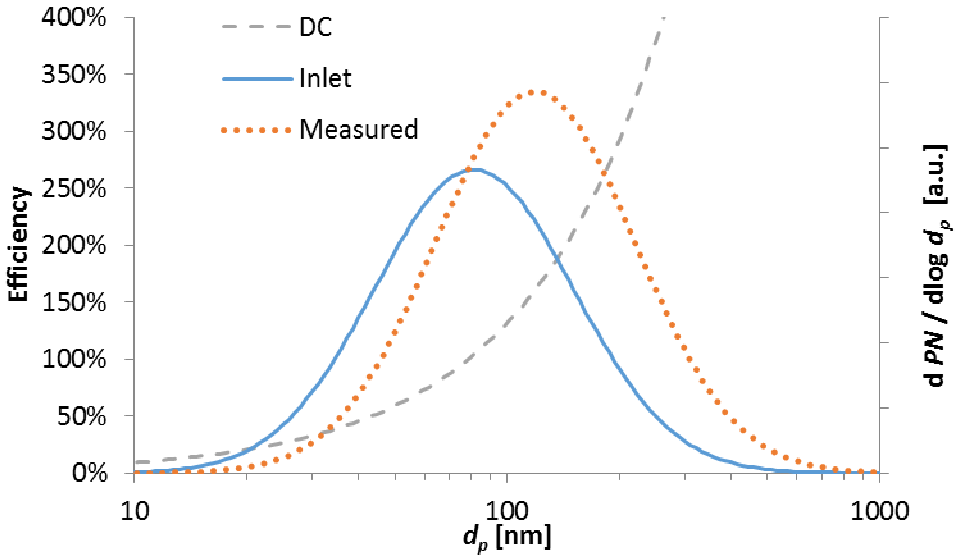

Figure 2.3: *Example of a DC efficiency curve and inlet and measured 'seen' size distributions (GMD=80 nm). DC with d_p^1.15 was calibrated at (monodisperse) 80 nm to have 100% efficiency.*

Comparison of response functions of PMP and DC

What is of interest in this report is the difference *D* of the DC from a PMP system. **Figure 2.4** gives as an example DCs with different efficiency (response) functions, all calibrated at 80 nm (i.e. their efficiency is 100% at 80 nm monodisperse aerosol). In the same figure the PMP efficiency curve is also given (which is almost 100% at 80 nm). This

size was chosen arbitrarily, as a size that all PMP systems would have reached 100% efficiency (for monodisperse aerosol). In addition it is the recommended size for 100% efficiency for instruments for construction machinery in Switzerland (Schlatter, 2012)

$$D = \frac{R}{PN_{PMP}} - 1 \qquad 2.9$$

Figure 2.5 shows the difference D of each DC from the PMP measuring monodisperse aerosol of different sizes focusing on the area of interest (20-200 nm), where the majority of particles is expected. As expected the difference is 0% at 80 nm. It becomes negative (DC measuring lower) at smaller sizes and bigger at bigger sizes.

Even more relevant is the difference of DC from PMP system measuring polydisperse aerosol, because the contribution of each size on the response of the DC is weighted according to their contribution in number concentration. This is shown in **Figure 2.6**. The size distributions with Geometric Mean Diameters (GMD) around 70 nm were assumed to have standard deviations of around 1.8 (Harris and Maricq 2001). Narrower size distributions were assumed for smaller GMDs and wider for bigger (see **Table 2.2**).

Focusing on the DC with response d_p^1.0, which can be assumed an ideal case, it can be observed that there is no difference to the PMP system at 55 nm geometric mean diameter (GMD). The difference remains in acceptable levels (<50%) up to GMD 90 nm approximately. For a DC with response d_p ^1.3, which is the most realistic case, the range with differences <50% is reduced to <80 nm. **Table 2.2** shows the theoretical efficiencies of the PMP and DCs and their differences for the previous DCs. In blue the acceptable differences (-33% to +50%). Note that theoretically two PMP systems should have less than ±15% differences in the whole range examined (Giechaskiel et al. 2012), but higher differences can be found between systems at the CVS and the tailpipe (±30%). Thus a -33% to +50% difference should be reasonable especially considering that it is an on-board application.

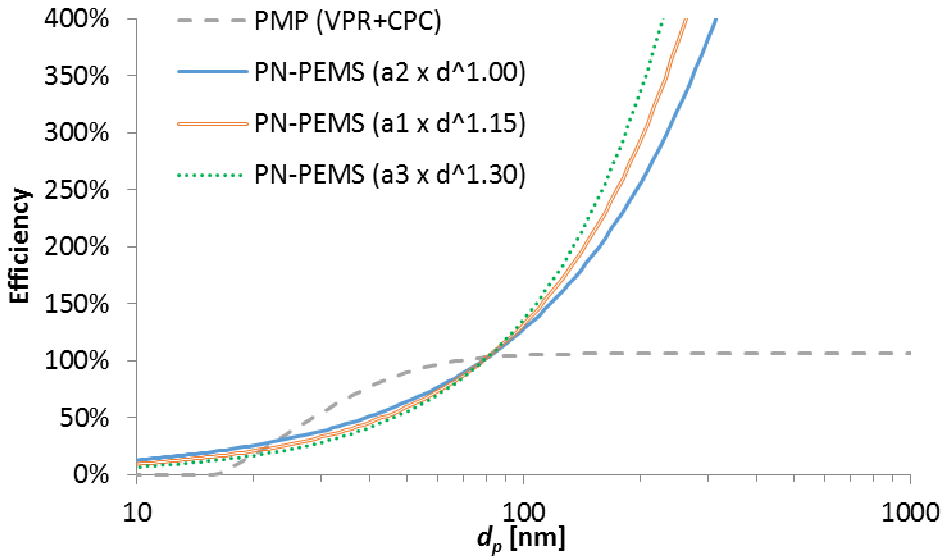

Figure 2.4: *Efficiency curves of a PMP system and three DCs with different response functions.*

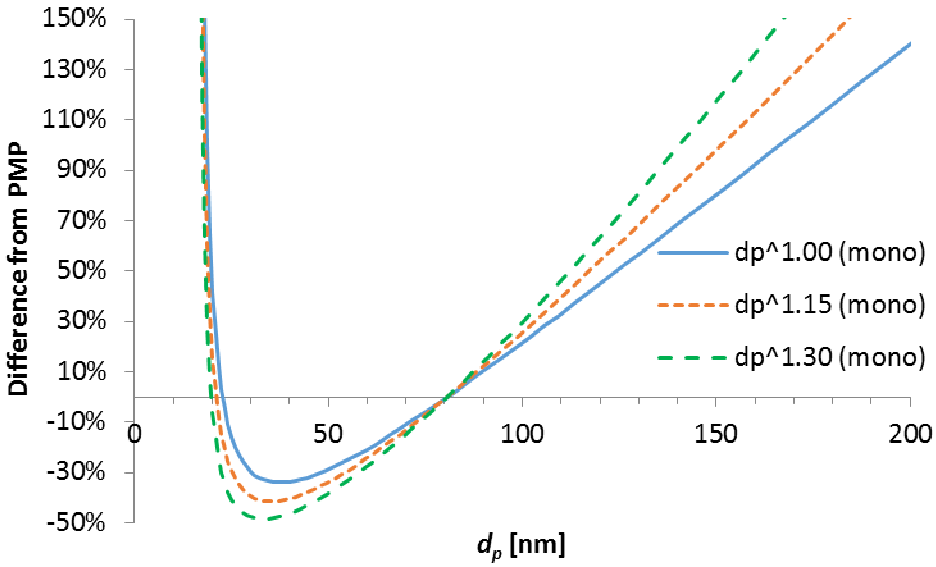

Figure 2.5: *Differences of three DCs with different response functions to a PMP system measuring monodisperse aerosol. All DCs calibrated to measure 100% at 80 nm.*

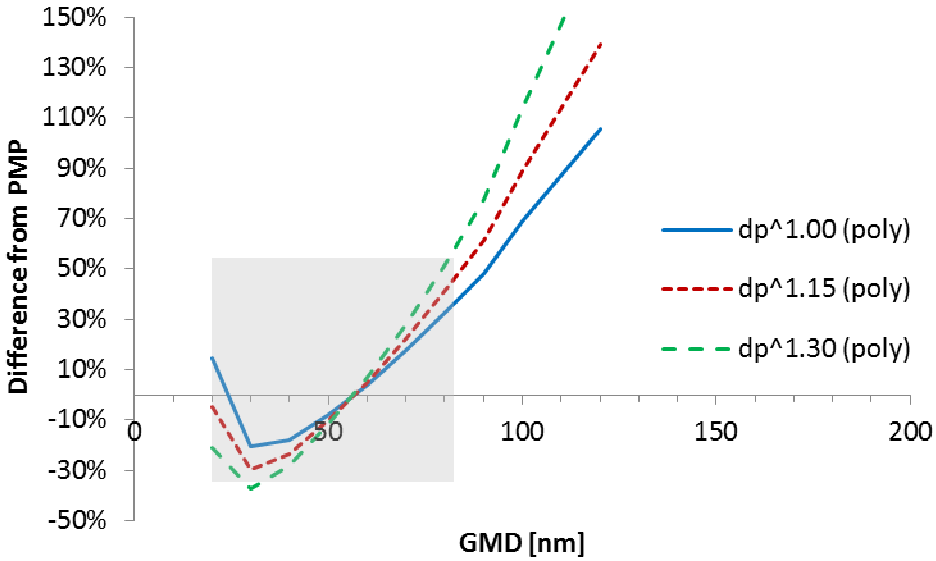

Figure 2.6: *Differences of three DCs with different response functions to a PMP system measuring polydisperse aerosol. All DCs calibrated to measure 100% at monodisperse 80 nm.*

However, typical vehicle size distributions lie on the range of 40-100 nm and thus it would be desirable to minimize the difference of DC and PMP in that polydisperse size range. In a next step the efficiencies of the DCs were optimized for polydisperse aerosol around 75 nm (and thus monodisperse around 100 nm), where most cases are expected. **Figure 2.7** and **Figure 2.8** show the monodisperse and polydisperse results respectively. **Table 2.3** gives the results in more detail. Calibrating the DCs with 100 nm monodisperse particles can result in small differences (15%) for 60-90 nm geometric mean diameters (GMD) for a DC with response dp^1.0. The differences are still acceptable (-33% to +50%) up to 100 nm GMD.

Table 2.2: *Responses of a PMP system and three DCs with different response functions and their differences to a PMP system measuring polydisperse aerosol. All DCs calibrated to measure 100% at monodisperse 80 nm.*

		Actual differences to inlet				Differences to PMP		
GMD	s	PMP	dp^1.00	dp^1.15	dp^1.30	dp^1.00	dp^1.15	dp^1.30
10	1.30	0%	13%	10%	7%			
20	1.40	24%	28%	23%	19%	15%	-5%	-21%
30	1.50	53%	42%	38%	33%	-21%	-30%	-37%
40	1.60	71%	58%	54%	51%	-18%	-23%	-28%
50	1.70	81%	75%	73%	72%	-8%	-10%	-11%
60	1.75	88%	91%	92%	94%	4%	5%	7%
70	1.80	92%	108%	112%	117%	18%	22%	28%
80	1.85	95%	126%	134%	144%	32%	41%	51%
90	1.90	97%	144%	157%	172%	48%	62%	78%
100	2.00	98%	165%	185%	209%	69%	89%	114%
120	2.10	100%	205%	239%	281%	106%	139%	182%

The monodisperse calibration is in agreement with Fierz et al. (2014) who suggested this size for optimizing the response of DCs for ambient aerosol. However, the Swiss regulation for construction machinery (Schlatter, 2012) requires a counting efficiency of 70%-130% at 80 nm. Thus it would be desirable to find a compromise for all applications. This could be done e.g. by calibrating an instrument to achieve 70-80% efficiency at 80 nm and 100% at 100 nm. The <200% efficiency at 200 nm could be achieved with an instrument with response <1.15. Nevertheless, the optimal calibration reference size depends on the size area that needs optimizations and the exponent of the DC.

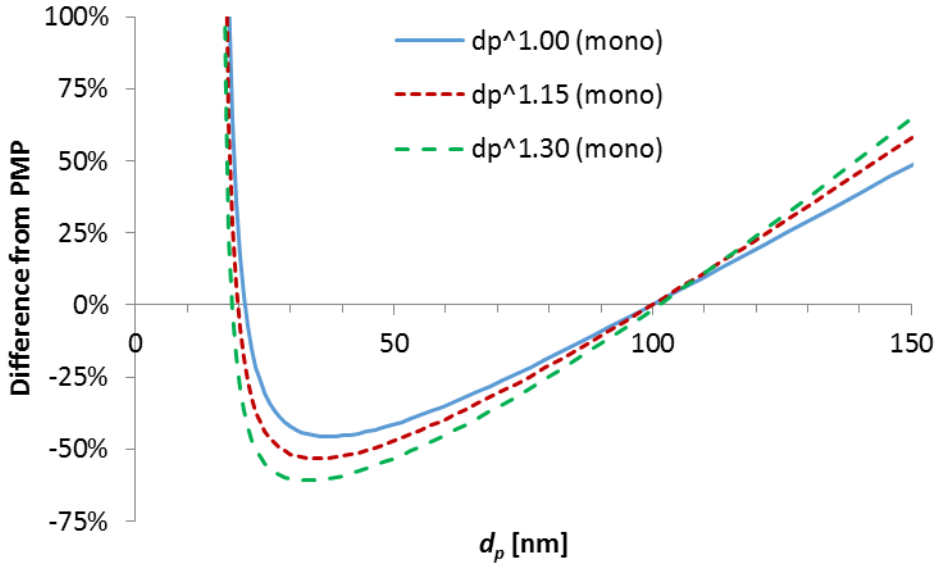

Figure 2.7: *Differences of three DCs with different response functions to a PMP system measuring monodisperse aerosol. All DCs calibrated to measure 100% at 100 nm.*

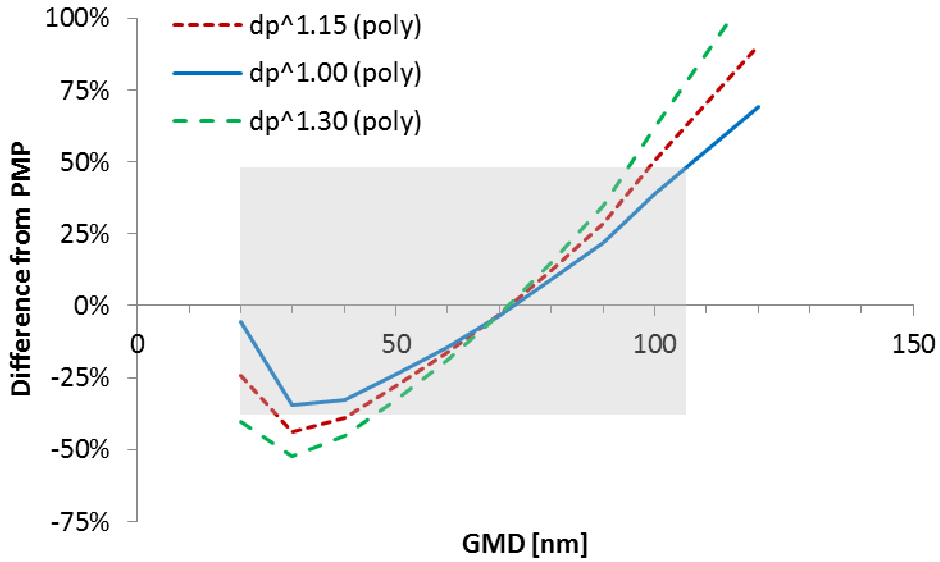

Figure 2.8: *Differences of three DCs with different response functions to a PMP system measuring polydisperse aerosol. All DCs calibrated to measure 100% at monodisperse 100 nm.*

Table 2.3: *Responses of a PMP system and three DCs with different response functions and their differences to a PMP system measuring polydisperse aerosol. All DCs calibrated to measure 100% at monodisperse 100 nm.*

		Actual differences to inlet				Differences to PMP		
GMD	s	PMP	dp^1.00	dp^1.15	dp^1.30	dp^1.00	dp^1.15	dp^1.30
10	1.30	0%	11%	8%	6%			
20	1.40	24%	23%	18%	14%	-6%	-24%	-40%
30	1.50	53%	35%	30%	25%	-35%	-44%	-52%
40	1.60	71%	48%	43%	39%	-33%	-39%	-45%
50	1.70	81%	62%	58%	54%	-24%	-28%	-33%
60	1.75	88%	75%	73%	71%	-14%	-16%	-19%
70	1.80	92%	89%	89%	89%	-3%	-3%	-3%
80	1.85	95%	103%	107%	109%	9%	12%	15%
90	1.90	97%	118%	125%	131%	22%	29%	35%
100	2.00	98%	136%	147%	159%	39%	51%	62%
120	2.10	100%	169%	190%	213%	69%	91%	114%

Discussion on other parameters affecting the results

The main assumption of the above analysis (monodisperse calibration and normalization at 100 nm) is that the GMD of the generated size distributions remains in the 40-100 nm range and the response is optimised for size distributions with GMD around 75 nm (and GSD=1.85). However, typically the (light-duty) vehicles have smaller mean sizes. This will result to underestimation of the emissions with the DCs. This could be solved by normalizing to a different size (e.g. 80 nm, which corresponds to approximately 60 nm polydisperse mean).

The monodisperse calibration will lead to differences between different systems with different response functions when measuring the same aerosol, even though they are calibrated with the same procedure. This effect could be minimized (but not solved) by calibrating with a polydisperse size distribution. This will be examined at **Chapter 10**.

Another topic that has to be discussed is the case of particle sizes outside the assumed range. Smaller particles are often observed (even <23 nm), however in this case even the PMP system underestimates significantly the particle concentration and gives a big error. For example with a GMD of 30 nm the PMP measures only 50% of the true inlet concentration. Thus one could argue, that the error of the DC, although much bigger than the expected range, is not so important. Nevertheless, there is a big risk of calibrating an engine to produce particles around 40 nm, thus under-counting the emissions with the DC (much more than the PMP system). This under-counting could be -33% or even more. On the other hand, extremely high emissions of sub23 nm, which are not counted by PMP might be counted by a DC, which doesn't have so steep counting efficiency for low sizes. This, over-counting due to volatiles (e.g. nucleation mode) should be avoided by DCs. This can be done only by a proper VPR. This is however out of the scope of this report.

Bigger particles is an issue that needs attention. Impactors and cyclones are recommended to remove these particles, however they shouldn't increase significantly the pump demands because the indent of the PN-PEMS is on-board application. Note however that the cut-point of the impactor is an aerodynamic diameter and for typical soot densities it corresponds to at least 3 times higher mobility diameter (depending on the size due to the different effective density). Thus a 500 nm (aerodynamic) cut-point impactor would cut in reality 1500 nm (mobility) particles, thus practically making it relevant for non-engine exhaust particles (e.g. from re-entrainment). Significant concentration of particles between 100 nm and the cut-off size of the impactor will be a concern, because will result in over-counting the emissions. On the other hand they could also indicate malfunction of the tested vehicle (e.g. oil particles escaping). Based on this discussion, the cyclone and the impactor is not necessary and only recommended.

The above analysis is based on the assumption that the other parameters that affect the DCs signal (see **Chapter 2**) do not change much during the measurement. Based on the discussion of **Chapter 2** the effect of parameters like humidity, temperature, pressure, morphology of particles should remain small by controlling these parameters (e.g. dilution with low humidity air, constant temperature of the DC). The change of ambient pressure, which cannot be controlled during an on-road test, should give an extra uncertainty of <10%.

Most theories of unipolar diffusion charging assume spherical particles. Laframboise and Chang (1977) developed the theory of charge deposition on charged aerosol particles of arbitrary shape for the unipolar charging process. Chang (1981) proposed equations for the mean charge of arbitrarily shaped particles in unipolar diffusion charging process. The proposed equations indicate that in the continuum regime mean charge per particle is determined by the electrical capacitance of a particle while in the free molecule regime it is determined by the geometric surface area as well as the capacitance of the particle. Han and Gentry (1994) showed that large surface area and low electric potential enhance the rate of charge acquisition using computational method based on population balance equations. Shin et al. (2009) performed unipolar charging experiments and showed that the mean charge on silver agglomerates was larger than that on fully coalesced silver spheres by about 30%. Their analysis indicated that the electrical capacitance of loose agglomerates is larger than that of spherical particles with the same mobility, therefore loose agglomerates can gain more charges in a charger. This information of current per particle after unipolar charging can then be used for morphology characterization (Wang et al. 2010).

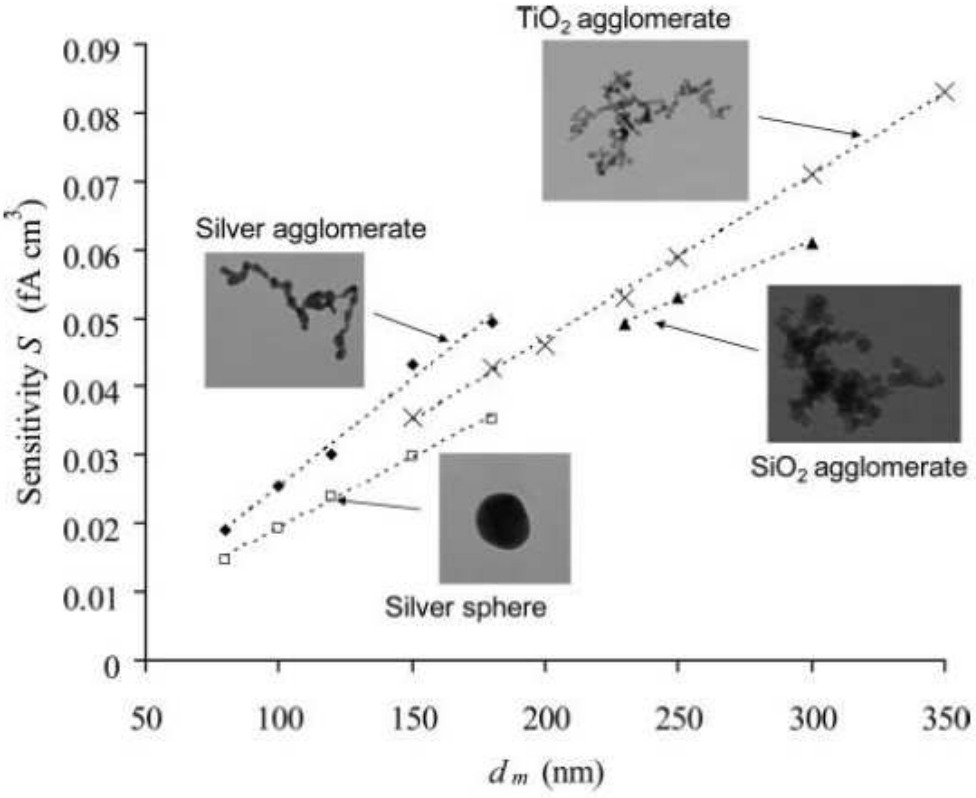

Figure 2.9: *Measured sensitivity (ratio of LDSA to PN) for silver agglomerates and spheres, SiO_2 and TiO_2 agglomerates (from Wang et al. 2010).*

The key message from this analysis is that DCs will have different response for spherical and agglomerate particles, with differences reaching easily 30%. At small sizes, where particles are more spherical the differences should be smaller. Note that different particle morphologies can also have differences among them. This raises some concerns regarding the 'reference' material that could be used for calibration of DCs. This problem is not unique: It's the same for the PMP systems' calibration and investigations are still going on. However for PMP systems, the effect is important in the cut-off range of the CPCs (around 20-240 nm) and is almost negligible for bigger sizes, thus the opposite from DCs. This issue is not the topic of this report, so another approach will be followed in the next chapters: Most tests will be conducted with soot agglomerates, as this is closer to what the DCs will measure. Spherical particles will also be checked for comparisons with values in the literature. Nevertheless, based on the previous literature survey, DCs have a response of 1.1 or higher and thus for soot particles a response of 1.3 is probably the most realistic.

Main theoretical conclusions

Efficiency is defined as the ratio of the reading of the instrument compared to the true inlet concentration. For a PMP system the efficiency is around 50% at 23 nm and reaches 100% for bigger particles. The efficiency of DCs strongly depends on the particle size and usually is a function of d_p to the power of 1 to 1.3.

The difference between the DC and the PMP increases as the particle size increases. It reaches a minimum around 30-40 nm and then increases again because the PMP

system doesn't count any more. By calibrating the size at which the difference of DC and PMP is 0%, one can achieve acceptable differences between the two systems for a wide range of sizes. For an 'ideal' DC which has a response d_p^1.0 and is calibrated at 100 nm (monodisperse) particles to have 0% difference to the PMP system, differences of -33% to +50% are seen for polydisperse aerosol with GMDs from 40 nm up to 110 nm. For the realsitic cases of d_p^1.15 and d_p^1.30 the ranges are 45-100 nm and 50-95 nm respectively. Note that these results are based on comparisons with a PMP system that can have >100% efficiency at 100 nm. In all cases above the agreement with the PMP is perfect (0% difference) for polydisperse size distributions of 75 nm (GSD=1.85).

Based on the theoretical calculations the efficiencies of **Table 2.4** could be recommended (column proposal), which are based on a d_p^1.30 response function (for soot particles). Such a response function, which is possible with existing DCs would probably mean lower exponent for spherical particles (e.g. PAO). However, a common agreeement has to be reached for calibration aerosol (and the limis could be adjusted accordingly). Since these values are for a size distribution of 75 nm in ti possible that with such a calibration the emissions with DCs will be underestimated in most cases (because the mean sizes are usually smaller). Alternatively, another normalization size could be selected (e.g. 80 nm), which has higher risk of overestimation of the emissions at bigger sizes.

Table 2.4: *Efficiencies (monodisperse) of a PMP system and a DCs calibrated to measure 100% at monodisperse 100 nm. The proposal refers to soot as calibration aerosol.*

d_p [nm]	PMP	DC (d_p^1.00)	DC (d_p^1.15)	DC (d_p^1.30)	Swiss	Proposal soot
23	30% – 65%	24%	19%	15%	<50%	<50%
30	56% – 89%	32%	27%	22%		
41	78% – 95%	43%	37%	33%	>50%	
50	90% – 100%	53%	48%	43%		>40%
80	100% – 105%	85%	82%	78%	70-130%	
100	100% – 105%	105%	105%	105%		100%
150	100% – 105%	159%	169%	175%		
200	100% – 105%	212%	235%	255%	<200%	<250%

With such response function (d_p^1.30 for soot particles), a calibrated DC could be used to measure a wide range of vehicle technologies. And it could be used, not only for on-road light duty vehicles but also heavy duty vehicles or non-road mobile machinery with the same calibration value. Based on the theoretical efficiencies of PMP and DCs, one could estimate the difference of the DCs compared to the PMP system for various polydisperse aerosols (**Table 2.5**). With response of 1.30, the differences would be -33% and +62% respectively for CMD sizes between 50 and 100 nm. It is thus evident that as the exponent increases the range of differences for typical vehicle exhust size distributions becomes very wide, increasing the risk of false conclusion (pass or fail an in-service conformity test). Higher exponents will result in higher uncertaitnies due to changes in particle size and thus a specific calibration each time (vehicle) would be

preferable. On the other hand, lower exponents would decrease this emasurement uncertainty. The limits of **Table 2.5** ensure that the response function of the DC will not be higher than 1.3 (for soot).

Table 2.5: *Efficiencies of a PMP system and a DCs calibrated to measure 100% at monodisperse 100 nm when measuring polydisperse aerosol with various GMD. The differences of the DCs compared to the PMP are also given.*

	Efficiencies				Difference from PMP		
GMD [nm]	PMP	DC (d_p^1.00)	DC (d_p^1.15)	DC (d_p^1.30)	DC (d_p^1.00)	DC (d_p^1.15)	DC (d_p^1.30)
30	53%	35%	30%	25%	-35%	-44%	-52%
50	81%	62%	58%	54%	-24%	-28%	-33%
80	95%	103%	107%	109%	9%	12%	15%
100	98%	136%	147%	159%	39%	51%	62%

3. EXPERIMENTAL

The previous chapter examined the possibility to use a DC to estimate the particle number concentration as it would be measured by a PMP system. In this chapter the experimental setup used for the evaluation of different PN-PEMS (with DCs as sensors) will be given. The results of the PN-PEMS evaluations will be discussed in the next chapters.

Experimental setup

Two kinds of tests were conducted: Tests with monodisperse aerosol and tests with polydisperse aerosol. The tests with polydisperse aerosol should be representative to the real-world application of the devices with vehicle exhaust.

Monodisperse tests

In order to measure the efficiency of the PN-PEMS systems the following setup was used (**Figure 3.1**). Particles were produced in a Palas spark-discharge graphite generator (DPN 3000) or in an evaporation-condensation PAO generator (in-house made) and the concentration was adjusted with a dilution bridge. A few tests were also conducted with a diffusion based soot generator (APG from AVL) that also thermally pretreats the particles at 350°C. Then particles of a specific size were selected with a TSI 3080 long DMA with a 2 years old 3077A ^{85}Kr neutralizer (370 MBq, beta, estimated activity is >85%). Particles downstream of the DMA are positively charged (negative voltage is applied to the DMA center electrode) and this could affect the charging efficiencies of the PN-PEMS. For this reason, downstream of the DMA there was a neutralizer to 'neutralize' the aerosol (achieve an equilibrium bipolar distribution) (TSI 3077, ^{85}Kr, 74 MBq, beta, with estimated activity 40% and Grimm 5522, ^{241}Am, 3.7 MBq, alpha with estimated activity 98%). For some cases it was not used in order to see the effect of pre-existing charge on the PN-PEMS efficiencies. The monodisperse aerosol was drawn with the help of a home-made ejector diluter. With 1 bar over-pressure the sampled flow rate was around 1.4 l/min. At the outlet of the ejector diluter all instruments were sampling at ambient pressure and the excess flow was vented. A TSI 3772 CPC (cut-off 10 nm) and a TSI 3025A CPC (cut-off 3 nm) were used as reference instruments to check the absolute levels particle number concentration.

The effect of doubly charged particles was estimated with the equations given in the **Annex**. Charging efficiencies for spherical particles were considered, although the spark – discharge generator is known to produce agglomerate particles with higher charging fractions (Bau et al., 2010). The reason was that the charge equilibrium distribution is not known

Note that the PN-PEMS system was treated in most cases as a 'black box' because it was not always possible to check separately the VPR and the DC. Only for a few devices a Grimm 5.403 CPC (cut-off 5 nm) was connected at the outlet of the devices to measure the penetration of the VPR of the PN-PEMS based on the upstream concentration (2-CPC method). Sometimes the same CPC was used for upstream and downstream measurements (1-CPC method).

The monodisperse tests included size dependent efficiencies (by changing the size at the DMA) or linearity checks by changing the concentration from the dilution bridge. To calculate the efficiency of the PN-PEMS the reading R was divided with the total

number concentration *PN* given by the reference CPC (**Eq. 3.1**). To determine the instrument's difference from the PMP system *D*, the reading of the instrument was compared with the reading of the PMP system (whenever it was connected) or the simulated CPC readings based on the log fit efficiency of the PMP system (**Eq. 3.2**). Both are (mobility) size d_p dependent. The effect of multiply charged particles was taken into account as explained in the **Annex**. Generally, with 10-15% multiply charged particles, the effect of doubly charged particles on the efficiency was 5% (or less than -0.05 change of the exponent *x* in d_p^*x*).

$$E_{PN-PEMS} = \frac{R_{PN-PEMS}}{PN_{CPC}} \qquad 3.1$$

$$D = \frac{R_{PN-PEMS}}{PN_{PMP}} - 1 \qquad 3.2$$

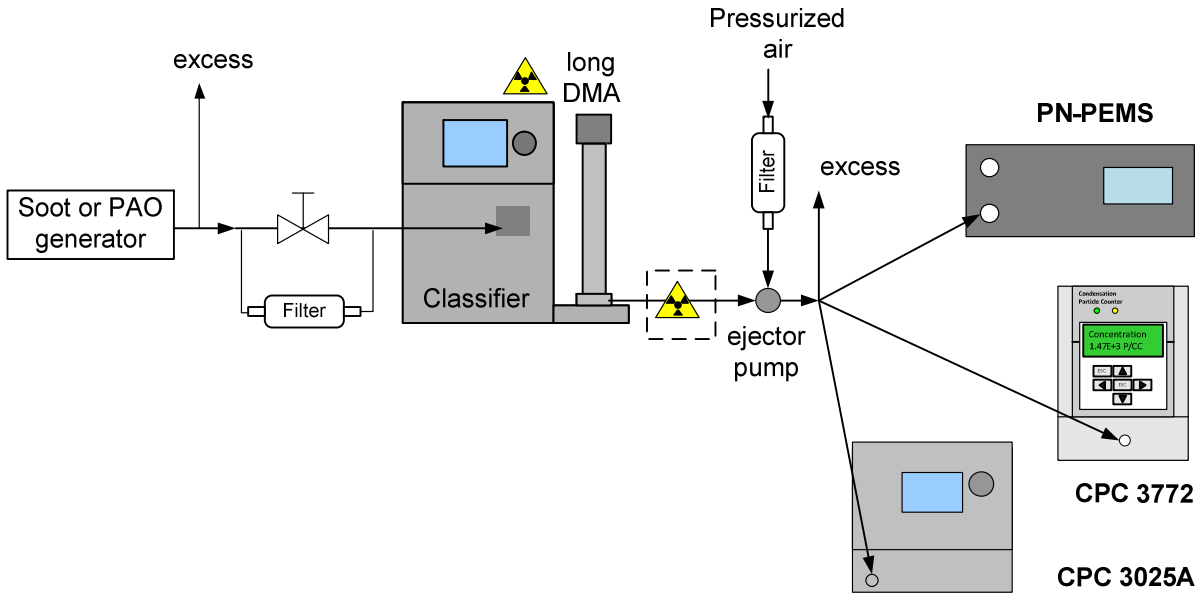

Figure 3.1: *Schematic setup for the monodisperse aerosol tests.*

Polydisperse tests

For the polydisperse checks the setup was similar (**Figure 3.2**). No DMA was used and the TSI 3025A CPC was combined with the DMA to have a SMPS that could measure size distributions from 10 to 400 nm (sheath 7 lpm and sample 0.3 lpm). Multiple charge and diffusion losses correction was taken into account by the software of the manufacturer. The software uses charging probabilities for spherical particles. However the spark-discharge soot is agglomerates. It was decided not use the internal software for agglomerates because there was not enough info for the degree of agglomeration and the primary size of particles. Although this correction is important for surface and volume estimations, the effect is smaller for the number concentration and the mean size of the size distribution (this will be discussed later). In addition, the same setup and operation points of the generator were used in order to minimize any differences during the evaluation of the different PN-PEMS. A 3772 was also used to confirm the estimated total

concentration by the SMPS. A Topas DDS 560 bifurcated diluter was used to bring the concentrations at the calibration range of the 3772. Usually evaporation-condensation generated polydisperse aerosol is considered to be on average neutral, thus no neutralizers are used. Nevertheless, for some PAO tests and in most of the spark-discharge tests, the neutralizers were used in order to investigate the charge effect on the PN-PEMS efficiencies.

To calculate the efficiency of the PN-PEMS the reading *R* was divided with the total number concentration *PN* given by the reference SMPS. To determine the instrument's difference *D* from the PMP system the reading of the instrument was compared with the reading of the PMP system (whenever it was connected) or the simulated SMPS readings based on the log fit efficiency of the PMP system (**Eq. 2.6 or 2.7**). Both are GMD dependent.

$$E_{PN-PEMS} = \frac{R_{PN-PEMS}}{PN_{SMPS}} \qquad 3.3$$

$$D = \frac{R_{PN-PEMS}}{PN_{DMP}} - 1 \qquad 3.4$$

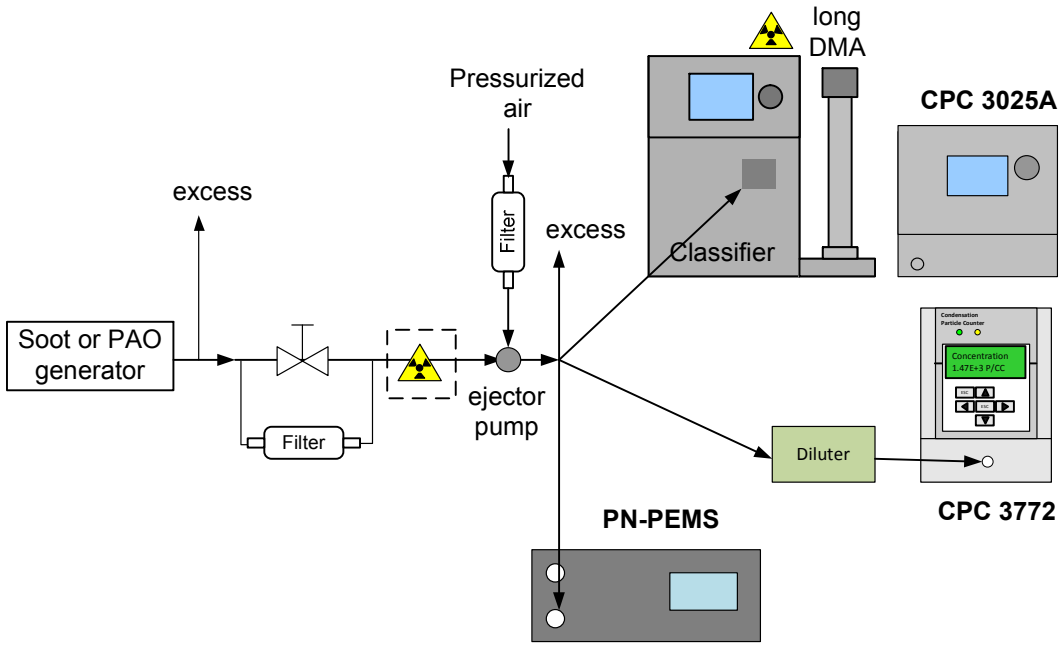

Figure 3.2: *Schematic setup for the polydisperse aerosol tests.*

Quality checks

The results that will be presented have some experimental uncertainties and target of these tests was to quantify them checking:

- Repeatability
- Calibration uncertainty of reference instruments
- Charges from the produced soot

Repeatability of PMP efficency measurement

The PMP theoretical efficiency curve was based on measurements with a CPC and a VPR (see previous **Figure 2.1**). The fit curve of the complete PMP system was based on multiplication of fits of separate curves for the CPC and VPR. The Efficiency of the PMP system measured experimentally twice: Experiments #1 and #2 with difference of a few weeks (**Figure 3.3**). It can be seen that the comparability is very good with differences within 5%.

Absolute levels

Quite often for the polydisperse check of the instruments a SMPS was considered as the reference instrument. For different size distributions the absolute levels of the SMPS were compared with a calibrated CPC 3772 after a dilution stage (300:1) (**Figure 3.4**). The differences are within 10% with no increasing or decreasing tedendy for concentration levels up to $1x10^7$ p/cm^3. Similarly the two reference CPCs (3772 and 3025A) were also within 10% for concentrations up to $1x10^6$ p/cm^3 with a slightly increasing differences for high concentrations (**Figure 3.5**). The 3772 was used with a dilution of 50:1 in that case in order to be in the single counting mode. Tests with differences >15% between the reference instruments (in their capable size range) were not taken into account.

Check of PMP simulated concentration from SMPS size distributions

In order to further confirm that the PMP fit curve was correct, the SMPS size distributions were fitted to PMP concentrations based on the PMP efficiency curve. Comparison of a PMP system with a SMPS using the fit of the PMP efficiency (**Eq. 2.6 or 2.7**) measuring polydisperse aerosol gave differens within 10% for different size distributions (concentrations and sizes) (**Figure 3.6**).

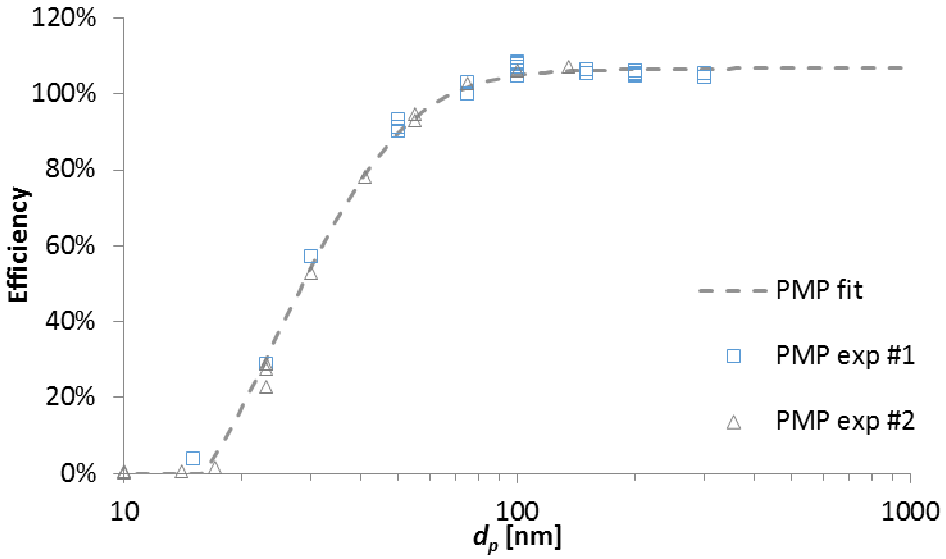

Figure 3.3: *Measured efficiencies of a PMP system (with a few weeks differences between them) and comparison with the fitted curve which was based on fitting seperately the CPC and the VPR.*

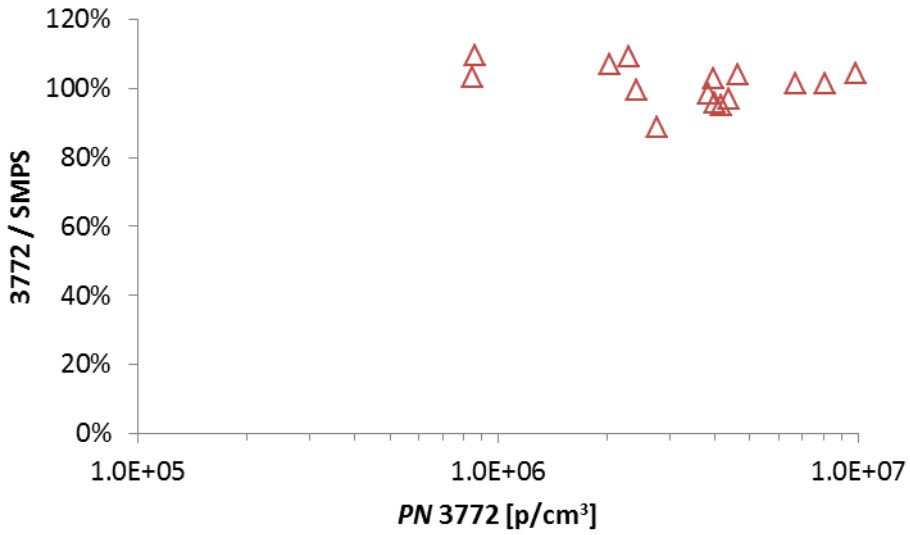

Figure 3.4: *Comparison of SMPS concentrations with a calibrated 3772 after a fixed dilution 300:1.*

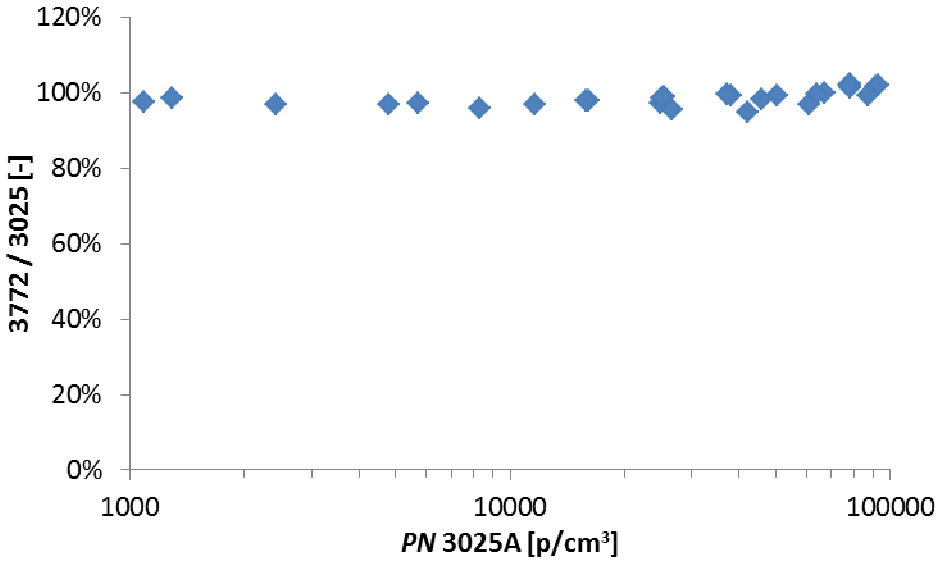

Figure 3.5: *Comparison of two reference CPCs (3772 and 3025A). A fixed dilution 50:1 was used upstream of the 3772.*

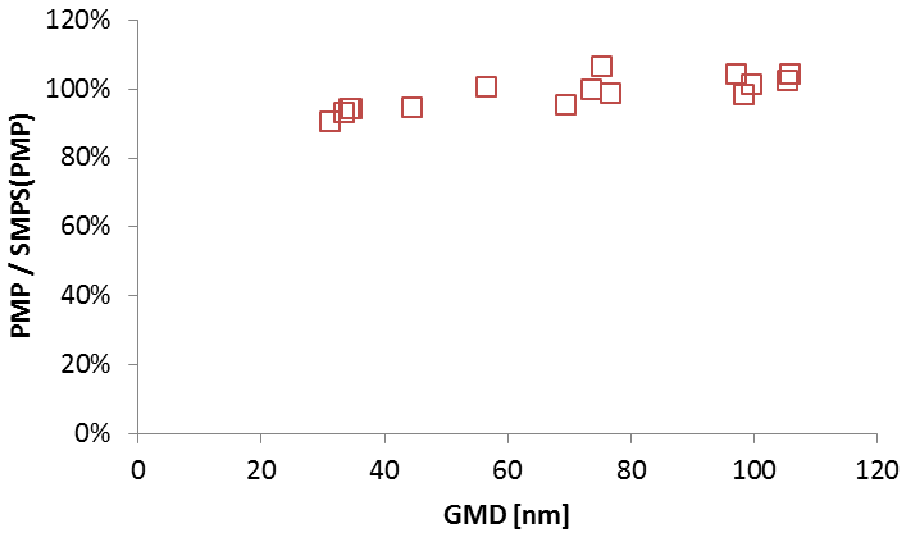

Figure 3.6: *Comparison of a PMP system with the SMPS multiplied with the theoretical PMP efficiency.*

Typical size distributions

Typical size distributions produced to check the PN-PEMS can be seen in **Figure 3.7** (poldisperse tests). Similar size distributions were also produced for the monodisperse tests (but a DMA was used to classify the particles).

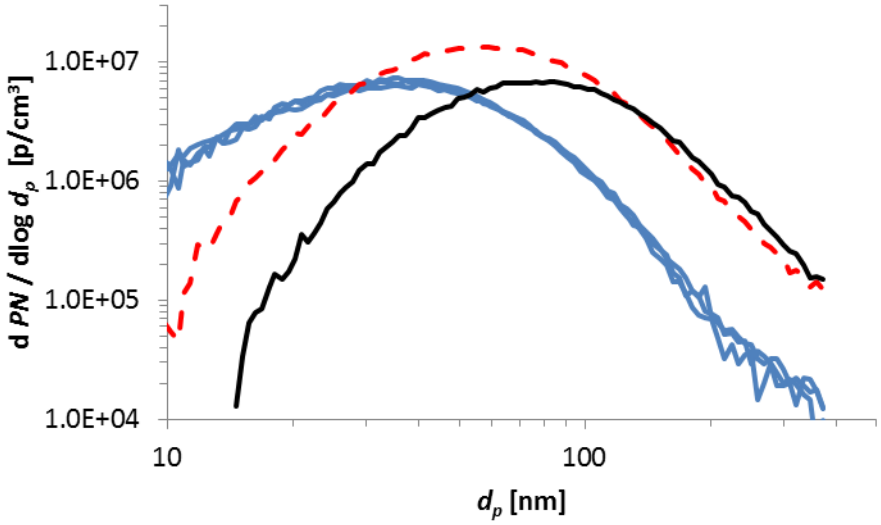

Figure 3.7: *Typical generated size distributions by the Palas spark-discharge graphite generator.*

Charging efficiency of SMPS neutralizer

Some tests were conducted with extra neutralizers upstream of the SMPS in order to ensure that the neutralizer of the SMPS was capable of achieving an equilibrium charge distribution. As **Figure 3.8** shows the size distributions were identical (within experimental error) confirming the proper operation of the SMPS.

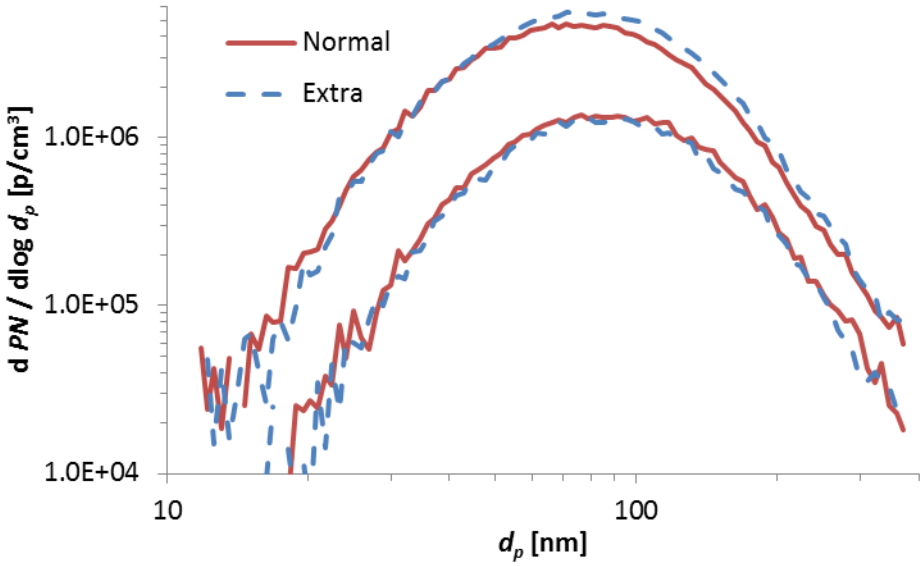

Figure 3.8: *Size distributions with the normal SMPS neutralizer and two extra upstream of the SMPS.*

Agglomerates charge distribution

The SMPS uses charging probabilities for spherical particles. However the spark-discharge graphite particles are agglomerates with different charge distribution. The exact charge distribution is not known, but the incorporated model insede the SMPS manufactuer's software was used to estimate the effect on the results. Primary sizes d_o of 8 and 14 nm were assumed and random and parallel orientation in the DMA.

As **Figure 3.9** and **Figure 3.10** show for two typically used size distributions (generator settings M-2-8-3 and M-5-3-3; energy-current-air-N_2) the effect is relatively small (10%) on number concentration (compare shperical with fractal 14 nm, random) and it increases with decreasing primary size or with parallel orientation in the DMA (unlikely for these sizes and flow rates that were used). **Table 3.1** summarizes the results.

Table 3.1: *Effect of agglomerate fractal correction on SMPS distributions.*

			M-2-8-3			M-5-3-3		
	do [nm]	orient.	GMD	s	PN	GMD	s	PN
Spheres			33.4	1.81	4.30E+06	56.5	1.73	7.94E+06
Fractals	14	parallel	35.4	1.74	3.62E+06	59	1.82	6.77E+06
Fractals	14	random	33.9	1.70	4.36E+06	55.2	1.8	7.66E+06
Fractals	8	random	24.4	1.98	5.25E+06	55.8	1.92	7.03E+06

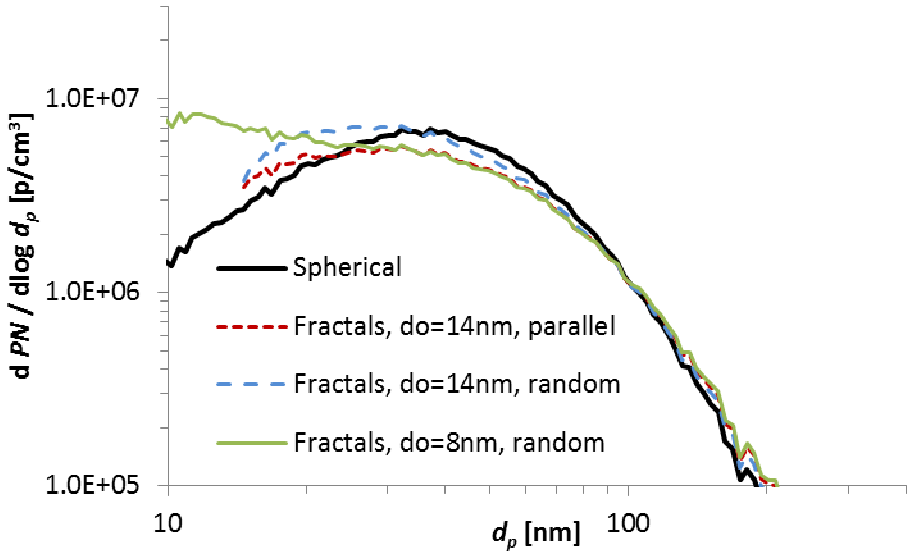

Figure 3.9: *Size distributions with different assumptions in the SMPS software.*

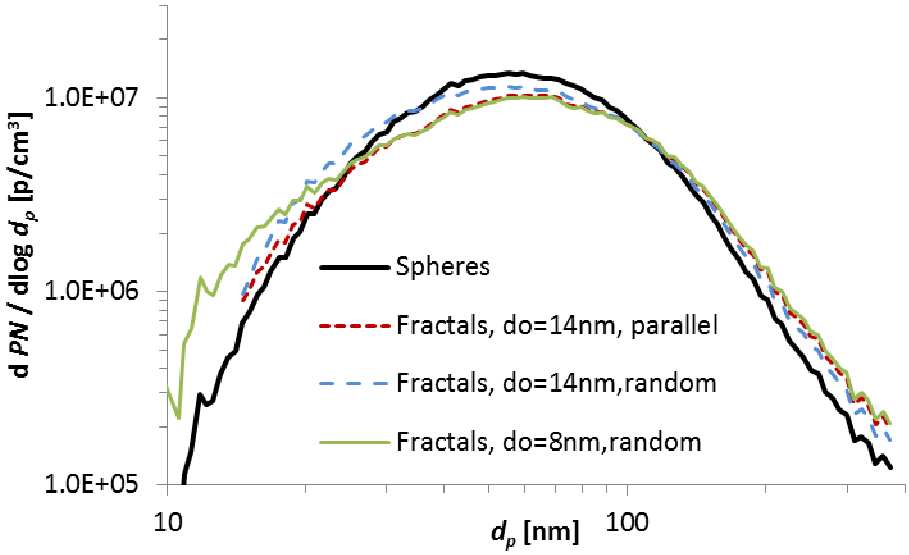

Figure 3.10: *Size distributions with different assumptions in the SMPS software.*

Multiply charged particles correction

Downstream of the DMA particles of one size should exist. However, bigger particles with more charges can also exist. Based on the charging probabilities of particles of different sizes, it is possible to estimate the concentration of the multiply charged particles and correct the number concentrations downstream of the DMA for them (see also **Annex**). However the spark-discharge graphite generated particles are agglomerates and not spherical and more charged than typical agglomerates. A specific test was done to see how close this correction brings the current from an electrometer to the concentration measured by a reference CPC. **Table 3.2** summarizes the results. The multiply charged correction (for double and triple-charged particles) brings the particle

number concentration from the electrometer close to the reference CPC for the sizes that were tested and the settings of the generator (those were mainly used in the tests of this report). However, it can be noticed that an uncertainty ±10% still remains.

Table 3.2: *Check of the multiply charged particles correction.*

Setting	Size [nm]	CPC [p/cm^3]	AE [fa]	f1 + 2 f2	AE [p/cm^3]	Difference
M-2-8-3	50	23000	340	5%	24742	-7%
GMD=35nm	50	12750	180	5%	13099	-3%
s=1.7	50	44000	690	5%	50212	-12%
	100	13850	190	8%	13370	4%
M-5-3-3	100	44500	750	14%	49149	-9%
GMD=50nm	100	12000	178	14%	11719	2%
s=1.7	200	7700	100	10%	6843	13%

Neutralization downstream of the DMA

Most DCs are sensitive to pre-existing charge on particles, which can affect their efficiency significantly. For this reason in most cases a neutralizer was used downstream of the DMA to bring a bipolar charge equilibrium to the particles entering the DC. The activity of the neutralizers that were used was checked with an electrometer downstream of the DMA and the neutralizers (position of PN-PEMS in **Figure 3.1**). Downstream of the DMA the particles are charged positively and the neutralizer(s) should bring the charge concentration to low levels. The two neutralizers that were used are:

- ^{85}Kr, 74 MBq, beta (TSI 3077): It was 13 years old and since the half-life of ^{85}Kr is around 10 years, the estimated activity is 40% (30 MBq).
- ^{241}Am, 3.7 MBq, alpha (Grimm 5522): It was 13 years old and since the half-life of ^{215}Am is around 430 years, the estimated activity is 98% (3.6 MBq).

Table 3.3 shows the results. Using filtered air the current was not zero but a few fA. Probably some ions were escaping from the neutralizers. Thus around 100 fA was assumed the concentration level of adequate 'neutralization'. The ^{215}Am was capable of neutralizing the aerosol (results not shown), but was always used in combination with the ^{85}Kr neutralizer. The two neutralizers could always neutralize the aerosol in all cases (sizes and concentrations). The ^{85}Kr neutralizer could neutralize the 100 nm monodisperse aerosol, but not the 50 nm at high concentrations. It has been shown that the specific ^{85}Kr chargers cannot bring the charge distribution close to equilibrium at 2 lpm, except at concentrations of monodisperse charged particles of $<10^3$ p/cm^3 or flow rates of 0.5 lpm (Covert et al. 1997). Thus the monodisperse aerosol tests with this neutralizer should be treated with care.

Table 3.3: *Check of the neutralizers for monodisperse aerosol.*

Generator	Neutralizer	Size [nm]	CPC [p/cm^3]	AE [fa]
Off	w/o	-	0	0
	Kr	-	0	80
	Kr+Am	-	0	80
M-2-8-3	w/o	50	23054	340
	Kr	50	24895	150
	Kr+Am	50	24438	62
M-2-8-3	w/o	50	12716	180
	Kr	50	12782	160
	Kr+Am	50	11208	74
M-2-8-3	w/o	50	43863	690
	Kr	50	43919	460
	Kr+Am	50	40474	45
M-2-8-3	w/o	100	13839	190
	Kr	100	13737	20
	Kr+Am	100	13112	60
M-5-3-3	w/o	100	44560	750
	Kr	100	43992	20
	Kr+Am	100	41103	-10
M-5-3-3	w/o	100	11915	178
	Kr	100	11990	20
	Kr+Am	100	11216	48
M-5-3-3	w/o	200	7635	100
	Kr	200	7925	5
	Kr+Am	200	7215	36

Neutralization of polydisperse aerosol

The spark-discharge aerosol can be charged due to its production procedure (Bau et al. 2010). This was examined using an electrometer at the position of the PN-PEMS in **Figure 3.2**. The results can be seen in **Table 3.4**. The size distribution with the small mean could be neutralized, but not the bigger one. The diffusion flame soot didn't have this issue.

Table 3.4: *Neutralization of the spark discharge graphite polydisperse aerosol with different neutralizers.*

Generator	Neutralizer	Size [nm]	CPC [p/cm^3]	AE [fa]
zero	w/o	-	4.38E+00	10
	Kr+Am	-	4.13E+01	80
M-2-8-3	w/o	poly	9.34E+05	10000
GMD=35nm	Kr	poly	8.37E+05	500
s=1.7	Kr+Am	poly	7.40E+05	-280
M-5-3-3	w/o	poly	2.06E+06	15630
GMD=50nm	Kr	poly	1.76E+06	15600
s=1.7	Kr+Am	poly	1.55E+06	-400

4. PN-PEMS #1

PN-PEMS #1 (prototype, AVL) consists of a VPR and a DC (Partector from Naneos). The VPR consists of a catalytic stripper at 170°C and a hot dilution around 10:1 at the same temperature. The dilution air and the diluted sample are heated at approximately 60°C. Description of the system can be found elsewhere. The VPR and the DC were calibrated separately by the manufacturer. The dilution factor (*DF*) that was used was 9. The DC gives Lung Deposited Surface (*LDSA*) in $\mu m^2/cm^3$. A constant factor *C* of 250 was also included to convert the LDSA to particle number (reading). This value, which was given by the manufacturer, was based on comparisons of the device with a PMP system for different vehicles, thus it should also account for the losses in the system. Thus the reading *R* of the instrument was:

$$R_{PN-PEMS} = C\ LDSA\ DF \quad (4.1)$$

The *LDSA* was always corrected for the zero offset. This value was around 1.5 $\mu m^2/cm^3$ and was important (>20%) for the low concentrations and/or small sizes (below 50 nm) during the monodisperse aerosol tests.

The study of the PN-PEMS #1 included:

- Checks of the VPR
- Checks of the DC
- Checks of the complete unit

VPR

For the VPR only one dilution stage was checked (9). Two CPCs (TSI 3772 with flow 1 lpm, Grimm 5.403 1.5 lpm) were used upstream and downstream of the VPR measuring monodisperse particles of different diameters. The downstream position was exactly where the DC is connected in the PN-PEMS. When the DC was disconnected it was sampling upstream of the PN-PEMS. Thus three *PCRF*s values were calculated for each diameter (two with the two CPCs and one with the DC). The results can be seen in **Figure 4.1**. The different pressure at the upstream and downstream position was taken into account only for the CPCs: Upstream it was ambient pressure due to the ejector diluter that was used downstream of the DMA. Downstream it was -5 mbar. In the same figure the actual dilution factors *DF* for each instrument connected are shown: The lower the flow of the instrument connected at the DC position, the higher the dilution. The DC had a flow of 0.75 lpm (close to the reported value 0.65 nlpm) and the mean PCRF was around 10 (for *DF* around 9). The 3772 had a flow of 1 lpm and the mean *PCRF* was around 7 (for DF around 6.1). The 5.403 had a flow of 1.5 lpm and the mean *PCRF* was 6.5 (for *DF* around 4.4). In all cases there was no flow (or other) warning from the instrument. It should be noted that the *PCRF* value from the DC strongly depended on the zero level used. In all cases, the losses at big sizes are low (<15%). Note also that the size dependent losses down to 30 nm are almost negligible (difference <7%).

The above results indicate that the calibration of the VPR must be done extremely careful, especially if any flow changes affect the dilution. For all results presented, the manufacturer's value (9) was used as it is considered more accurate. In addition the extra correction factor (C=250) to convert *LDSA* to *R* could mask any uncertainties in the *PCRF* or dilution determination.

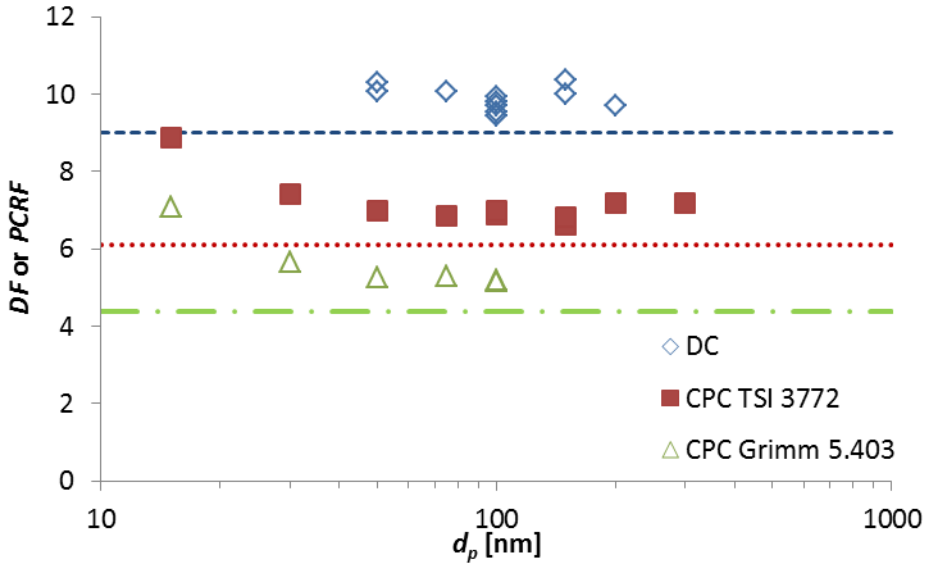

Figure 4.1: *PCRF measurements (symbols) and actual DFs (dotted lines) for different instruments connected (CPCs, DC).*

DC

The DC was investigated regarding the effect of pre-existing charges, its response function and linearity. A factor of 250 was assumed which might overestimate the emissions because it includes the losses in the VPR (around 15%).

Pre-existing charge effect

The specific DC measures differences in space (image) charge, i.e., it measures the charge transferred to the aerosol, and not the final charge state. For initially neutral aerosol, this is the same thing; however, for initially negatively charged aerosol the DC will give a higher *LDSA* value (since the charge difference is larger), and for initially positively charged aerosol it will give a lower *LDSA* value (Fierz et al. 2014). Thus, this method is less robust for pre-charged aerosols than the traditional filter-based collective method.

In the experiments without the neutralizer, the particles at the exit of the DMA are positively charged and thus the reading of the DC was lower 10% (200 nm) to 60% (50 nm) compared to the tests with neutralizer (**Figure 4.2**).

Some tests extra tests were conducted with the diffusion flame based soot generator (APG). The specific generator produces particles that have a charge distribution similar to the combustion generated charge distributions, which is similar to the Boltzmann distribution achieved by the neutralizer inside the DMA. For this reason the efficiencies without the neutralizer inside the DMA were similar to those using neutralizers both inside and downstream of the DMA.

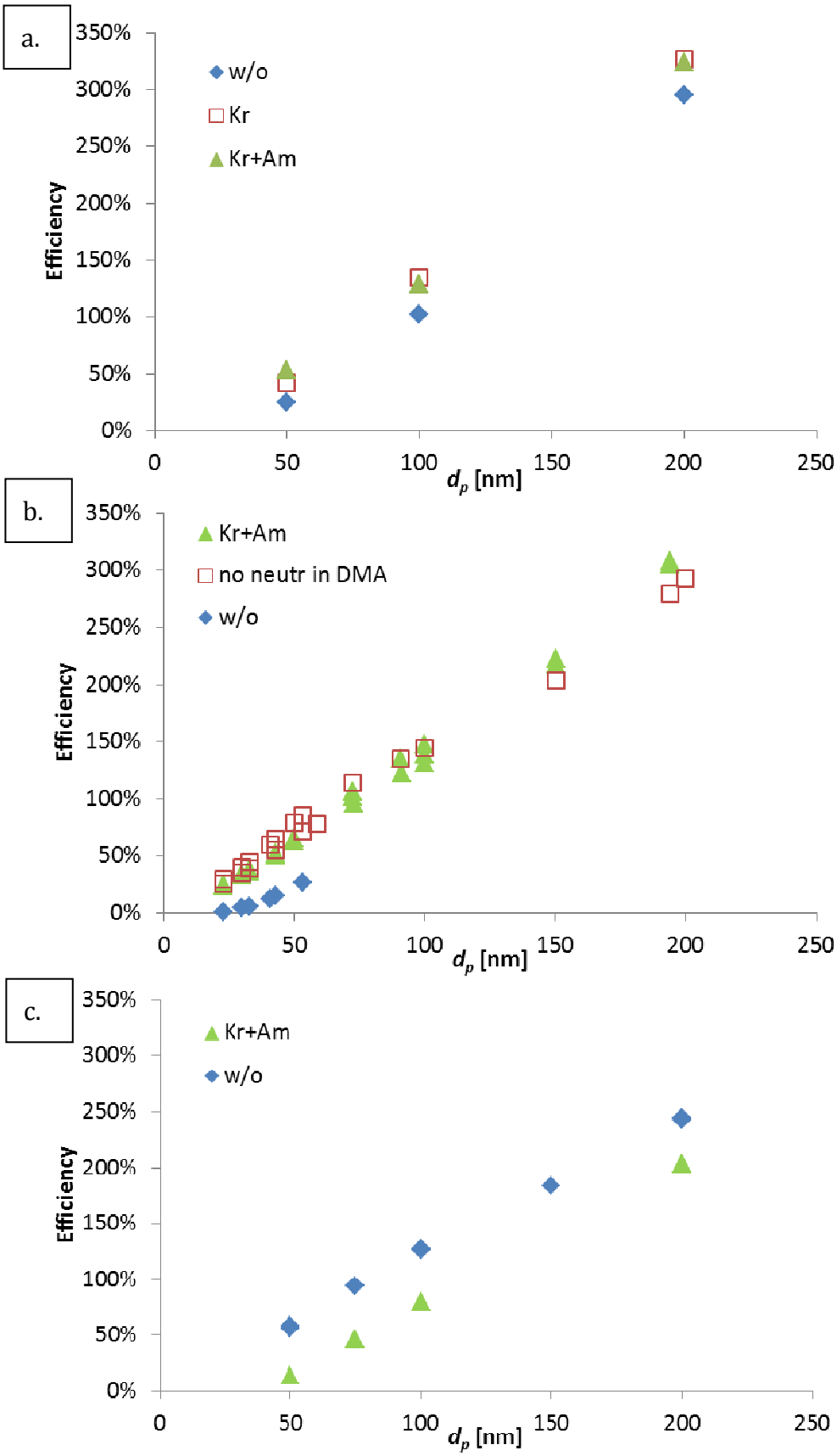

Figure 4.2: *Effect of pre-existing charge on the efficiency of PN-PEMS for monodisperse particles a) Spark-discharge soot b) diffusion flame with pre-treatment c) PAO. No multiple charge correction.*

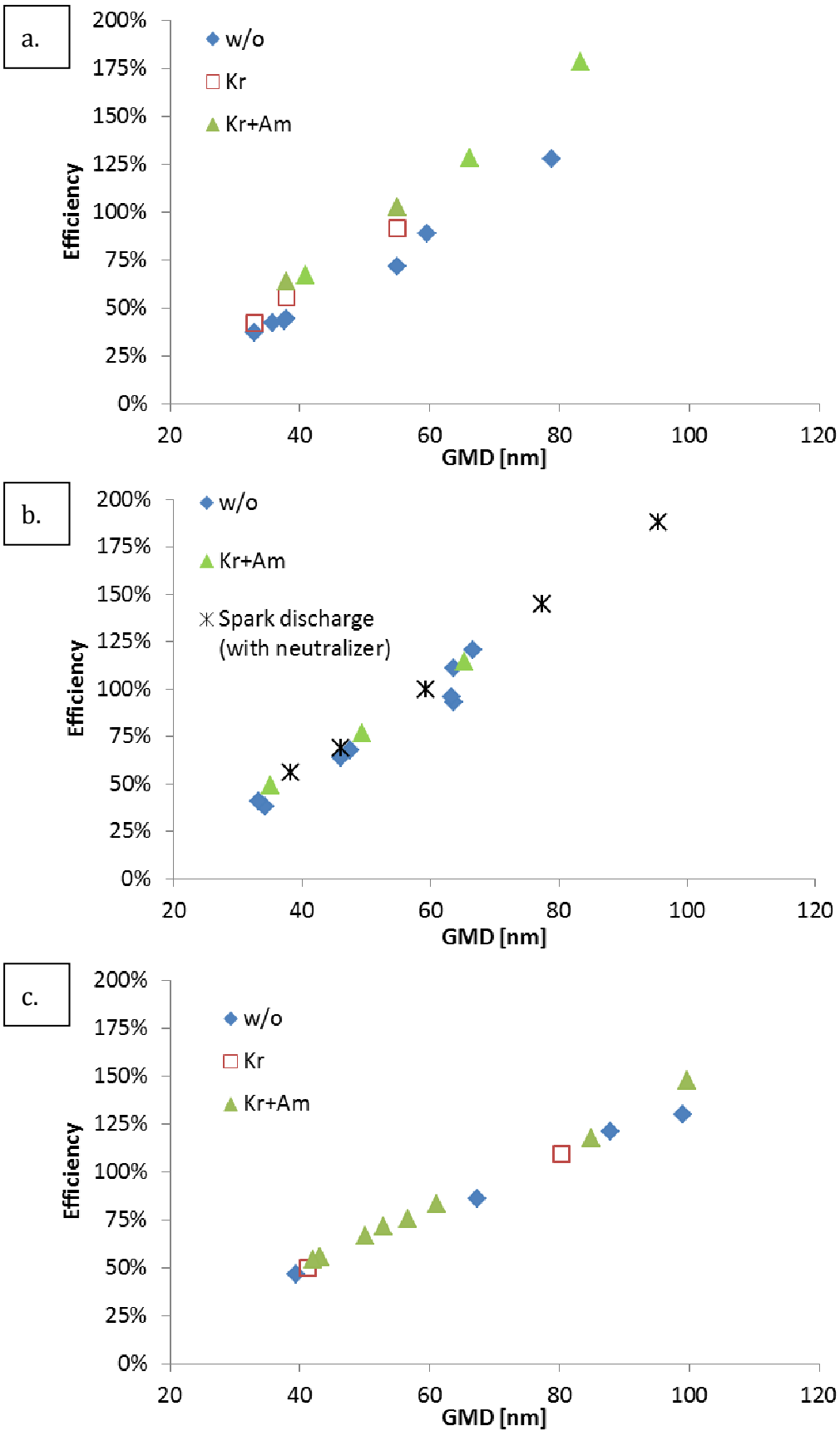

Figure 4.3: *Effect of pre-charge on the response of PN-PEMS for polydisperse aerosol. a) Spark-discharge soot b) diffusion flame with pre-treatment c) PAO.*

For polydisperse aerosol there was a 30% difference due to the highly charged aerosol of the graphite spark generator (**Figure 4.3**). For the PAO polydisperse test there was no effect of the neutralizers because the net charge of the aerosol is zero.

One important finding from these investigations was that the soot generators (spark discharge graphite and diffusion flame based with thermal pre-treatment) gave very similar efficiencies, which were in general higher than the PAO.

Linearity tests

The linearity of the DC was checked either stand-alone or connected to the VPR (PN-PEMS). **Figure 4.4** shows the results. The DC is linear at least in the range 1000 – 20000 p/cm^3. At low concentrations <1000 p/cm^3 (for 100 nm particles) the background correction is important and can lead to big errors. This background value is higher than the 200-600 p/cm^3 for 50 nm particles reported (Fierz et al. 2014).

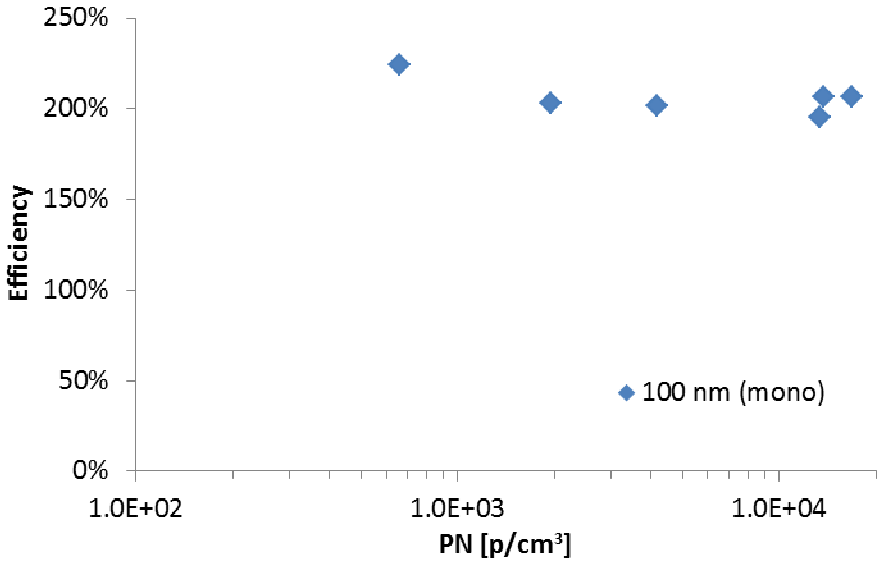

Figure 4.4: *Linearity of the DC.*

Efficiency of DC

The efficiency of the DC (with a neutralizer after the DMA, and corrected for multiple charges according to the equations of the **Annex**) can be seen in **Figure 4.5**. The exponent was found to be 1.1 for PAO (oil) particles and 1.26 for soot particles (spark-discharge in the figure); higher as expected due to the fractal structure of the soot. The manufacturer reported a value of 1.23 based on calibrations with mini CAST soot (unpublished data). However it should be noted that the uncertainty of the exponent was around 0.05 depending on the day and the size range examined, thus the results are very similar.

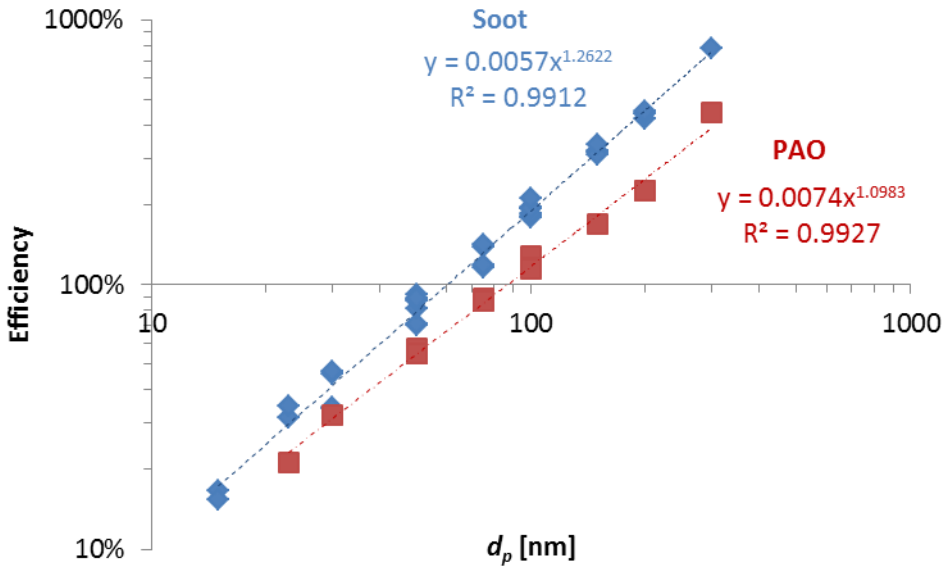

Figure 4.5: *Efficiency curve of the DC for PAO and spark-discharge soot.*

Theoretical evaluation

Following the analysis of **Chapter 2**, the monodisperse experimental data (blue open circles) for the DC were fitted in a linear function (solid blue line) (**Figure 4.6**). Then the efficiency (response) of the DC for polydisperse aerosol (various GMDs) was estimated (dashed green line) and was compared with the experimental polydisperse aerosol data (green open squares).

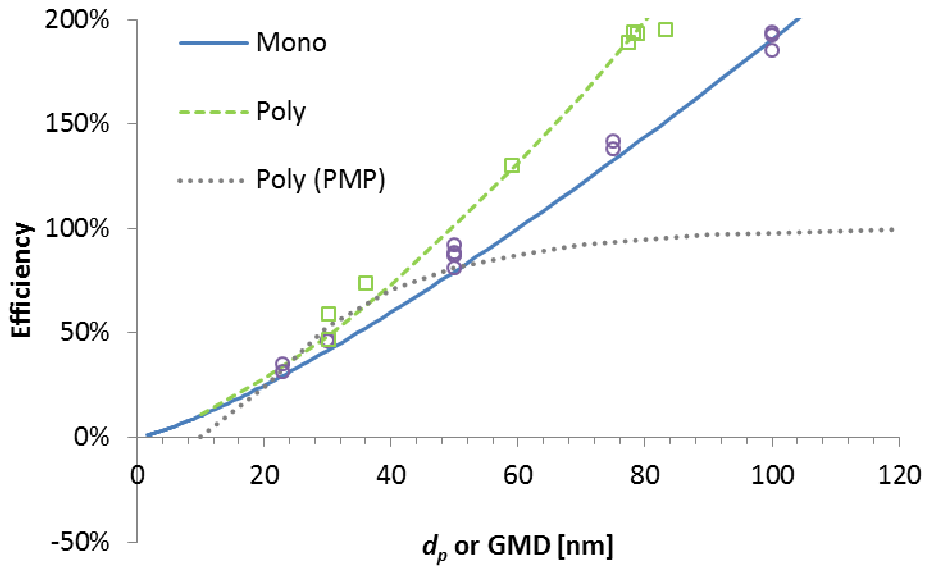

Figure 4.6: *Theoretical and experimental efficiencies for the DC and PMP systems.*

At a next step the difference of the PN-PEMS from the PMP system for different sizes was estimated (**Figure 4.7**). As previously, the monodisperse experimental data (open circles) were fitted (blue solid line). Then this monodisperse efficiency was used to estimate the efficiency (response) of the instrument for polydisperse aerosol (dashed green line) and the polydisperse estimation was compared with experimental data (open

squares). The open symbols were based on CPC and SMPS data that were fitted with the PMP efficiency curve.

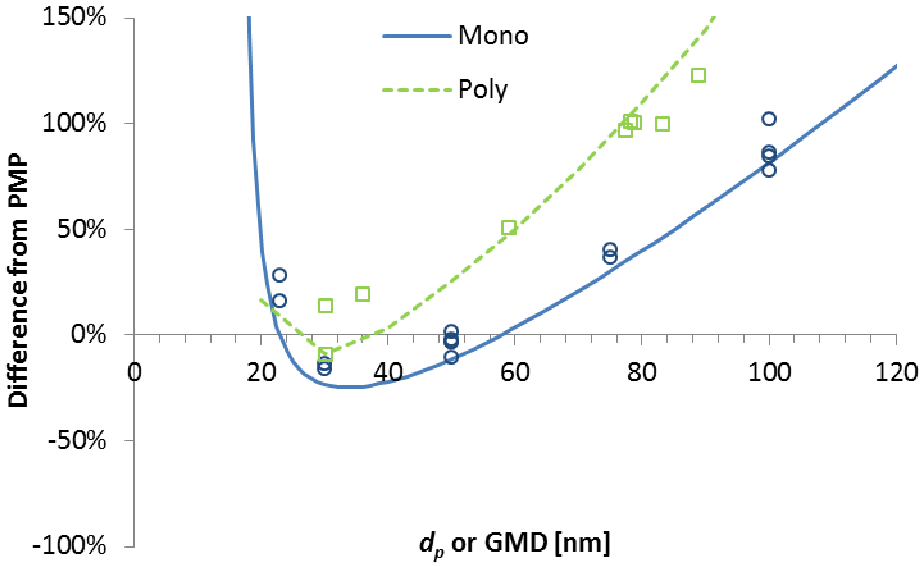

Figure 4.7: *Theoretical and experimental differences between PN-PEMS and PMP systems. Solid symbols are true PMP experimental data, while open symbols indicate CPC or SMPS data that were fitted with the PMP efficiency.*

PN-PEMS

Following the analysis of **Chapter 2**, the monodisperse experimental data (blue open circles) for the complete PN-PEMS were fitted in a linear curve (solid blue line) (**Figure 4.8**). Then the efficiency (response) of the PN-PEMS for polydisperse aerosol (various GMDs) was estimated (dashed green line) and was compared with the experimental polydisperse aerosol data (green open squares).

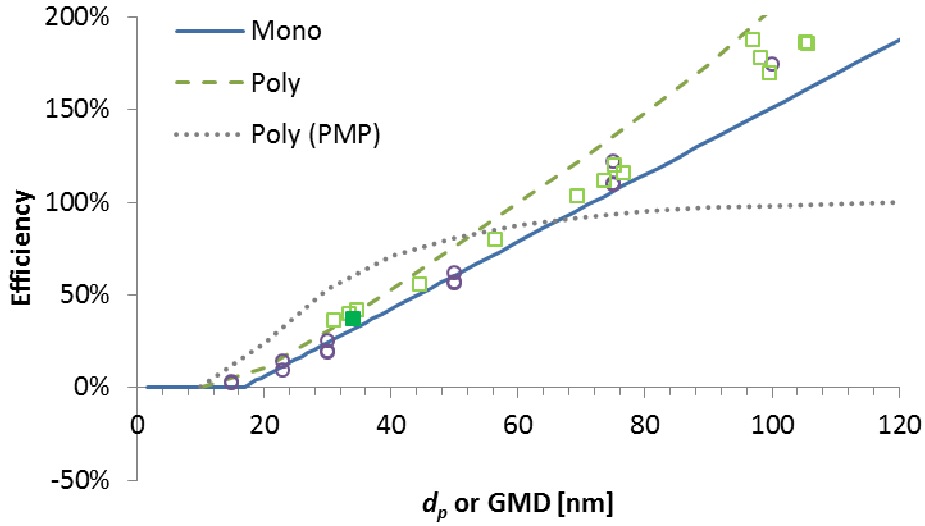

Figure 4.8: *Theoretical and experimental efficiencies for the PN-PEMS and PMP systems.*

The agreement is quite good, but the polydisperse experimental efficiencies are lower than the estimated one. One reason could be that the assumed standard deviation was different than the real one (see **Table 2.3**). Another reason for the deviations could be incorrect estimation of the multiply charged particles. In these results care was taken to use sizes on the right side of the generated distribution and with concentrations within the capabilities of the neutralizer (<1x10^7 p/cm^3 at the inlet of DMA). Thus the correction for doubly and triply charged particles should be adequate (see also discussion in **Chapter 3**), although the effect of bigger particles cannot be excluded, especially taking into account that no impactor was used at the inlet of DMA and knowing that the Palas soot is highly charged (Bau et al. 2010). Inadequate neutralization after the DMA would result in lower than the true efficiencies for the monodisperse tests (see **Figure 4.2**), thus the true monodisperse efficiencies would be higher (so it would be in the opposite direction).

At a next step the difference of the PN-PEMS from the PMP system for different sizes was estimated (**Figure 4.9**). As previously, the monodisperse experimental data (open circles) were fitted (blue solid line). Then this monodisperse efficiency was used to estimate the efficiency (response) of the instrument for polydisperse aerosol (dashed green line) and the polydisperse estimation was compared with experimental data (open squares). The open symbols were based on CPC and SMPS data that were fitted with the PMP efficiency curve, while the solid symbols were true PMP measurements. The simulation of PMP is very close to the true PMP measurements as already shown in **Chapter 2**.

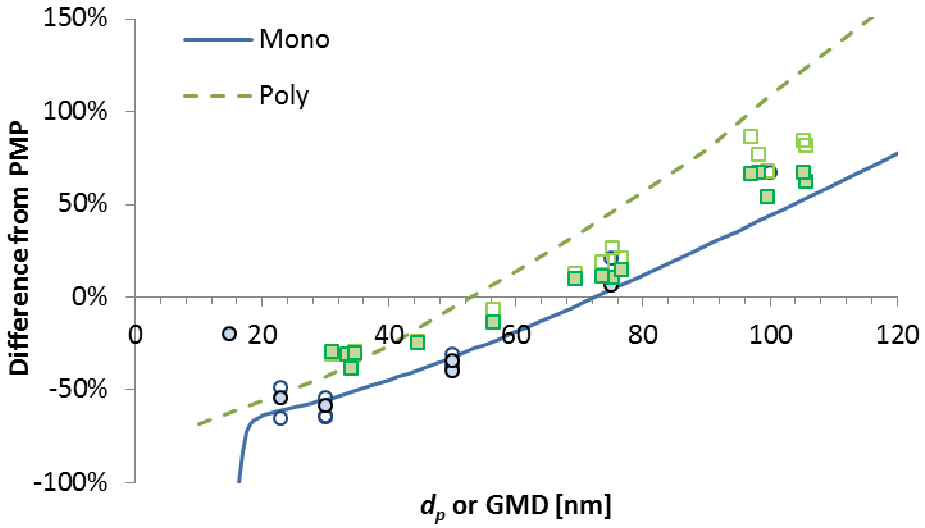

Figure 4.9: *Theoretical and experimental differences between PN-PEMS and PMP systems. Solid symbols are true PMP experimental data, while open symbols indicate CPC or SMPS data that were fitted with the PMP efficiency.*

The important message from this figure is that the expected differences between the PN-PEMS and the PMP system is -35% to +25% for GMDs between 30 and 75 nm. A +50% difference is expected at GMD around 90 nm. The difference is >50% for bigger sizes. Assuming that typical vehicle GMDs are between 40 and 80 nm, differences ±25% are expected. For a wider range, differences of -38% to +70-85% are expected. The vehicle tests (Riccobono et al. 2014) gave differences of -40% to +80% indicating current

technologies have wider range of GMDs (e.g. 30 to 100 nm) or wider size distributions. Other experimental uncertainties during the vehicle testing (e.g. sampling location, pressure and temperature effect etc.) also contribute and usually increase the differences.

Calibration

One open issue is whether the calibration of the PN-PEMS should be conducted for the complete unit or for its parts separately (i.e. VPR and DC). **Figure 4.10** shows the efficiencies of the VPR, the DC and the complete PN-PEMS. The estimated efficiency based on the separate parts (VPR and DC) is also shown. Note that for the VPR efficiency the size dependent *PCRF*s of **Figure 4.1** were used normalized to the mean *PCRF*. This will be further discussed in **Chapter 10**. It can be seen that the calibration of the complete system or its parts separately give similar results and the decision of which approach should be followed should be based on practical difficulties (e.g. when the complete PN-PEMS is calibrated the DC measures very low currents and has higher uncertainty). This applies for systems with small size dependent losses of the VPR.

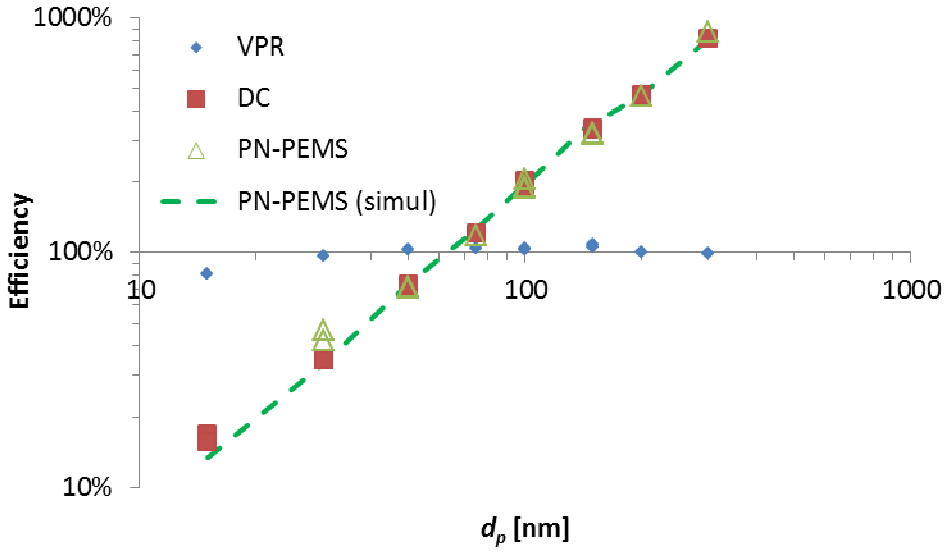

Figure 4.10: *Experimental efficiencies of VPR, DC, PN-PEMS and estimated efficiency of PN-PEMS based on the seperate VPR and DC calibration.*

5. PN-PEMS #2

PN-PEMS #2 (OBS-PN prototype, Horiba) consists of a VPR and a DC (DCS-100 from TSI). The VPR consists of a heated ejector diluter (180°C), a heated line (47°C) that brings the diluted sample to a secondary ejector diluter (ambient temperature). Description of the system and the DC can be found elsewhere (e.g. Riccobono et al. 2014, Wilson et al. 2007). Important note is that the specific DC was used with diffusion screens to reduce the sensitivity to sub 23 nm particles. The VPR was calibrated separately by the manufacturer and the (mean) *PCRF* used was 30. The DC gives 'aerosol length' *L* in mm/cm^3. This equals approximately with the current that is measured *I* [pA] multiplied by 6.1. A constant factor *C* of 10000 was also included to convert the length to particle number (reading). This value, which was given by the manufacturer, was based on comparisons of the device with a CPC with monodisperse particles of 55 nm. Thus the reading *R* of the instrument was:

$$R_{PN-PEMS} = C\ L\ PCRF_{mean} \qquad 5.1$$

The *L* was always corrected for the zero offset. This value was around 500 p/cm^3 and was not important (<10%) for sizes 50 nm and above during the monodisperse aerosol tests.

The analysis of the specific PN-PEMS included investigation of the DC with and without the diffusion screens and evaluation of the complete PN-PEMS.

VPR

Initially the VPR was checked by sampling upstream and downstream of the VPR (from the DC position) with a TSI CPC 3772. The results gave a *PCRF* of around 12 (independent of particle size down to 30 nm), although a *PCRF* value of 30 was expected. The above results indicate that the calibration of the VPR must be done extremely carefully, especially if any flow changes affect the dilution. For all results presented, the manufacturer's *PCRF* (30) was used as it is considered to be more accurate.

DC

Initially the DC was checked without the diffusion screens in order to compare its efficiency with published data. **Figure 5.1** shows the Penetration x average charge per particle (*Pn*) based on the raw data of the device and a flow rate of 2.5 lpm. The results are in agreement with TSI (manual), Jung and Kittelson (2005) and Fissan et al. (2007), who found exponents around 1.13 and pre-factors between 0.018 and 0.020. However the lower pre-factor in **Figure 5.1** could indicate less ion current produced by the charger. This was observed in a previous study where the ion current produced by the charger was lower than the nominal value (Mamakos et al. 2011).

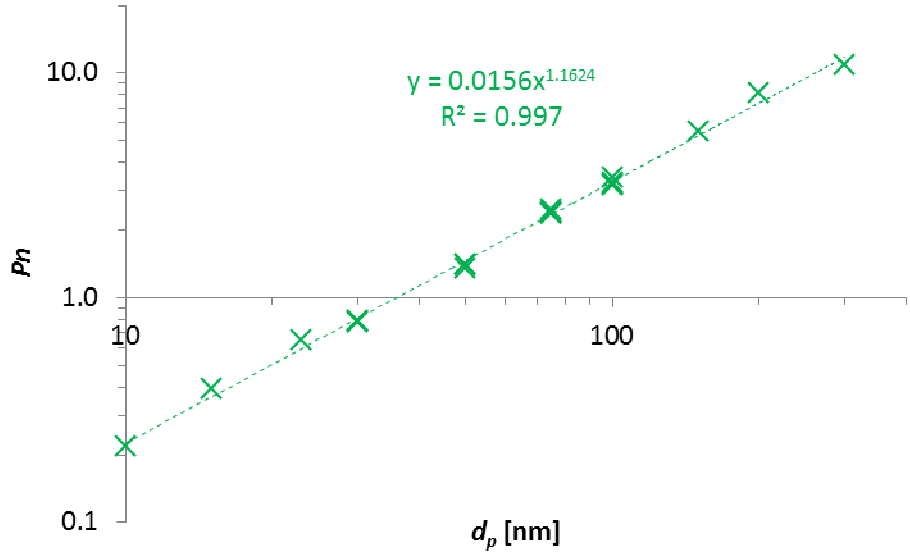

Figure 5.1: *Mean charge per particle*.

The specific DC gives particle length, thus a combination of this metric with the number concentration measured with a CPC can give estimation of a mean diameter $d_p(estim)$ (Frank et al. 2008).

$$d_p(estim) = \frac{L}{PN} \qquad 5.2$$

This diameter can be compared with the DMA setting (d_p) for the monodisperse tests or the GMD of the SMPS for the polydisperse tests. **Figure 5.2** shows that the size estimated is higher than the set size at the DMA. For small sizes the differences are <10%, they reach 10-15% for 50 nm particles, and they are >30% for >100 nm particles. The differences also increased as the concentration increased or the generated size distribution moved to bigger particles. This is an indication that the neutralization of the particles after the DMA was not efficient and the multiple charge contribution was significant. However, as it will be shown in **Figure 5.3** probably this was not the reason. The most possible explanation is the response of the instrument which is d_p^1.15 and not d_p^1 (see **Figure 5.1**). Frank et al. (2008) did the same test with polydisperse aerosol and found 30% underestimation of the estimated size compared to the GMD.

Pre-existing charge effect

The specific DC uses a positive unipolar charger and the effect of pre-existing charges on the aerosol has been investigated (Qi et al. 2009). For initially neutral and negatively charged particles, the final charge state is identical, whereas the final positive charge is a bit higher for initially positively charged particles. The final charge state, which is what the DC measures, is therefore nearly independent of the pre-existing charge. **Figure 5.3** shows that the efficiency of the DC with and without neutralizer after the DMA (monodisperse aerosol) was almost the same. Probably, the pre-existing charge was low compared to the charging capability of the charger (Ntziachristos et al. (2004), Biskos et al. (2005), Qi et al. (2009)). With polydisperse aerosol the efficiency was lower

without neutralizer (5-10% with GMD of 50 nm) (Figure not shown). However the reason is probably the change of the GMD and *s* between the two tests.

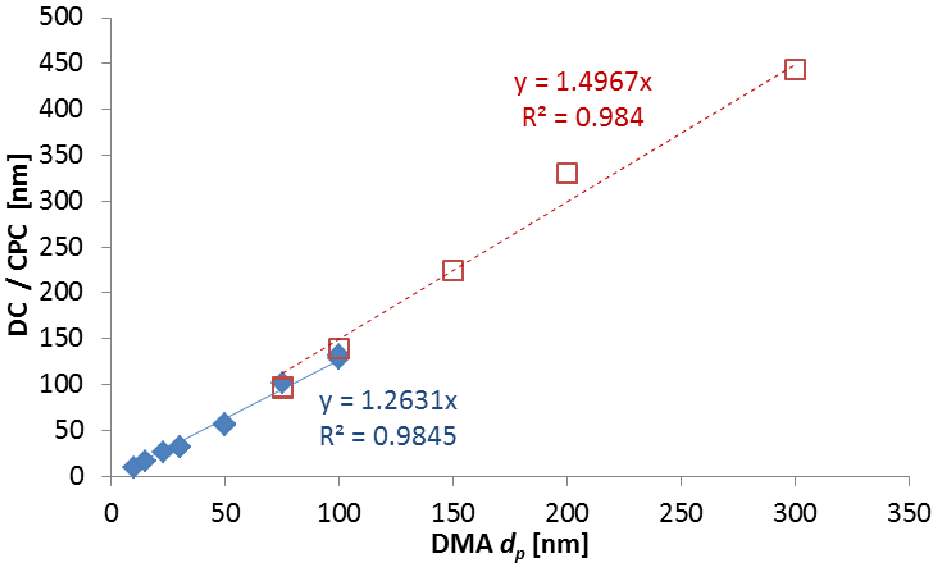

Figure 5.2: *Estimated particle size from DC and CPC.*

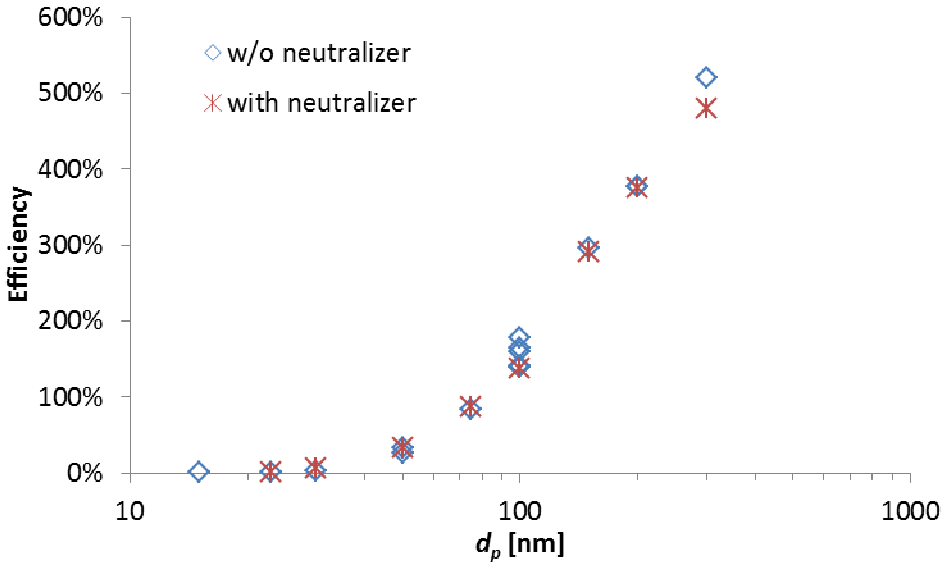

Figure 5.3: *Efficiency measurements with and without neutralized after the DMA.*

PN-PEMS

Following the analysis of **Chapter 2**, the monodisperse experimental data (blue open circles) for the complete PN-PEMS were fitted in a linear curve (solid blue line) (**Figure 5.4**). Then the efficiency (response) of the PN-PEMS for polydisperse aerosol (various GMDs) was estimated (dashed green line) and was compared with the experimental polydisperse aerosol data (green open squares).

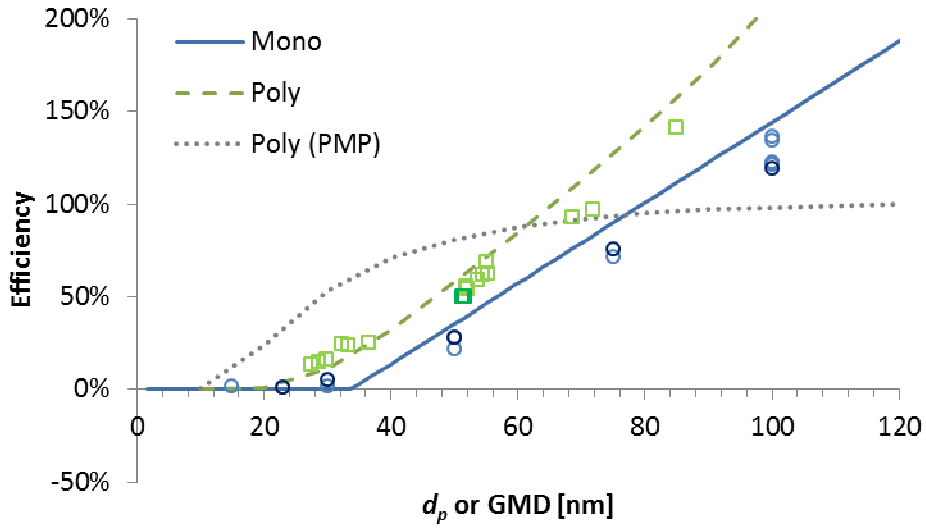

Figure 5.4: *Theoretical and experimental efficiencies for the PN-PEMS and PMP systems.*

At a next step the difference of the PN-PEMS from the PMP system for different sizes was estimated (**Figure 5.5**). As previously, the monodisperse experimental data (open circles) were fitted (blue solid line). Then this monodisperse efficiency was used to estimate the efficiency (response) of the instrument for polydisperse aerosol (dashed green line) and the polydisperse estimation was compared with experimental data (open squares). The open symbols were based on CPC and SMPS data that were fitted with the PMP efficiency curve.

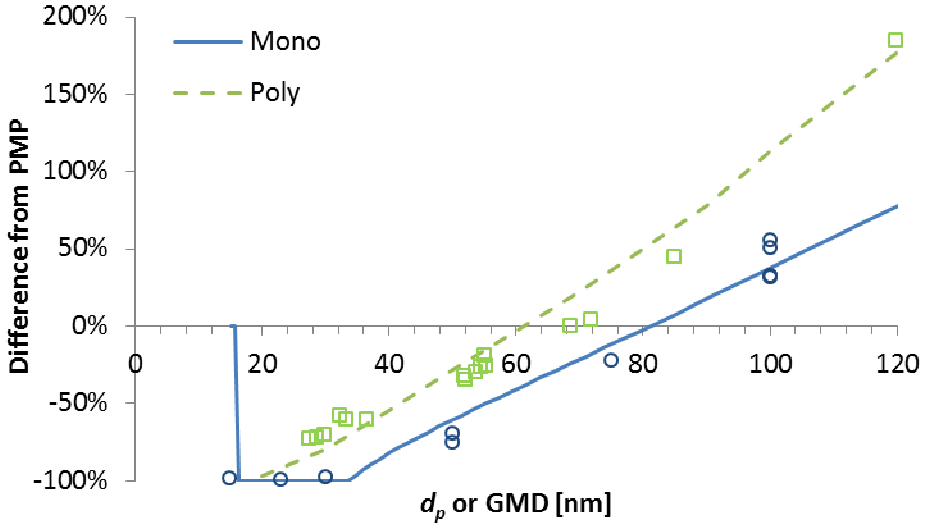

Figure 5.5: *Theoretical and experimental differences between PN-PEMS and PMP systems. Open symbols indicate CPC or SMPS data that were fitted with the PMP efficiency.*

The important message from this figure is that the expected differences between the PN-PEMS and the PMP system is -75% to +50% for GMD between 30 and 80 nm. A +50% difference is expected at GMD around 80-90 nm. The difference is >50% for bigger sizes (e.g. 200% for GMD 120 nm). Assuming that typical vehicle GMDs are between 40

and 80 nm, differences ±40% are expected. The vehicle tests (Riccobono et al. 2014) gave differences of -80% to +80% indicating current technologies have wider range of GMDs (e.g. 30 to 100 nm) or wider size distributions. Other experimental uncertainties during the vehicle testing (e.g. sampling location, pressure and temperature effect etc.) also contribute and usually increase the differences. Especially for this device dilution issues were identified that increased the differences to the PMP method.

Calibration

One concern is whether the calibration of the PN-PEMS should be conducted for the complete unit or for its parts separately (i.e. VPR and DC). **Figure 5.6** shows the efficiencies of the VPR, the DC and the complete PN-PEMS. The estimated efficiency based on the separate parts (VPR and DC) is also shown. Note that for the VPR efficiency the size dependent *PCRF*s of **Figure 4.1** were used normalized to the mean *PCRF* (see also **Chapter 10**). It can be seen that the calibration of the complete system or its parts separately do not give similar results. There is a factor of 1.4 missing: either the *PCRF* of the manufacturer is lower than 30 (see discussion of **VPR** above) or the DC is underestimating the emissions (see discussion of **Figure 5.1**). Actually the DC tests were conducted at the end and is possible that the internal orifice was contaminated and affected the internal flows.

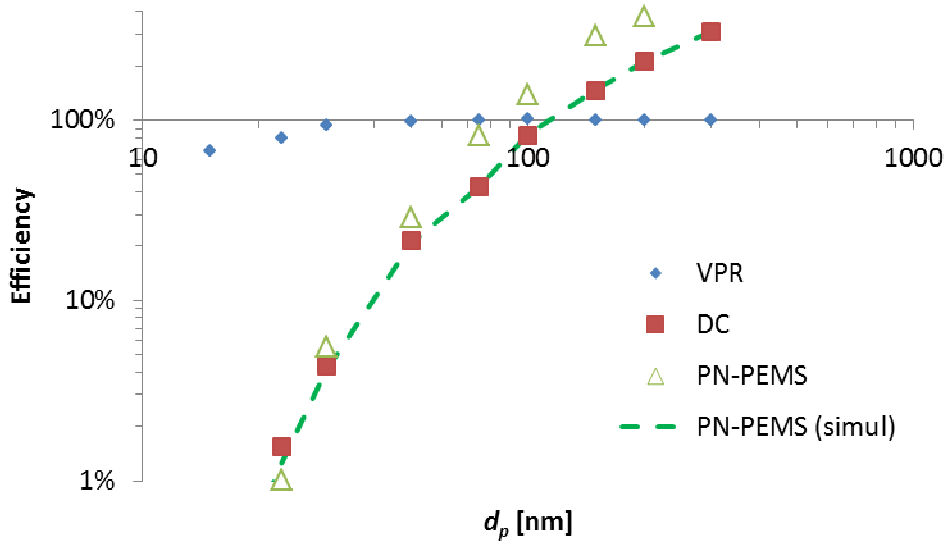

Figure 5.6: *Experimental efficiencies of VPR, DC, PN-PEMS and estimated efficiency of PN-PEMS based on the seprate VPR and DC calibration.*

6. PN-PEMS #3

PN-PEMS #3 (Nanomet 3-PS, Mater Aerosol) consists of a VPR and a DC (Diffusion Size Classifier miniature, DiSC mini). The VPR consists of a heated sampling line at 100°C, a heated rotating disk diluter, and an evaporation tube at 300°C. Description of the system can be found elsewhere. The VPR and the DC were calibrated separately by the manufacturer. The (mean) *PCRF* that was used was 9.9, based on the manufacturer's calibration with NaCl particles at 90 nm. The DC gives Lung Deposited Surface (*LDSA*) in $\mu m^2/cm^3$. A constant factor *C* of 200 was also included to convert the LDSA to particle number (reading). This value was based on the calibration conducted at JRC (see below). Thus the reading *R* of the instrument was:

$$R_{PN-PEMS} = C\ LDSA\ PCRF_{mean} \qquad 6.1$$

The *LDSA* was always corrected for the zero offset. This value was around 1 $\mu m^2/cm^3$ and was not important (<10%) for the sizes 23 nm and above during the monodisperse aerosol tests. The following results refer to the LDSA value of the device. The estimated size and PN will be examined separately at the end of the chapter.

VPR

The VPR was not checked. The primary diluter of the device is a rotating disk and there is no secondary dilution after the evaporation tube. Thus at least 35% losses are expected. Most of them should be included with the one point particle calibration.

DC / PN-PEMS

The DC was not checked separately. However, the Penetration x average charge per particle (*Pn*) based on the raw data of the device was estimated from the PN-PEMS results (**Figure 6.1).** The exponent (1.18) is between the NaCl experiments (1.11 in Fierz et al. (2008), 1.125 in Fierz et al. (2011), 1.13 reported value by the manufacturer) and soot (1.34 in Maricq (2013)). Partly this could be due the low current that was measured from the DC due to the extra dilution in the VPR. Here the VPR is also included and the results are not easily comparable. The pre-factor 0.013 is similar to Fierz et al. 2008 (0.013) and 2011 (0.015) and the reported value by the manufacturer (0.013). The results without neutralizer downstream of the DMA were quite close for the sizes examined. Based on the results of Maricq (2013) there is no measurable difference for particles >100 nm and negligible for 50 nm particles. Particle polarity doesn't affect the diffusion screen response, because data are normalized by total current, so the charging efficiency cancels out. The result is higher measured efficiencies for particles <50 nm without the neutralizer downstream of the DMA.

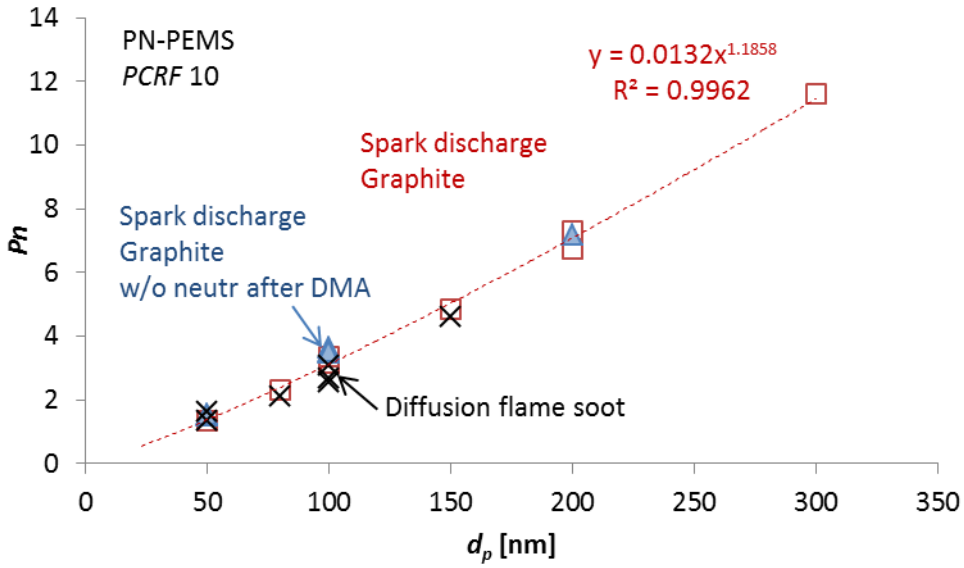

Figure 6.1: *Mean charge per particle.*

Linearity

Figure 6.2 shows the linearity response of the PN-PEMS (*PCRF* 10) for 30 and 100 nm monodisperse particles and a polydisperse aerosol with GMD around 55 nm. The concentrations below 10000 p/cm³ have high uncertainty due to the low current measured. For 30 nm and 100 nm monodisperse particles the response is quite linear. The same applies for polydisperse aerosol.

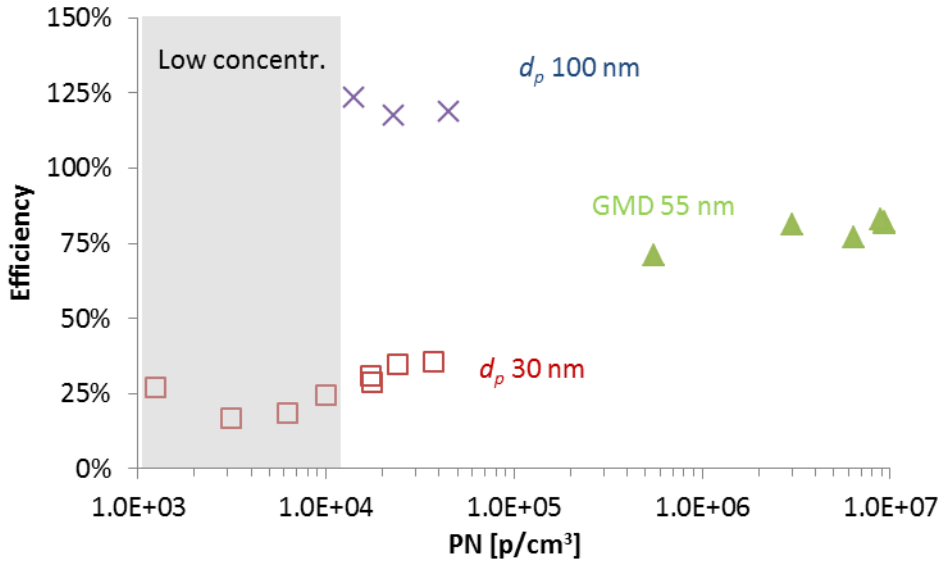

Figure 6.2: *Linearity checks.*

Efficiency

Following the analysis of **Chapter 2**, the monodisperse experimental data (blue open circles) for the complete PN-PEMS were fitted in a linear curve (solid blue line) (**Figure 6.3**). Then the efficiency (response) of the PN-PEMS for polydisperse aerosol

(various GMDs) was estimated (dashed green line) and was compared with the experimental polydisperse aerosol data (green open squares).

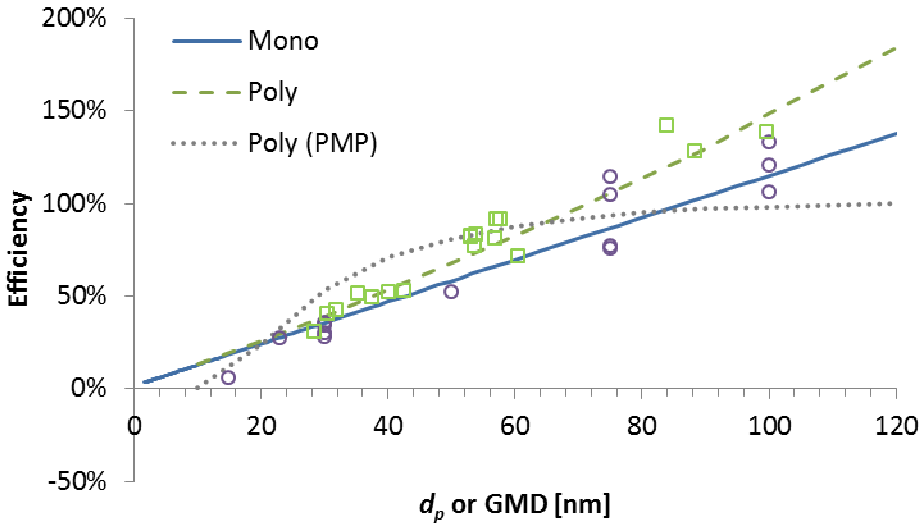

Figure 6.3: *Theoretical and experimental efficiencies for the PN-PEMS and PMP systems.*

At a next step the difference of the PN-PEMS from the PMP system for different sizes was estimated (**Figure 6.4**). As previously, the monodisperse experimental data (open circles) were fitted (blue solid line). Then this monodisperse efficiency was used to estimate the efficiency (response) of the instrument for polydisperse aerosol (dashed green line) and the polydisperse estimation was compared with experimental data (open squares). The open symbols were based on CPC and SMPS data that were fitted with the PMP efficiency curve.

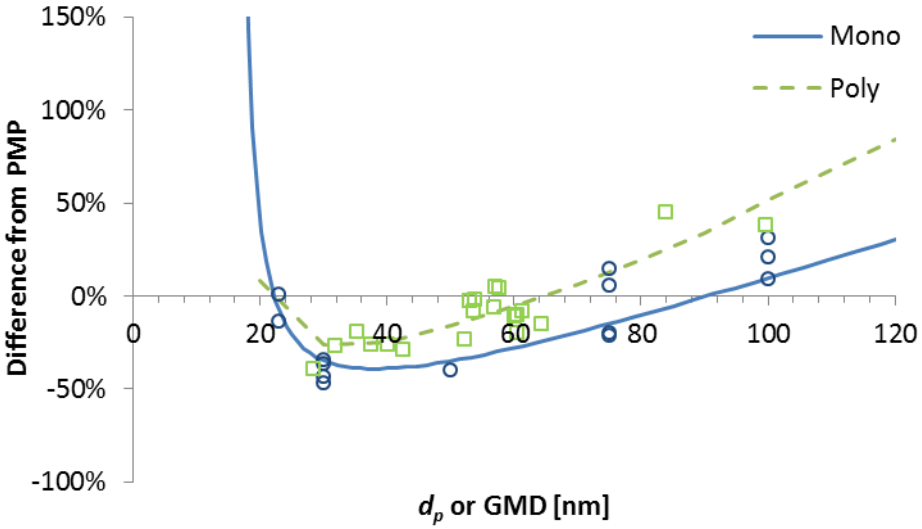

Figure 6.4: *Theoretical and experimental differences between PN-PEMS and PMP systems. Open symbols indicate CPC or SMPS data that were fitted with the PMP efficiency.*

The important message from this figure is that the expected differences between the PN-PEMS and the PMP system is -30% to +20% for GMD between 30 and 80 nm. A +50% difference is expected at GMD around 100 nm. The difference will be >50% for bigger sizes. Assuming that typical vehicle GMDs are between 40 and 80 nm, differences ±30% are expected. The vehicle tests (Riccobono et al. 2014) gave differences of -40% to +45% indicating current technologies have wider range of GMDs (e.g. 30 to 100 nm) or wider size distributions. Other experimental uncertainties during the vehicle testing (e.g. sampling location, pressure and temperature effect etc.) also contribute and usually increase the differences.

Estimation of mean size and PN

Theoretical background

A unique characteristic of the device is that the DC has two electrometers and can estimate a mean size based on their ratio (Fierz et al. 2008, 2011). The charged particles first flow through a diffusion stage. Some of the particles are captured in this stage and generate a current I_{diff}, while the remaining particles flow into a second stage that is equipped with a HEPA filter. Here, all particles are captured, and a current I_{filter} is measured with an electrometer. The ratio I_{filter}/I_{diff} is a measure of the average particle size, because smaller particles undergo larger Brownian motion, and are therefore more likely to be captured in the diffusion stage. This ratio is fitted to a curve (exponential curve below) by the manufacturer:

$$\frac{I_{filter}}{I_{diff}} = a d_p^{\ c} \qquad 6.2$$

Then during a measurement, based on the ratio of filter and diffusion stage currents, a size can be estimated d_{estim}. Then, the number concentration (of a monodisperse aerosol) can be calculated with the following equation:

$$PN_{estim} = \frac{I}{Q\ a d_{estim}^{\ c}} \qquad 6.3$$

Where $I=I_{filter}+I_{diff}$ and Q the flow rate of the DC. For polydisperse aerosol the width of the size distribution is assumed to be 1.9 (1.7 is typical for vehicle emissions, 2.1 is typical for immissions) and the calibration factors for the estimation of the size are adjusted accordingly. The exponent c remains the same as in Equation (6.2), but the pre-factor a is approximately 20% larger for polydisperse aerosol (0.017 from 0.013). For details see Fierz et al. (2008).

Obviously any error at the size estimation will be transferred to the number concentration estimation. Moreover, the calculated average particle diameter is sensitive to the shape of the particle size distribution. Of course if the ratio is not accurate (e.g. one of the stages is at its min or max detection limit) big errors can occur.

The DC is calibrated with NaCl particles but the behavior of soot particles in the diffusion screen stage is different (Maricq 2013): Enhanced interception by the diffusion screen of fractal-like versus spherical particles with the same mobility diameter is observed.

There is one more drawback of this approach: The DC is calibrated on separately from the VPR, but then the same equation is used for the complete PN-PEMS, and thus the size dependent losses of the VPR are not taken into account. Due to the higher losses of small particles in the VPR, a larger d_p (or GMD) will be estimated and the estimated number concentration will be overestimated.

Estimated particle size

The estimated diameter can be compared with the DMA setting (d_p) for the monodisperse tests or the GMD of the SMPS for the polydisperse tests. **Figure 6.5** shows that the size estimated is approximately ±15% of the set size at the DMA. Some outliers (>30% difference) were excluded, because in those cases the current at the electrometers was very low.

However the mean size given is usually lower compared to the GMD of the polydisperse aerosol distribution. The underestimation of the polydisperse aerosol can be explained by the narrower size distributions that were generated (standard deviation s of 1.7 instead of 1.9 assumed by the manufacturer) (Fierz et al. 2011). The results are in agreement with Maricq (2013) who found that the specific DC underestimates size for soot polydisperse particles. Kaminski et al. (2013) also found underestimation of the GMD of 5-10% for 35-40 nm NaCl particles, 15% for 60-100 nm soot particles (spark discharge).

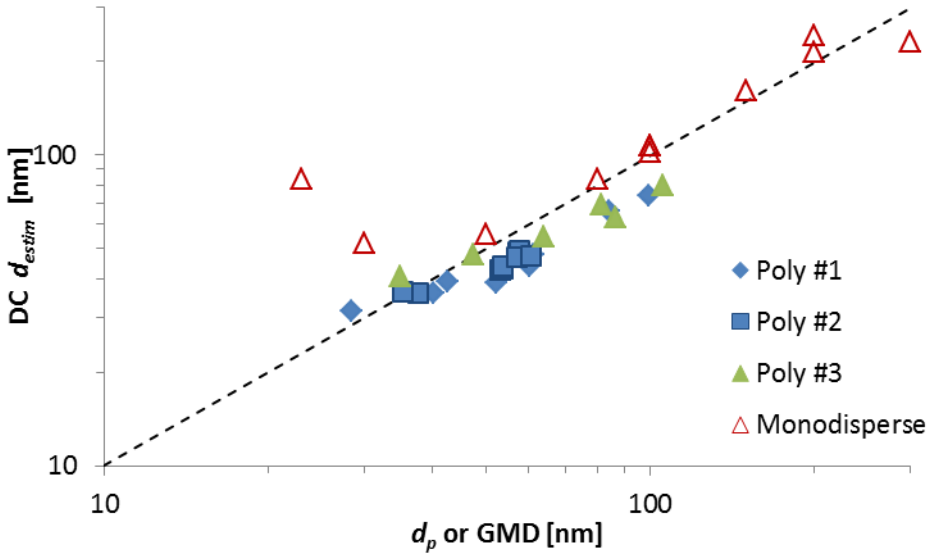

Figure 6.5: *Estimated size from the DC compared to the experimental ones set at the DMA or the GMD given by the SMPS.*

PN estimation

The estimated PN concentration can be seen in **Figure 6.6** for monodisperse and polydisperse aerosols of various sizes. The results show a 15-20% underestimation of the

concentration. The particle number determination should be quite robust, and the error should be within 20% (Fierz et al. 2011). Kaminski et al. (2013) found differences of <10% for NaCl and around 15% for soot (spark discharge). The results here are in agreement with the previous researchers. In addition it is possible that the reference instrument that was used for these measurements was overestimating 10% as comparison with another PNC showed after these tests.

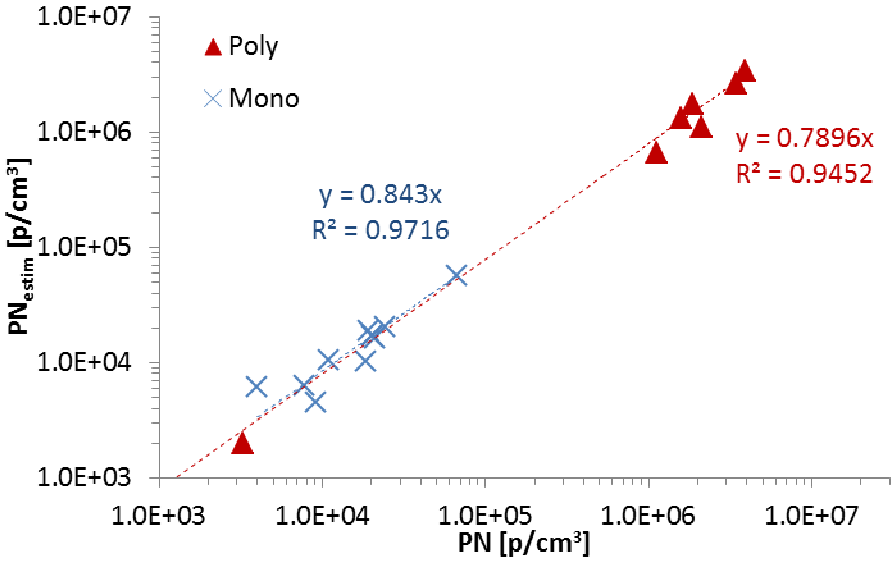

Figure 6.6: *Estimated number concentration from the DC compared to the experimental ones measured by a CPC or SMPS.*

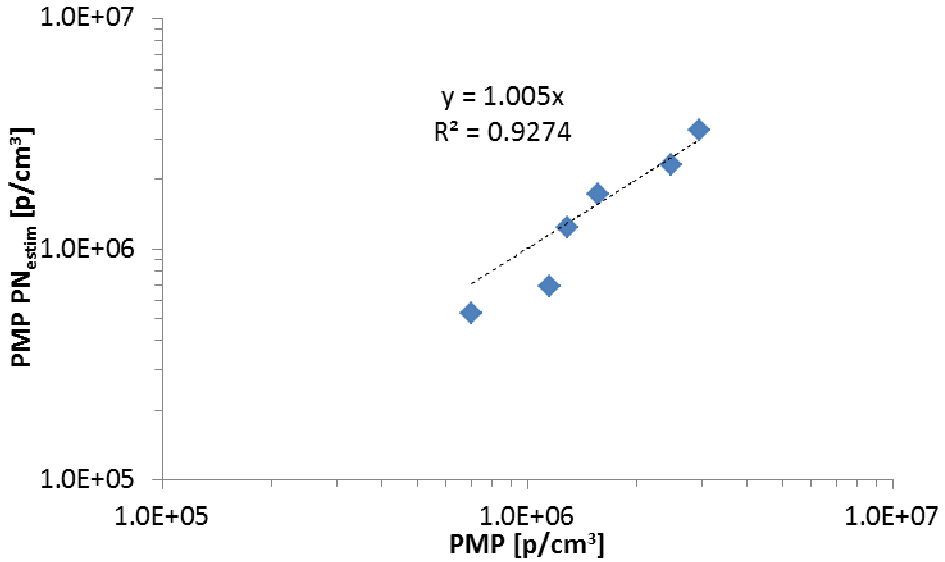

Figure 6.7: *Difference between adjusted PN-PEMS and PMP system.*

A next question is: Which method has higher uncertainty for a specific size range (e.g. 40-100 nm)? The *LDSA which makes no size assumptions* or the PN estimation method which has uncertainties from the assumptions included? **Figure 6.7** shows the comparison of the particle number concentration of the PN-PEMS *adjusted with a PMP*

polydisperse efficiency correction (e.g. correction around 50% for GMD around 30 nm) with a PMP system. The results are quite promising (GMDs examined 35-105 nm).

7. PN-PEMS #4

PN-PEMS #4 (Pegasor) consists of a VPR and DC at the same unit. Description can be found elsewhere (e.g. Ntziachristos et al. 2011, Besch et al., 2011). In a few lines, the sample is drawn through a 2 m heated line by an ejector pump. The sample line and the whole unit with the DC are heated at 200°C. Three devices were checked:

- PN-PEMS #4a (Mi3-1, Pegasor): It was the unit that was used for the vehicle testing. It consists of a heated line at 200°C and the unit heated at 200°C.
- PN-PEMS #4b (4438, Pegasor): It was a unit for garage testing. It's identical to the PN-PEMS #4a. This was the unit was evaluated in the laboratory (not the actual unit that was used for the vehicle testing). This unit was also tested cold and without the heated line.
- PN-PEMS #4c (Pegasor DC from PN-PEMS #5): It's identical with PN-PEMS #4a but without the heated line and heated at only 47°C.

The DC is based on the electrical detection of aerosol following the "escaping current" technique. A sample of the exhaust gas is charged by a corona-ionized flow as it is being pumped by an ejector diluter built in the sensor's construction. While the majority of the corona ions return to the grounded sensor's body due to their high electrical mobility, a small quantity is lost with the charged particles exiting the sensor. This "escaping current" is a measurement of the particle concentration in the exhaust gas. The charge level of the particles as such is not detected, only the charge particles acquire and carry away is detected. Therefore the initial charge of the particles could affect the measurement significantly. The measured current is proportional to the particle flux through the sensor and the charge that particles acquire inside the charger.

More specifically, the PN-PEMS gives a current I [pA] which is proportional to the active surface of the particles and a factor C. However, based on the flow rate of the device Q [lpm], the current can be converted to particle number concentration. Thus the reading of the instrument is (see Ntziachristos et al. 2013):

$$PN_{PN-PEMS} = C\,I \qquad 7.1$$

$$C = \frac{288000}{Q} \qquad 7.2$$

The signal was always corrected for the zero offset. This value was around -3500 p/cm^3 and was <20%) for the sizes 50 nm and above during the monodisperse aerosol tests. All results were corrected with the true flow rate of the devices All tests were conducted with the complete PN-PEMS.

Figure 7.1 shows the penetrations of the 3 devices based on CPC measurements upstream and downstream of the devices. For the heated unit (200°C) the penetrations reach 65% (PN-PEMS #4a). However around 20% thermophoretic losses are expected after the device due to the cooling of the hot aerosol at ambient temperature at the inlet of the CPC. Thus the true penetrations should reach at least 80%. The cold units reached

>80% penetrations (PN-PEMS #4b and #4c). The penetration of the 15 nm particles is <15% which is in agreement with Lanki et al. (2011) who showed approximately 20% penetration for a size distribution with GMD 15 nm. PN-PEMS #4c further increased the penetration reached >90% when the trap voltage was decreased from 400 V to 50 V (Figure not shown).

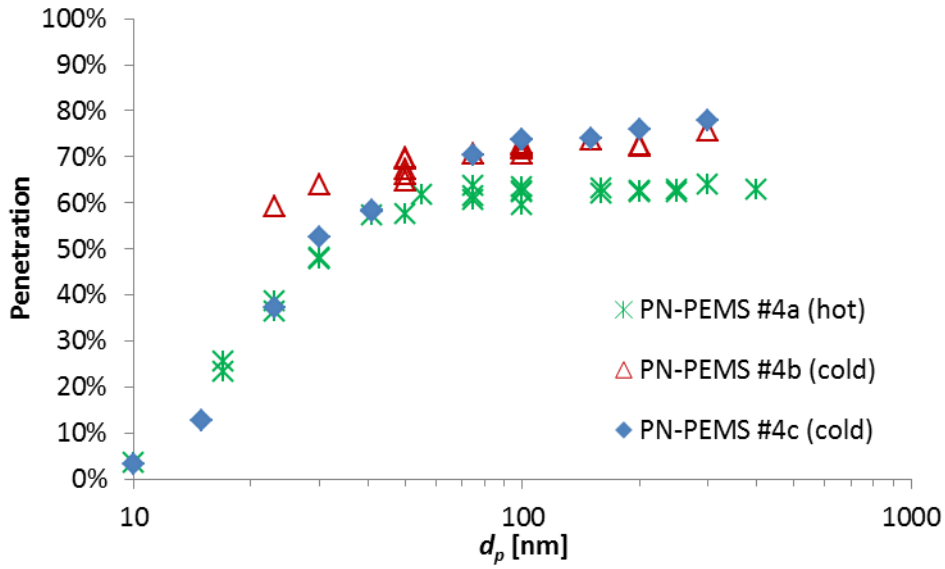

Figure 7.1: *Penetration.*

Effect of pre-existing charge

In the experiments without the neutralizer, the particles at the exit of the DMA are positively charged and thus the reading of the DC will be lower. **Figure 7.2** shows the effect of pre-existing charge on the efficiency of PN-PEMS #4b (cold) with soot and PAO. The effect is very big when no neutralizer exists. Similar behaviour was observed with soot and PAO particles. For example, for 50 nm particles the efficiency changed from almost 100% to 25% and for 100 nm particles from 215% to 145%. Nevertheless, a not so strong neutralizer (<30 MBq) seems enough to neutralize the particles and minimize the effect. Generally the effect is different for positive, neutral and negatively charged particles (Maricq 2013). The charge dependence originates from the combination of positive corona and escaping charge detection. Particles entering the sensor reach a final state of charge that depends on their size but not their initial charge. This means that a negative particle removes more positive ions (charge) from the corona than a neutral particle when it exits the sensor, whereas a positive particle removes less.

For polydisperse aerosol there was also an effect on the efficiencies due to the highly charged soot aerosol (**Figure 7.3**). On average a 50% change of the efficiency was observed. For the PAO polydisperse test there was no effect of the neutralizers because the net charge of the aerosol is zero. However the response of the system to soot and PAO particles is different (i.e. different efficiencies were measured).

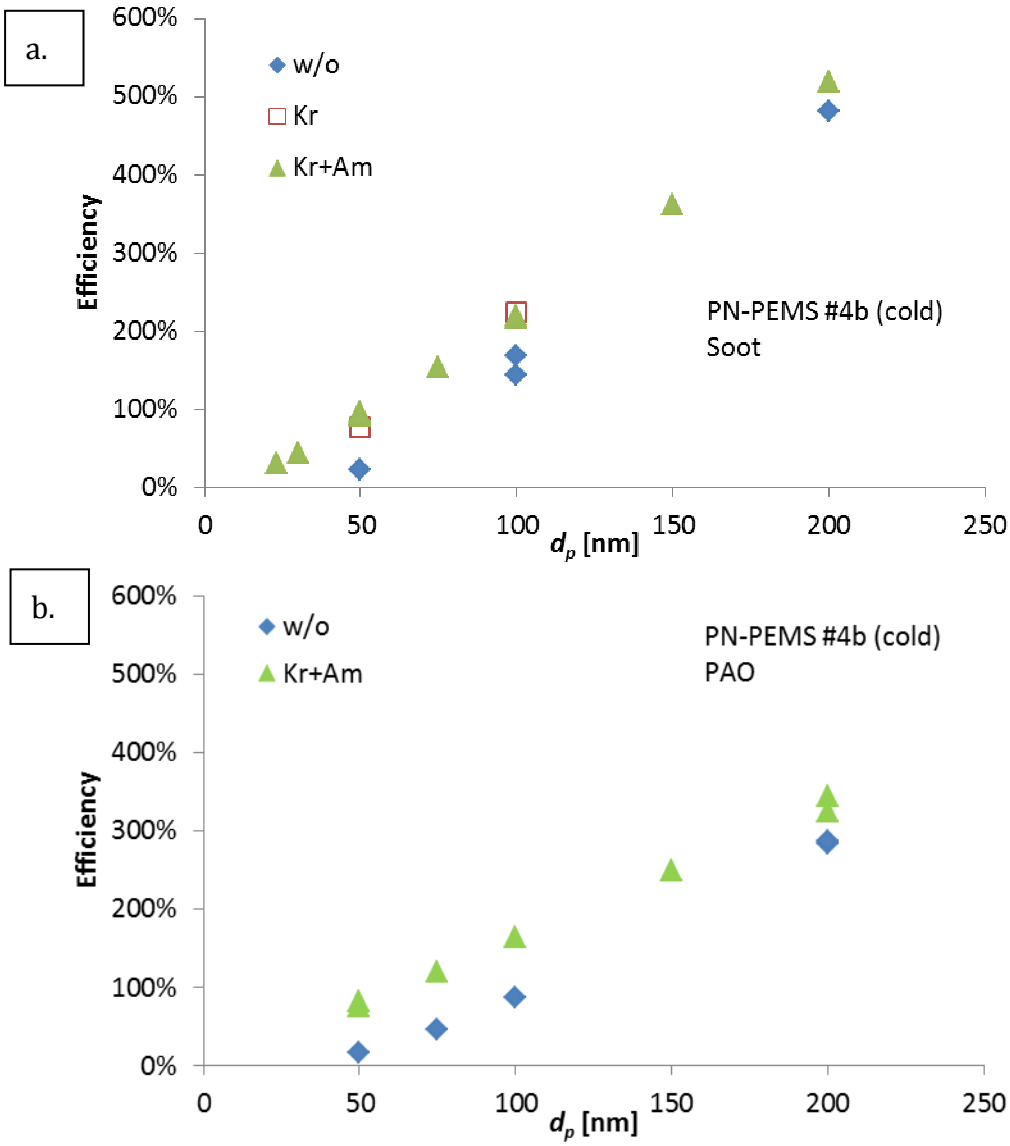

Figure 7.2: *Effect of pre-existing charge on the efficiency of PN-PEMS for monodisperse particles a) Spark-discharge soot b) PAO. With multiple charge correction applied.*

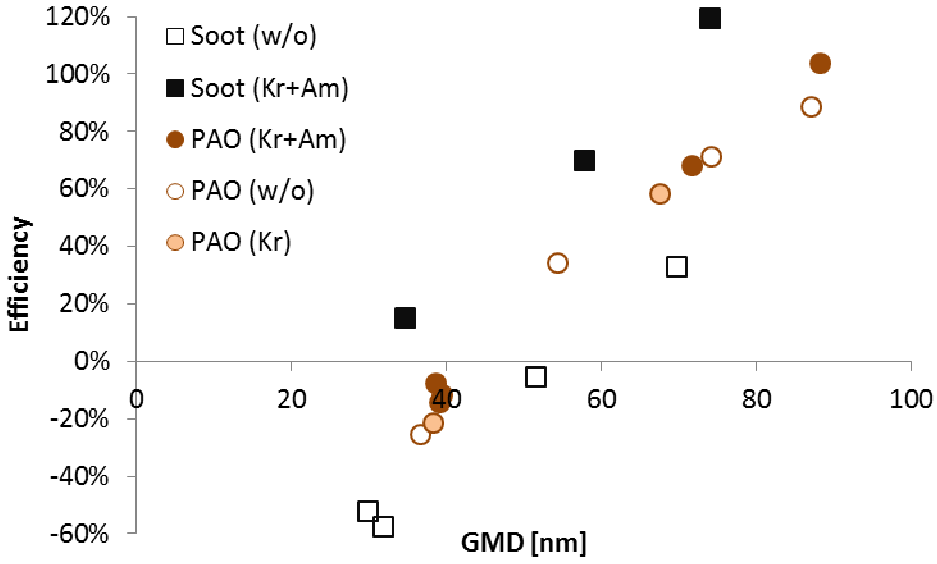

Figure 7.3: *Effect of pre-charge on the response of PN-PEMS for polydisperse aerosol.*

Average charge per particle

Figure 7.4 shows the Penetration x average charge per particle (*Pn*) based on the raw data of the device and the measured flow rate (around 5 lpm). The results are in agreement with Maricq (2013), who found exponents around 1.15 (PAO) and 1.29 (soot). Higher exponent was found by Mamakos et al. (2012) for a hot unit, in agreement with the findings of this study (figure not shown).

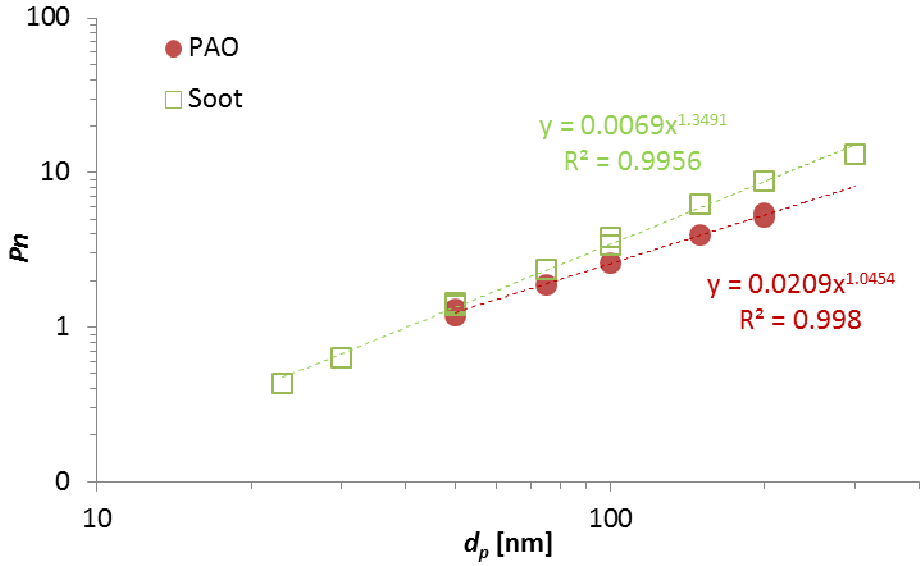

Figure 7.4: *Mean charge per particle.*

Theoretical evaluation

Following the analysis of **Chapter 2**, the monodisperse experimental data (blue open circles) for the complete PN-PEMS#4b (hot, soot data) were fitted in a linear curve (solid blue line) (**Figure 7.5**). Then the efficiency (response) of the PN-PEMS for polydisperse aerosol (various GMDs) was estimated (dashed green line) and was compared with the experimental polydisperse aerosol data (green open squares).

At a next step the difference of the PN-PEMS from the PMP system for different sizes was estimated (**Figure 7.6**). As previously, the monodisperse experimental data (open circles) were fitted (blue solid line). Then this monodisperse efficiency was used to estimate the efficiency (response) of the instrument for polydisperse aerosol (dashed green line) and the polydisperse estimation was compared with experimental data (open squares). The open symbols were based on CPC and SMPS data that were fitted with the PMP efficiency curve.

The important message from this figure is that the expected differences between the PN-PEMS and the PMP system are 0%-150% for GMD between 30 and 90 nm. The vehicle tests with the other unit (PN-PEMS #4a) (Riccobono et al. 2014) gave differences of -45% to +120% indicating that there was a 50% overestimation with the specific unit tested in the laboratory (PN-PEMS #4a), at least for the specific soot. Because with PAO the difference was in the expected range: -30% to +100% for GMDs ranging from 35 nm to 90 nm. The PAO results are in agreement with Amanatidis et al (2013) that found +75% overestimation of the system compared to the PMP when the GMD was around 80 nm. The results also agree with Ntziachristos et al (2012) showed an uncertainty of ±25% for size distributions with GMDs ranging from 40 to 66 nm.

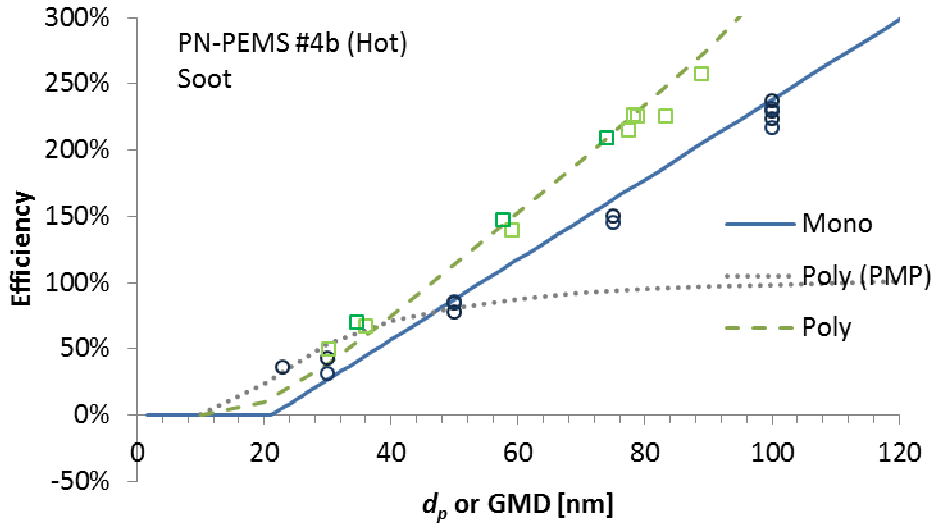

Figure 7.5: *Theoretical and experimental efficiencies for the PN-PEMS and PMP systems.*

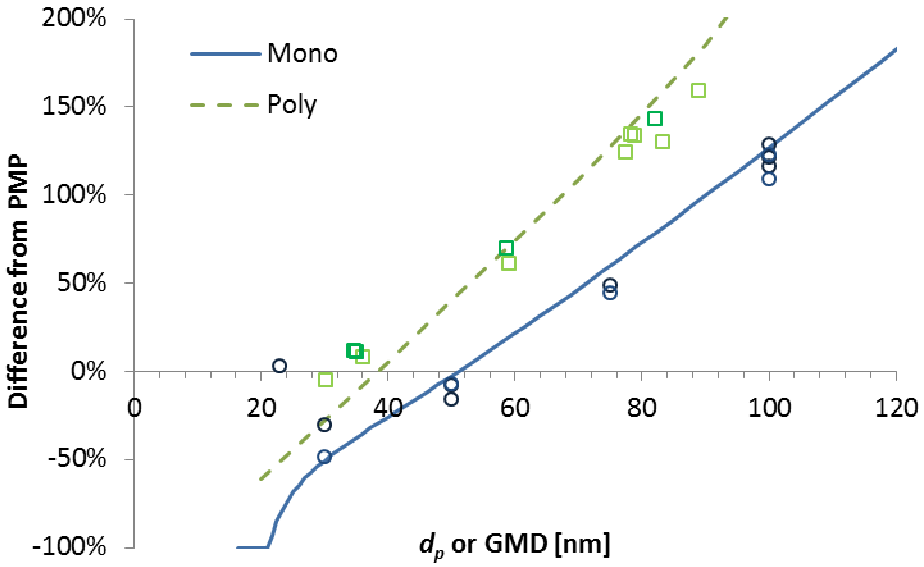

Figure 7.6: *Theoretical and experimental differences between PN-PEMS and PMP systems. Open symbols indicate CPC or SMPS data that were fitted with the PMP efficiency.*

8. PN-PEMS #5

PN-PEMS #5a (Ecostar, Sensors) consists of a VPR and a DC (PPS from Pegasor). The VPR consists of a primary diluter and a heated line at 47°C. This system was used at the vehicle campaign and detailed description of the system can be found elsewhere (Riccobono et al. 2014). The VPR was calibrated with flows by the manufacturer and the dilution factor *DF* was 10. No particle losses were taken into account, but nevertheless the dilution will be used as (mean) *PCRF* in this report (i.e. no losses correction will be applied). The losses were investigated at JRC and will be presented below. The DC primarily measures the escaping current *I* which is proportional to the active surface S_{act} (see Ntziachristos et al. 2013). It converts it to particle number concentration with an internal constant *C* which was 80000 for the specific system. Thus the reading *R* of the instrument was:

$$R_{PN-PEMS} = C\, S_{act}\, DF \qquad 8.1$$

The constant *C* is actually a function of the flow *Q* [lpm] of the DC (see Ntziachristos et al. 2013).

$$C = \frac{288000}{Q} \qquad 8.2$$

The constant used by the manufacturer corresponds to a flow rate of 3.6 lpm which was close to the flow rate measured inside the device (3.9 lpm). When the DC was removed from the PN-PEMS a flow rate of 4.9 lpm was measured. The difference of the flow rates originates from the backpressures inside the device. The true flow rate (4.9 lpm) was used for the tests of the DC standalone.

The study of the PN-PEMS #5 included:

- Checks of the VPR
- Checks of the DC
- Checks of the complete unit

After the vehicle tests and the update of the technical requirements, the VPR was updated: The diluter and the heated line were heated to 200°C and a catalytic stripper (Catalytic Instruments) at 300°C was added at the end of the heated line. The heated line was changed from the previous version, smaller diameter flexible stainless steel that would increase the penetration efficiency from the previous line. The hot aerosol was cooled down in a spiral coil before entering the DC. This system (PN-PEMS #5b) was also investigated and the results will be shown separately.

PN-PEMS #5a

VPR

For the VPR only one dilution setting was checked (10). Two CPCs (3772 with flow 1 lpm, Grimm 1.5 lpm) were used upstream and downstream of the VPR measuring monodisperse particles of different diameters. The downstream position was at the excess flow of the PN-PEMS. The VPR was used with and without the 4 m heated line. The results can be seen in **Figure 8.1**.

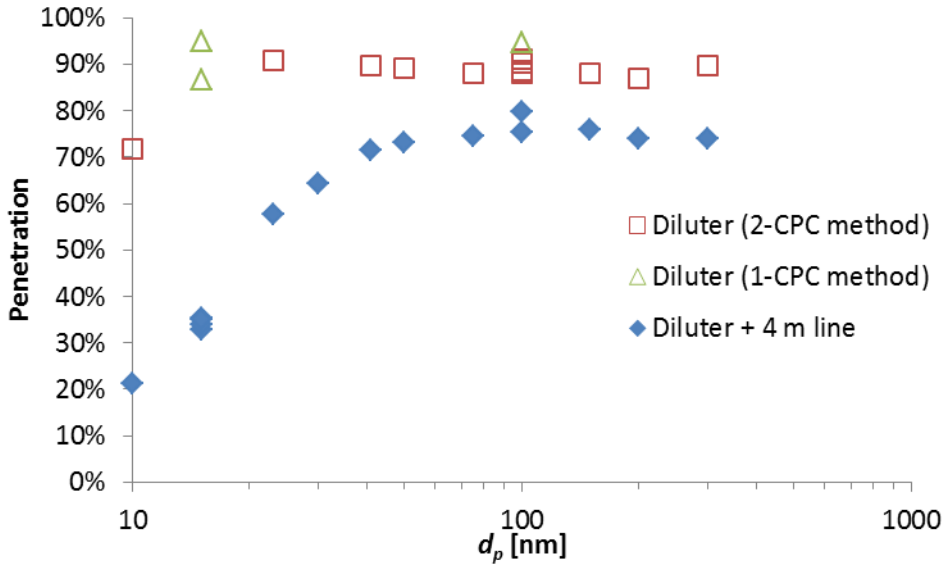

Figure 8.1: *Penetration measurements of the VPR with and without the 4 m heated line.*

The size dependent losses down to 20 nm are almost negligible for the diluter only without the heated line. The overall losses are around 10% which could be due to the design of the diluter or uncertainties of the flow calibration. The 4 m sampling line introduces significant losses: Around 25% for 100 nm particles and around 50% for 23 nm particles. The PN-PEMS was always used with the 4 m line during the measurement campaign (in the laboratory and with the vehicle testing).

DC

The DC was investigated separately at the temperature that was used in the device (47°C) regarding its penetration and efficiency.

Figure 8.2 shows the penetration measurements of the VPR. The losses are 20% at big sizes and reach 65% at 23 nm. When the trap voltage was reduced to 50 V the losses decreased to 10% and 30% for 100 nm and 23 nm respectively. All tests in the laboratory calibration and in the vehicles campaign were conducted with 400 V trap voltage. Note that the penetration measurements are only for informative reasons, since the losses are taken into account by the calibration factor of the efficiency.

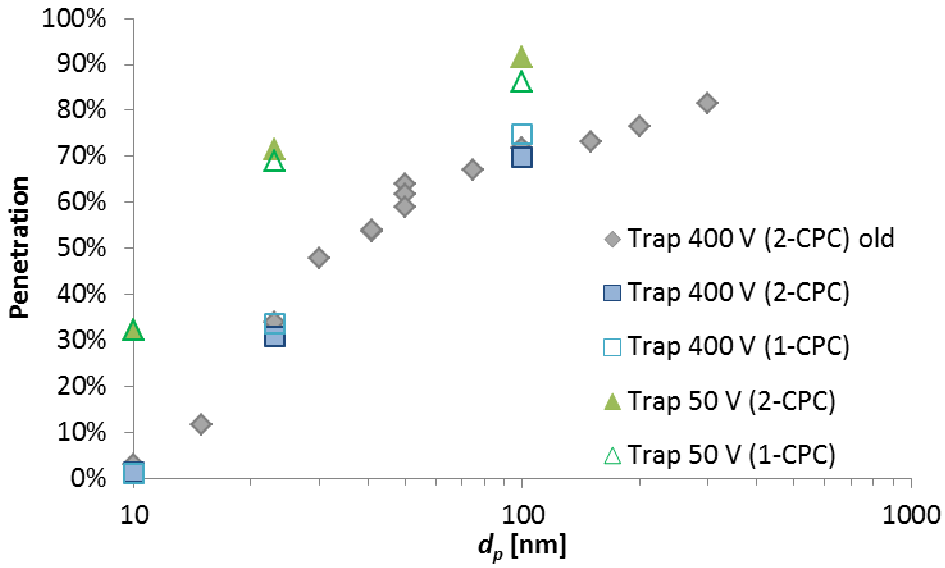

Figure 8.2: *Penetration of the DC (47°C).*

Linearity

Figure 8.3 shows the linearity results of the PN-PEMS with monodisperse aerosol of 50 nm. The response of the instrument is linear.

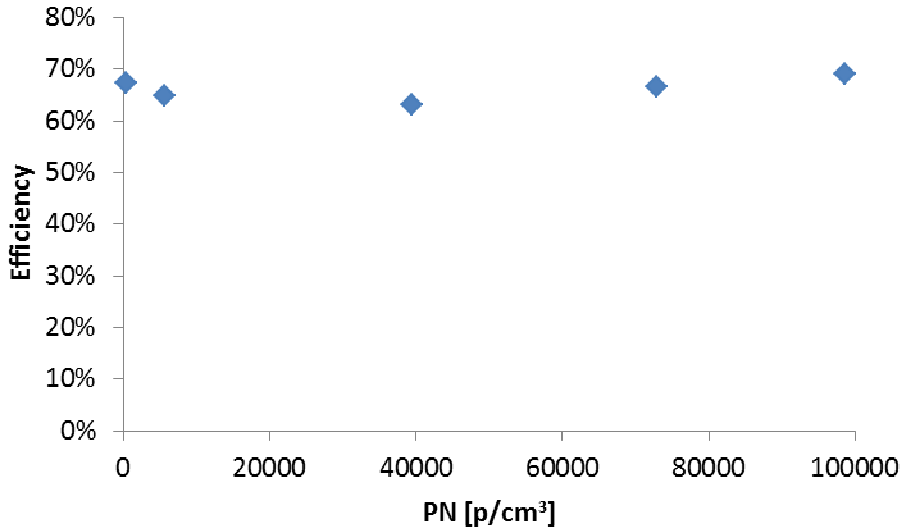

Figure 8.3: Linearity.

Calibration

One concern is whether the calibration of the PN-PEMS should be conducted for the complete unit or for its parts separately (i.e. VPR and DC). **Figure 8.4** shows the efficiencies of the VPR, the DC and the complete PN-PEMS. The estimated efficiency based on the separate parts (VPR and DC) is also shown. Note that for the VPR efficiency the size dependent *PCRF*s of **Figure 8.1** were used. It can be seen that the calibration of the

complete system or its parts separately give similar results and the decision of which approach should be followed should be based on practical difficulties (e.g. when the complete PN-PEMS is calibrated the DC measures very low currents and has higher uncertainty).

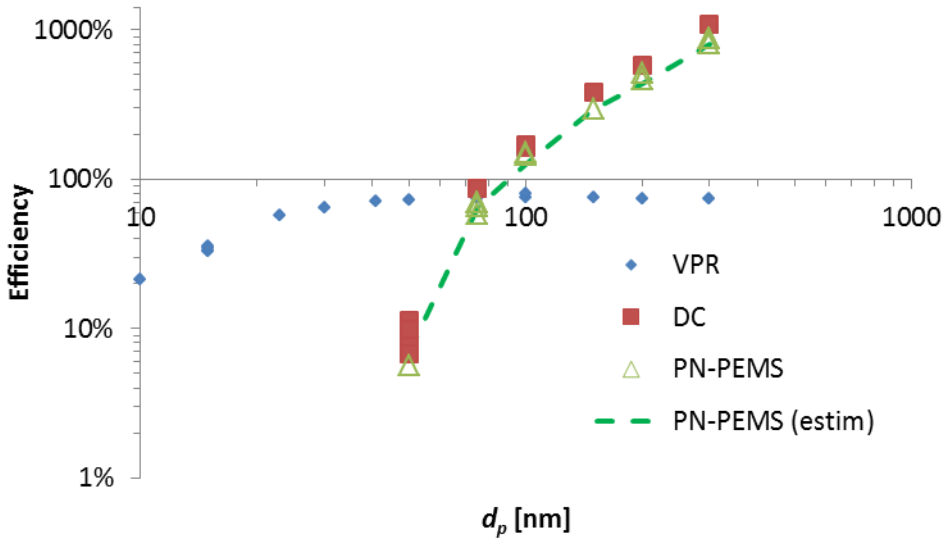

Figure 8.4: *Experimental efficiencies of VPR, DC, PN-PEMS and estimated efficiency of PN-PEMS based on the seprate VPR and DC calibration.*

PN-PEMS #5b

The penetration of the VPR was investigating measuring upstream and downstream of the VPR with a 10 nm PNC (**Figure 8.5**). It was around 65% for sizes >50 nm. Most of the losses are expected to originate from the thermophoretic losses downstream of the CS as the aerosol cools down. An error in the estimation of the dilution factor is also possible.

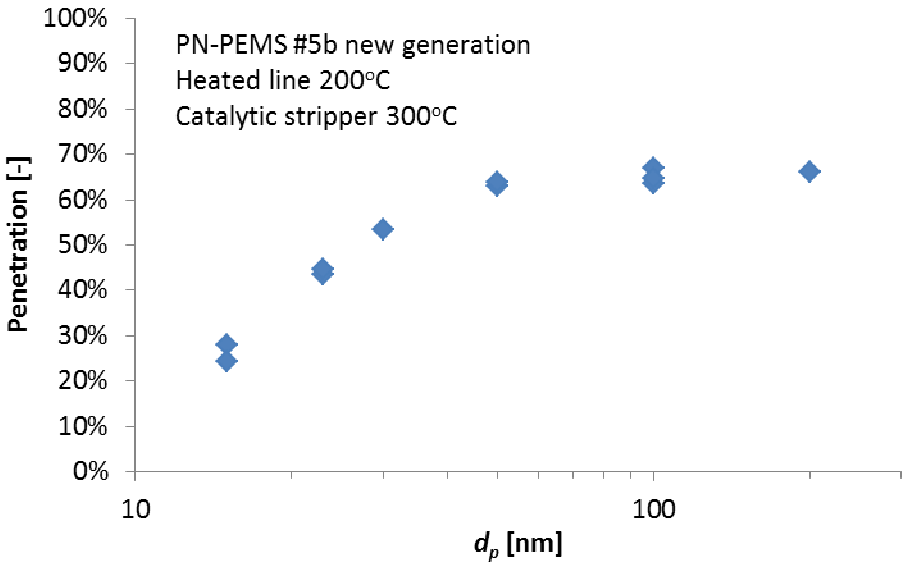

Figure 8.5: *Penetration of the VPR.*

The tetracontane removal efficiency was very high (>99.9%) even for 100 nm particles (heated line 200°C, CS 300°C). Polydisperse aerosol (GMD 30 nm) was also tested with concentration around $6x10^6$ p/cm^3 and the removal was much higher than 99.9%. **Figure 8.6** shows the removal efficiency as a function of the CS temperature when keeping the heated line at 140°C. The inlet polydisperse aerosol >$4x10^6$ p/cm^3, around 80000 p/cm^3 were surviving when the heated line temperatures was around 140°C. The CS efficiency was >99% at 300°C (less than 650 p/cm^3 were penetrating). The efficiency was increased to >99.9% when the heated line temperature was increased to 200°C (less than 15 p/cm^3 could penetrate). These tests showed that the removal efficiency of the CS is very high when the particles have been evaporated.

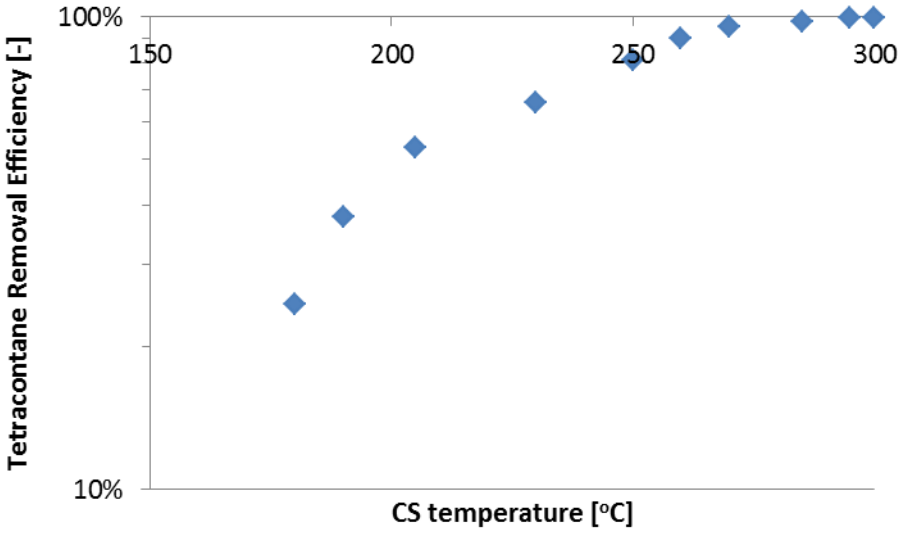

Figure 8.6: *Tetracontane removal efficiency (heated line at 140°C).*

At a next step the PN-PEMS #5b was checked with monodisperse graphite particles to measure the efficiency and normalize it to 100 nm. Then the corrected signal was checked with polydisperse aerosol. The results are summarized in **Figure 8.7** and **Figure 8.8**.

More specifically, following the analysis of **Chapter 2**, the monodisperse experimental data (blue open circles) for the complete PN-PEMS#5b (hot, soot data) were fitted in a linear curve (solid blue line) (**Figure 8.7**). Then the efficiency (response) of the PN-PEMS for polydisperse aerosol (various GMDs) was estimated (dashed green line) and was compared with the experimental polydisperse aerosol data (green open squares).

At a next step the difference of the PN-PEMS from the PMP system for different sizes was estimated (**Figure 8.8**). As previously, the monodisperse experimental data (open circles) were fitted (blue solid line). Then this monodisperse efficiency was used to estimate the efficiency (response) of the instrument for polydisperse aerosol (dashed green line) and the polydisperse estimation was compared with experimental data (open squares). The open symbols were based on CPC and SMPS data that were fitted with the PMP efficiency curve.

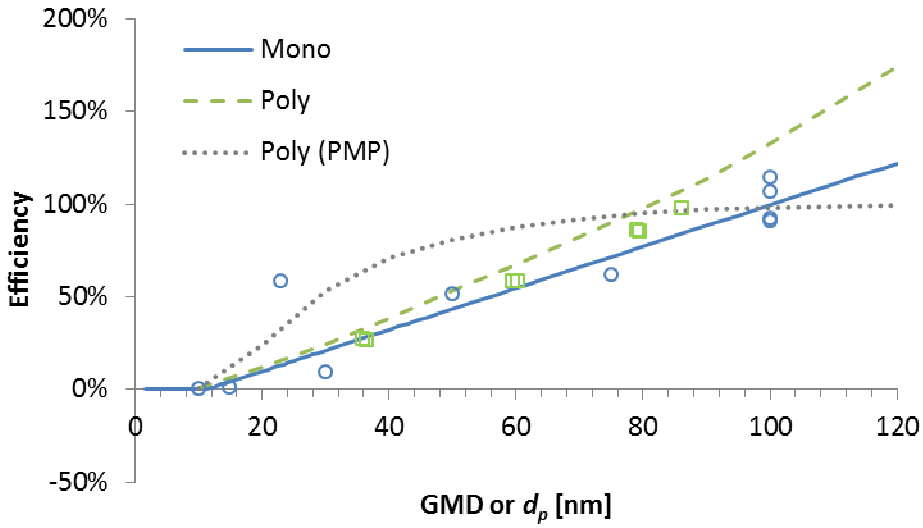

Figure 8.7: *Theoretical and experimental efficiencies for the PN-PEMS and PMP systems.*

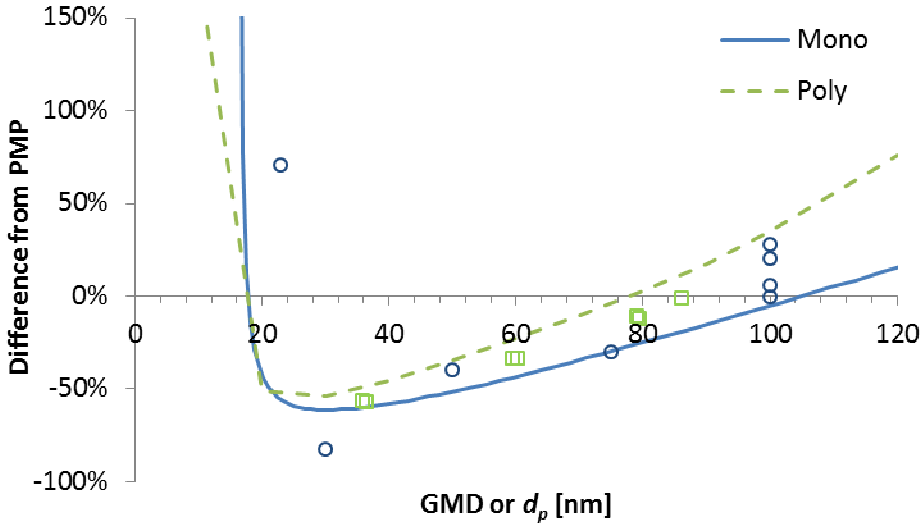

Figure 8.8: *Theoretical and experimental differences between PN-PEMS and PMP systems. Open symbols indicate CPC or SMPS data that were fitted with the PMP efficiency.*

The important message from this figure is that the expected differences between the PN-PEMS and the PMP system are -50% to +50% for GMD between 30 and 110 nm. The difference is minimized for sizes around 80 nm. Obviously, if optimizing the system for lower sizes is desirable, a lower calibration factor should be applied.

The tests were repeated with 400 V at the DC. Higher correction factor was needed due to higher particle losses in the DC and the sensitivity was slightly lower for small particles (results not shown). Based on these tests and the high hydrocarbons removal efficiency it seems it's better to operate the system at lower trap voltage.

9. Comparisons of PN-PEMS

In this chapter the efficiencies of the PN-PEMS will be compared. The polydisperse tests, which should be closest to the behavior of the instruments with vehicle exhaust aerosol, are summarized in **Figure 9.1**. Based on a limited number of tests slopes between 0.166 and 0.270 were determined. A low slope has the advantage of less influence of the particle size on the final result. The offset had also quite big variability: from -0.18 to -0.56.

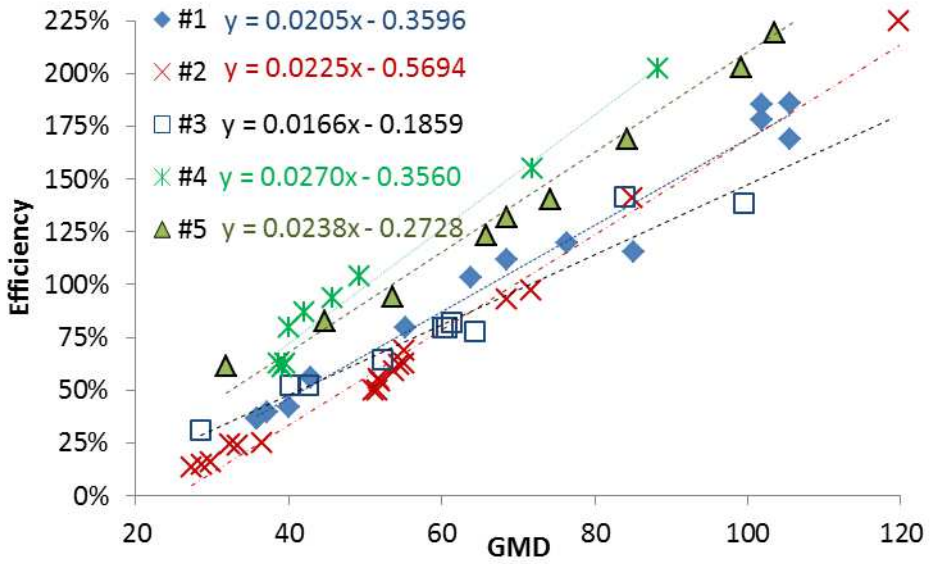

Figure 9.1: *Comparison of PN-PEMS with polydisperse aerosol.*

Figure 9.2 presents the differences of the PN-PEMS to the PMP system. Some PN-PEMS agree with the PMP system for GMDs between 60 and 75 nm. PN-PEMS #4 and PN-PEMS #5 were optimized for lower sizes and have big differences in the range of interest. Re-calibration would solve this issue. The slope of the linear fits will determine the uncertainty during the tests where the size is unknown and can also change even during a test: Systems with higher slopes had higher scatter. PN-PEMS #3, followed by PN-PEMS #1 seem those with the lowest slope and size uncertainty (Note that the results of PN-PEMS #3 are based on calibration at JRC). **Table 9.1** summarizes the experimental results for all PN-PEMS.

Table 9.1: *Difference to PMP for different GMDs.*

Difference to PMP	**#1**	**#2**	**#3**	**#4**	**#5**
D=0% at GMD	60 nm	70 nm	70 nm	45 nm	45 nm
D=-33% at GMD	35 nm	50 nm	35 nm	30 nm	30 nm
D=+50% at GMD	90 nm	85 nm	100 nm	70 nm	70 nm
D at 40 nm is	-30%	-50%	-30%	-5%	-5%
D at 100 nm is	+75%	+55%	+50%	+110%	+110%

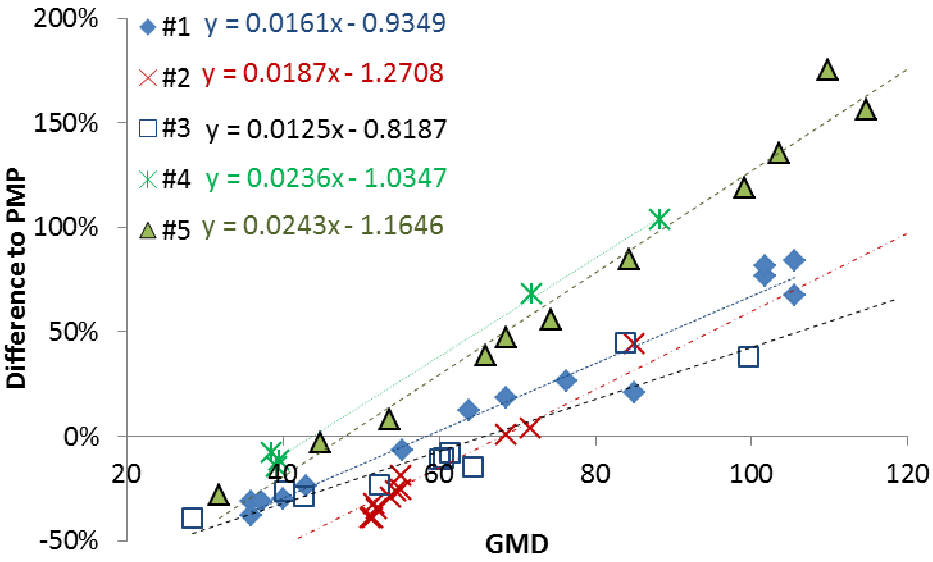

Figure 9.2: *Differences of PN-PEMS from the PMP system measuring polydisperse aerosol.*

10. CALIBRATION OF PN-PEMS

The PN-PEMS that were presented so far were calibrated by the manufacturers following various procedures. Based on the theoretical evaluation of **Chapter 2**, it seems possible to have a common calibration procedure, which however shouldn't be much different from the existing one for the PMP systems. So far the following assumptions can be made:

- The systems can be calibrated separately (VPR, DC) or as a complete unit (PN-PEMS)
- The calibration should be based on monodisperse aerosol that should be normalized to a size such as that the PN-PEMS and the PMP systems give similar results when measuring polydisperse distributions with GMD around 75 nm.

The above assumptions were true for some systems but not for all. In this section a detailed characterization of three systems was conducted in order to confirm them. Then based on the results the final calibration procedure is discussed.

Calibration of PN-PEMS or its parts separately

PN-PEMS #1b (next generation) was calibrated as a complete unit or separately the DC and the VPR. For the DC and the PN-PEMS the setup of **Figure 3.1** was followed, i.e. the DC or the PN-PEMS were measuring monodisperse aerosol in parallel with a reference PNC. The ratio of the DC or PN-PEMS to the PNC concentration (efficiency) was normalized to 100 nm (100%). The VPR calibration was conducted as with the calibration of the PMP VPRs, i.e. a PNC was measuring upstream and downstream of the VPR monodisperse aerosol. The ratio of the two concentrations is the PCRF at the specific size. The PCRFs were normalized to 100 nm.

Figure 10.1 shows the efficiencies of the PN-PEMS and those estimated by multiplying the DC efficiency with the PCRF efficiency. Note that the PCRF efficiency is higher for smaller than 100 nm particles (actually it's the same number as defined in the PMP procedure as the ratio of e.g. 30 to 100 nm PCRFs). The efficiencies are in very good agreement.

The conclusion is that both methods give similar results, i.e. the PN-PEMS can be calibrated as a complete unit or its parts can be calibrated separately and their efficiencies have to be multiplied. Some points should be kept in mind though:

- The reference PNC should be well calibrated. At the moment reliable calibrations in single counting mode are up to 20.000 p/cm^3 thus limiting the concentration that the PN-PEMS measure close to their detection limit (assuming they have an internal dilution of 10:1). Thus separate calibration seems more accurate. Restrictions for the lowest concentration of the PN-PEMS (or DC) should be added (e.g. at least 3 times the Limit of Detection LoD). On the other hand, the separate calibration of DC and VPR introduces the uncertainty of two calibrations.
- When the separate method is used, the reported efficiencies should be the multiplication of the measured efficiencies of the DC and the VPR at the specific size (i.e. not an average dilution or PCRF for the VPR). This is plotted in **Figure 10.1**.
- The same aerosol should be used for the VPR and the DC and should be thermally stable at the temperatures of the PN-PEMS. Based on the limited investigations of

this study the material should be spark discharge graphite or diffusion flame and thermally treated soot.

- The 'calibration constant' is the constant that normalizes the results to 100 nm. For the complete PN-PEMS calibration is the single value. For the separate method it's the multiplication of the DC calibration constant (that normalizes the efficiency of the DC 100% at 100 nm) and the 100 nm PCRF (not the average PCRF). The calibrations of **Figure 10.1** gave a calibration factor of 1400 for the complete PN-PEMS and 179x8.8=1574 for the separate parts (8.8 was the 100 nm PCRF).
- The 12.5% difference of the two factors shows the importance of measurements above the LoD. However the PN-PEMS tests of **Figure 10.1** were conducted at concentrations much higher (especially for the 100 nm point) and thus can be considered as experimental uncertainty.

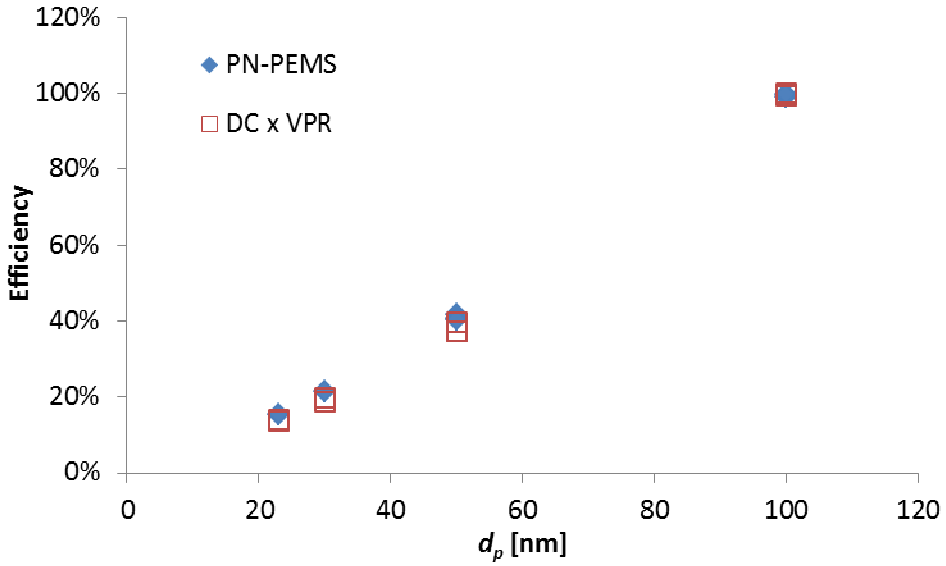

Figure 10.1: *Experimental efficiency of PN-PEMS and estimated efficiency of PN-PEMS based on the seprate VPR and DC calibration.*

Polydisperse aerosol measurements

PN-PEMS #1b, #3b and #5b, were calibrated according to the above mentioned procedure (as complete units). More specifically, the calibration factor that was found to normalize the 100 nm efficiency to 100% was used for polydisperse checks. The calibrated PN-PEMS were compared with a PMP system in **Figure 10.2**. The PN-PEMS had the same results with the PMP system at around 75-85 nm. The reason of the higher size than expected (75 nm) is that their slopes were different and/or the generated size distributions were narrower (GSD 1.65 instead of 1.85). In order to minimize such differences optimizing the PN-PEMS calibration for an assumed typical size distribution is another option. In any case, the results confirm that the proper calibration ensures small differences from the PMP systems in the GMDs range of 40 to 100 nm (-45% to +10%), however there is a tendency of underestimating typical vehicle emissions with GMDs around 65 nm.

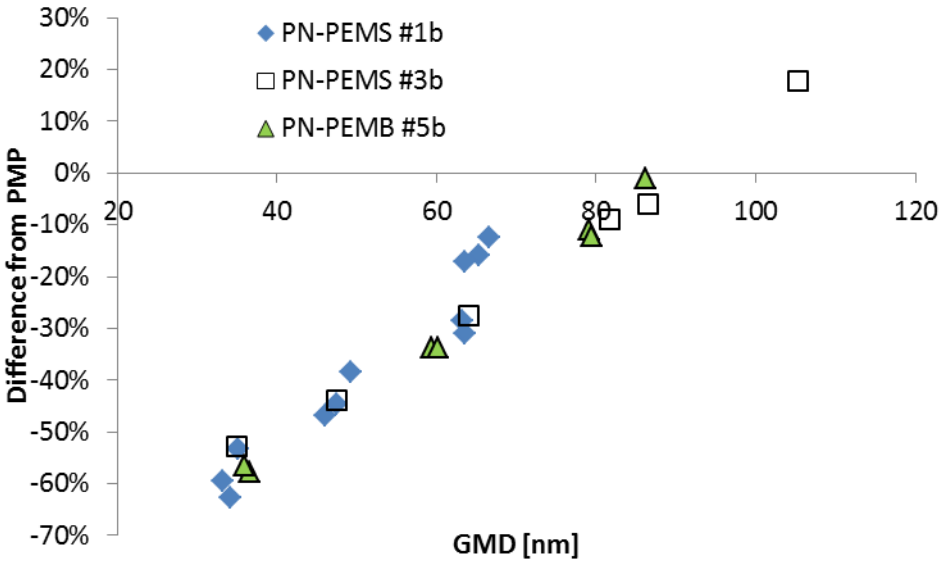

Figure 10.2: *Difference of PN-PEMS from the PMP system (simulated) measuring polydisperse aerosol.*

Calibration material

The calibration material was not thoroughly investigated. Target was to use a soot like material to simulate as possible the response of the instruments with engine exhaust aerosol. Most tests were conducted with spark discharge graphite that was neutralized (even the polydisperse aerosol). Individual PN-PEMS tests showed that there is not difference between spark discharge graphite and thermally pre-treated diffusion flame soot. **Figure 10.3** gives such an example. Other material such as PAO cannot be used due to the temperatures employed in PN-PEMS. NaCl, could be an alternative but due to the non-fractal structure it will give lower exponent. These two materials, spherical and compact, give lower exponents for the response of the DCs.

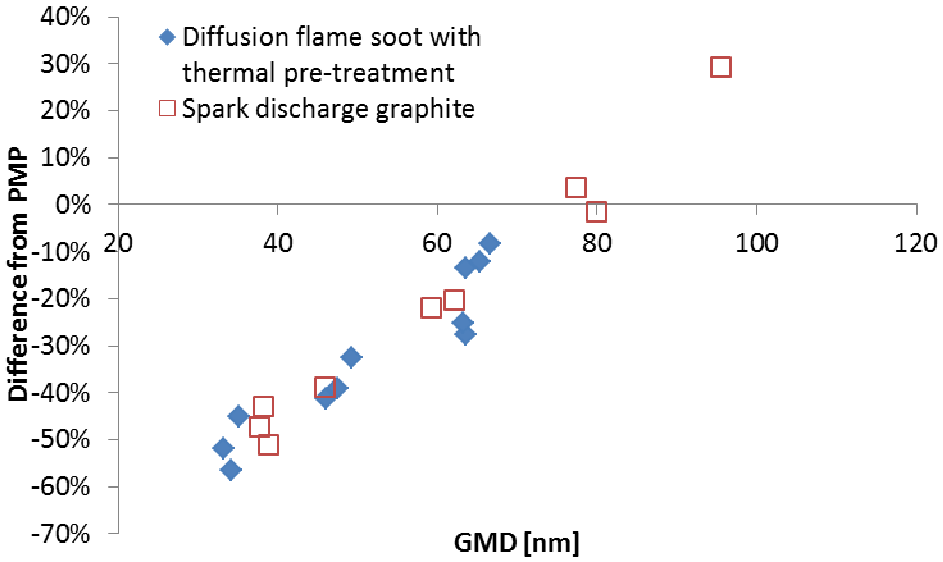

Figure 10.3: *Difference of PN-PEMS from the PMP system (simulated) measuring soot like polydisperse aerosol.*

Comparison of monodisperse and polydisperse calibration

Instead of normalizing at a specific size (e.g. 100 nm), another possibility is to calibrate the system to a specific size distribution. **Table 10.1** gives the efficiencies normalized such as that the difference of the PN-PEMS from the PMP system is 0% for polydisperse size distribution of GMD 75 nm. The first two columns give theoretical system with exponents 1.15 and 1.30. The results show that the commercial systems behave similarly but compared to the theoretical systems the optimum size is below 100 nm, close to 96-97 nm. Or in other words, they give the same result with PMP systems for wider size distribution (1.9) or bigger GMD (80 nm). Although monodisperse and polydisperse calibration give similar results a polydipserse calibration (i.e. optimizing the response of the PN-PEMS with an assumed size distribution) ensures minimum differences of systems with very different response functions.

Table 10.1: *Efficiencies of PN-PEMS after calibration with theoretical polydisperse aerosol GMD 75 nm and GSD 1.85.*

d_p	^1.15	^1.30	#1	#1b	#2	#3	3b	#4	#5	#5b
23	19%	15%	7%	17%	0%	14%	1%	12%	14%	13%
30	25%	20%	16%	25%	7%	22%	10%	20%	22%	21%
50	46%	40%	42%	48%	36%	46%	38%	45%	46%	45%
70	66%	61%	66%	69%	63%	68%	64%	68%	68%	68%
80	78%	74%	80%	81%	78%	81%	79%	81%	81%	81%
90	89%	85%	91%	92%	91%	92%	91%	92%	92%	92%
100	100%	98%	104%	103%	106%	103%	105%	104%	103%	104%
200	225%	243%	233%	217%	250%	222%	243%	225%	222%	223%

The equation that was used is:

C=1/(*pre_factor**GMD^*exponent**EXP(*exponent*^2*(LN(GSD))^2/2))

Where

GMD: Geometric mean diameter of the size distribution to be optimized

GSD: Geometric standard deviation of the size distribution to be optimized

Pre-factor and *exponent* are the fit parameters of the power curve fit of the measured monodisperse efficiencies for the PN-PEMS.

11. CONCLUSIONS

The particle number method based on the Particle Measurement Programme (PMP) is part of the light duty legislation and starts to expand to other sectors as well. As a consequence systems for in service conformity and real driving emissions procedures will be necessary. These systems should be small and compact. The commercial systems at the moment are not ready for on-road use because the Particle Number Counters (PNCs) sensors (condensation particle counters, CPC) are sensitive to vibrations. For this reason a different concept has been suggested: Diffusion chargers (DC). The main target of this report was to evaluate theoretically and experimentally in the laboratory various PN-PEMS using diffusion chargers as PNCs as alternative technique to the PMP method for on-road measurements.

The main conclusions of this study are the following:

Efficiency / Response function: Typically the response of the DCs is a function of the diameter to the power of around 1.1 (spherical particles) to 1.3 (soot). With this response function and a proper calibration of the DC (i.e. monodisperse aerosol and normalization at 100 nm), the difference between the DC and the PMP system is between -45% and +60% for polydisperse aerosol with GMDs 45-100 nm particles (theoretically). Note that in all cases the theoretical difference between two PMP systems is expected to be ±15%. Thus the DCs introduce an extra 50% uncertainty due to a size dependency that is not known during a test (i.e. there is no size info).

Calibration setup: The calibration setup of **Figure 3.1** is highly recommended. An ejector diluter downstream of the DMA ensures ambient pressure at the inlet of the PN-PEMS, which is exactly the pressure that they will face during the on-board measurements. An efficient neutralizer between the DMA and the ejector is very important because some DCs are sensitive to pre-existing charge. It's recommended to use an impactor upstream of the DMA. In addition the generated size distribution should have always GMD smaller than the selected size at the DMA. This way the multiply charged articles should remain <10-15% and their effect to the efficiency of the DC should be <5%. A particle generator with a dilution system that doesn't affect the size distribution for linearity checks of the DCs would be also very helpful.

PN-PEMS #1: This system has a response in function of the diameter to the power of 1.1 (PAO) to 1.3 (soot). The pre-existing charge strongly affected its response. The lower detection limit of the DC was around 1000 p/cm^3 (of 100 nm) (or 10000 p/cm^3 for the complete PN-PEMS). The difference of the system from the PMP for GMDs 35-90 nm was acceptable (-33% to +50%).

PN-PEMS #2: This system has a response in function of the diameter to the power of 1.15 with small effect of pre-existing charge. The diffusion screens decreased significantly the efficiency for small particles. The effect of pre-existing charge was found to be negligible. For the specific system some concerns were raised for the *PCRF* value that was used and the charging efficiency of the DC. Nevertheless, the difference of the system from the PMP for GMDs 50-85 nm was acceptable (-33% to +50%).

PN-PEMS #3: This system was calibrated using its original signal. This system has a response in function of the diameter to the power of 1.15. The difference of the system from the PMP for GMDs 35-100 nm was acceptable (-33% to +50%). The estimated size and number concentration from the system was found to be in good agreement with the

monodisperse size for concentrations 5 times higher than the zero levels. For low measured currents, the error was quite high. The re-estimated PN multiplied with a simulated PMP efficiency curve gave good agreement with the PMP method for the size range examined (35-105 nm).

PN-PEMS #4: The unit that was tested was a garage unit and not the one that was used in the vehicle testing. The pre-existing charge strongly affected its response. Significant difference was also found between PAO and soot particles. The difference of the system from the PMP was small at sizes <60 nm, but much bigger for bigger sizes.

PN-PEMS #5: This system had a VPR with a diluter with high penetration. However the heated line (at 47°C) had 25% losses at big sizes and improved material should be used to reduce them. The system had low penetration of sub 50 nm particles and the response was quite steep. It gave acceptable differences to the PMP for small sizes. The improved version (heated at 200°C with less losses and catalytic stripper at 300°C) resulted in slightly higher losses (35%). However, the high tetracontane removal efficiency of the system, permits to use the DC at lower trap voltage (50V) increasing the sensitivity of the system.

Comparisons: Different slopes and offsets were measured from the various PN-PEMS indicating the need of common calibration procedures. It was shown experimentally that it is feasible to cover a size range of 35-90 nm (for polydisperse aerosol) with differences within -33% and +50% to the PMP system.

Calibration: In most cases the PN-PEMS were calibrated as a 'black box', resulting in low currents measured and thus high uncertainty. The PN-PEMS that their parts were also calibrated separately (#1, #2, #5) gave in general similar results to the complete unit calibration (differences around 10%). These results indicate that it is possible to do the VPR and DC calibration separately, then have a combined efficiency of the PN-PEMS for possible onsite checks. However, it was noticed that in some cases the pressure conditions at the inlet of the DC might be different in the PN-PEMS and in the calibration setup. If this affects the efficiency of the DC it should be taken into account. In addition, it was found that if the VPR has high size dependent losses, it might affect the combined efficiency that could be important for systems that use assumptions for estimated particle size.

Calibration of second generation PN-PEMS systems (#1b, #3b, #5b) showed that calibration with monodisperse aerosol and normalization at 100 nm gives similar results to the PMP systems for polydisperse aerosol with GMD around 75 nm (or higher for narrow size distributions). However vehicle tests showed that typical size distributions peak at smaller sizes (at least as measured with real time electrical aerosol sizers) and an optimization at 100 nm might result in underestimation of the emissions.

Proposal: Based on the above mentioned findings, suggested ratios of efficiencies for DCs (and PN-PEMS) normalized to 100 nm are given in **Table 11.1** (as a control of the response function). For a PMP system these ratios are equivalent to the inverse of the PCRF.

Table 11.1: *Proposed PN-PEMS efficiency ratios.*

	23 nm	50 nm	100 nm	200 nm
Efficiency ratios	<0.5	0.4 - 1	1	<2.5
PMP (estim)	0.5	0.9	1	1

The calibration factor can be either the value needed to normalize the response function to a specific monodisperse size or to a theoretical polydispere size distribution.

Regarding the monodisperse calibration, if a correction factor is applied to set the efficiency of the PN-PEMS at 100% for 100 nm, polydisperse checks with GMDs between 50 and 80 nm should give differences to PMP systems within -33% and +15% and good agreement for 75 nm. These values are sensitive to the standard deviation of the size distributions and the response functions of the DCs. The 100 nm size is a size that for typical vehicle application will lead to underestimation of the emissions, as typically modern vehicles have lower mean sizes. A better agreement can be found by normalizing to a lower size (e.g. monodisperse 80 nm).

A second approach is to normalize the response of the system to a given (theoretical) polydisperse distribution. The advantage of this approach is that more realistic calibration factor can be achieved. A size distribution close to 75 nm would be almost equivalent to a monodisperse calibration at 100 nm.

References

Amanatidis, S., Ntziachristos, L. Samaras, Z. Janka, K., Tikkanen, J. (2013). Applicability of the Pegasor particle sensor to measure particle number, mass and PM Emissions. SAE, 2013-24-0167.

Asbach, C., Kaminski, H., von Barany, D., Kuhlbusch, T., Monz, C., Dziurowitz, N., Pelzer, J., Vossen, K., Berlin, K., Dietrich, S., Götz, U., Kiesling,H.J., Schierl, R., & Dahmann, D. (2012). Comparability of portable nanoparticle exposure monitors. Annals of Occupational Hygiene, 56, 606–621.

Barrios, C., Domínguez-Sáez, A., Rubio, J., & Pujadas, M. (2011). Development and evaluation of on-board measurement system for nanoparticle emissions from diesel engine. Aerosol Sci. Technol., 45, 570-580.

Bau, S., Witschger, O., Gensdarmes, F., Thomas, D. (2009). Experimental study of the response functions of direct-reading instruments measuring surface-area concentration of airborne nanostructured particles. J. Physics: Conference series, 170, 012006.

Bau, S., Witschger, O., Gensdarmes, F., Thomas, D. (2011). Response of three instruments devoted to surface-area for monodisperse and polydisperse aerosols in molecular and transition regimes. J. Physics: Conference series, 304, 012015.

Bau, S., Witschger, O., Gensdarmes, F., Thomas D. (2012). Evaluating three direct-reading instruments based on diffusion charging to measure surface area concentrations in polydisperse nanoaerosols in molecular and transition regimes. J. Nanopart. Res., 14, 1217.

Bau, S., Witschger, O., Gensdarmes, F., Thomas D., Borra J. (2010). Electrical properties of airborne nanoparticles produced by a commercial spark-discharge generator. J. Nanopart. Res. 12, 1989-1995.

Besch, M., Thiruvengadam, A., Kappanna, H., Cozzolini, A., Carder, D., Gautam, M. (2011). Assessment of novel in-line particulate matter sensor with respect to OBD and emissions control applications. ASME ICEF 2011-60142, Oct 2-5, West Virginia USA.

Biskos, G., Reavell, K., & Collings, N. (2005). Unipolar diffusion charging of aerosol particles in the transition regime. J Aerosol Sci., 36, 247-265.

Bukowiecki, N., Kittelson, D., Watts, W., Burtscher, H., Weingartner, E., & Baltensperger, U. (2002). Real-time characterization of ultrafine and accumulation mode particles in ambient combustion aerosols. J. Aerosol Sci., 33, 1139-1154.

Chang, J.-S. (1981). Theory of diffusion charging of arbitrarily shaped conductive aerosol particles by unipolar ions. J. Aerosol Sci., 12, 19–26.

Covert, D., Wiedensohler, A., & Russell, L. (1997). Particle charging and transmission efficiencies of aerosol charge neutralizers Aerosol Sci. Technol., 27, 206–214.

Davidson, J., & McKinney, P. (1998). Chemical vapor deposition in the corona discharge of electrostatic air cleaners. Aerosol Sci. Technol., 29, 102-110.

EU 459/2012. Commission Regulation (EU) No 459/2012 of 29 May 2012 "amending Regulation (EC) No 715/2007 of the European Parliament and of the Council and Commission Regulation (EC) No 692/2008 as regards emissions from light passenger and commercial vehicles (Euro 6)", Official Journal of the European Union L 142, 16-24, 2012.

EU 595/2009. Regulation (EC) No 595/2009 of the European Parliament and of the Council of 18 June 2009 “on type-approval of motor vehicles and engines with respect to emissions from heavy-duty vehicles (Euro VI) and on access to vehicle repair and maintenance information and amending Regulation (EC) No 715/2007 and Directive 2007/46/EC and repealing Directives 80/1269/EEC, 2005/55/EC and 2005/78/EC”, Official Journal of the European Union L 188, 1-13, 2009.

EU 715/2007. Regulation (EC) No 715/2007 of the European Parliament and of the Council of 20 June 2007 “on type approval of motor vehicles with respect to emissions from light passenger and commercial vehicles (Euro 5 and Euro 6) and on access to vehicle repair and maintenance information”, Official Journal of the European Union L 171, 1-16, 2007.

Fierz, M., Meier, D., Steigmeier, P., Burtscher, H. (2014). Aerosol measurement by induced currents. Aerosol Sci. Technol., 48, 350-357.

Fierz, M., Burtscher, H., Steigmeier, P., & Kasper, M. (2008). Field measurement of particle size and number concentration with the diffusion size classifier (DiSC). SAE 2008-01-1179.

Fierz, M., Houle, C., Steigmeier, P., & Burtscher, H. (2011). Design, calibration and field performance of a miniature diffusion size classifier. Aerosol Sci. Technol., 45, 1-10.

Fissan, H., Kaminski, H., Asbach, C., Pui, D., Wang, J. (2013). Rationale for data evaluation of the size distribution measurements of agglomerates and aggregates in gases with extended SMPS-technology. Aerosol and Air Quality Research, 13, 1393-1403.

Fissan, H., Neumann, S., Trampe, A., Pui, D., Shin, W. (2007). Rationale and principle of an instrument measuring lung deposited nanoparticle surface area. J. Nanopart. Res., 9, 53-59.

Frank, B, Saltiel, S, Hogrefe, O, Grygas, J, & Lala, G. (2008). Determination of mean particle size using the electrical aerosol detector and the condensation particle counter: comparison with the scanning mobility particle sizer. J. Aerosol Sci., 39, 19-29.

Giechaskiel, B., Mamakos, A., Andersson, J., Dilara, P., Martini, G., Schindler, W., & Bergmann, A. (2012). Measurement of automotive non-volatile particle number emissions within the European legislative framework: a review. Aerosol Sci. Technol., 46, 719-749.

Han, R., & Gentry, J. (1994). Evolution of charge distribution of non-spherical particles undergoing unipolar charging. J. Aerosol Sci., 25, 499–508.

Harris, S., & Maricq, M. (2001). Signature size distributions for diesel and gasoline engine exhaust particle matter. J. Aerosol Sci., 32, 749-764.

Heitbrink, W., Evans, D., Ku, B., Maynard, A., Slavin, T., Peters, T. (2009). Relationships among particle number, surface area, and respirable mass concentrations in automotive engine manufacturing. J. Occupational and Environmental Hygiene, 6, 19-31.

Jung, H., & Kittelson, D. (2005). Characterization of aerosol surface instruments in transition regime. Aerosol Sci. Technol., 39, 902-911.

Kaminski, H., Kuhlbusch, T., Rath, S., Götz, U., Sprenger, M., Wels, D., Polloczek, J., Bachmann, V., Dziurowitz, N., Kiesling, H., Schwiegelshohn, A., Monz, C., Dahmann, D., & Asbach, C. (2013). Comparability of mobility particle sizers and diffusion chargers. J. Aerosol Sci., 57, 156-178.

Kasper, M. (2004). The number concentration of non-volatile particles - design study for an instrument according to the PMP recommendations. SAE, 2004-01-0960.

Kittelson, D., Watts, W., Savstrom, J., & Johnson, J. (2005). Influence of a catalytic stripper on the response of real time aerosol instruments to diesel exhaust aerosol. J. Aerosol Sci., 36, 1089-1107.

Ku, B. (2010). Determination of the ratio of diffusion charging-based surface area to geometric surface area for spherical particles in the size range of 100-900 nm. J. Aerosol Sci., 41, 835-847.

Ku, B. and Maynard, A. (2005). Comparing aerosol surface-area measurements of monodisperse ultrafine silver agglomerates by mobility analysis, transmission electron microscopy and diffusion charging. J. Aerosol Sci., 36, 1108-1124.

Kulkarni, P., Baron, P., & Willeke, K. (2011). Aerosol Measurement: Principles, Techniques, and Applications. Wiley-Blackwell; 3rd edition, New Jersey. US.

Laframboise, J., & Chang, J. (1977). Theory of charge deposition on charged aerosol particles of arbitrary shape. J. Aerosol Sci., 8, 331–338.

Mamakos, A., Carriero, M., Bonnel, P., Demircioglu, H., Douglas, K. Alessandrini, S., Forni, F., Montigny, F., Lesueur, D. (2011). EU-PEMS PM evaluation program -Third report – Further study on post DPF PM/PN emissions, EUR 24883

Maricq, M. (2103). Monitoring motor vehicle PM emissions: An evaluation of three portable low cost aerosol instruments. Aerosol Sci. Technol., 47, 564-573.

Maricq, M., Szente, J., Loos, M., & Vogt R. (2011). Motor vehicle PM emissions measurements at LEV III levels. SAE, 2011-01-0623.

Matson U., Ekberg L. E. & Afshari, A. (2004). Measurement of ultrafine particles: A comparison of two handheld condensation particle counters, Aerosol Sci. Technol., 38, 487-495,

Meier, R., Clark, K., & Riediker, M. (2013). Comparative testing of a miniature diffusion size classifier to assess airborne ultrafine particles under field conditions. Aerosol Sci. Technol., 47, 22-28.

Mohr, M., Lehmann, U., & Rutter J. (2005). Comparison of mass-based and non-mass-based particle measurement systems for ultra-low emissions from automotive sources. Environ. Sci. Technol., 39, 2229-2238.

Mordas, G., Manninen, H., Petäjä, T., Aalto, P., Hämeri, K., & Kulmala, M. (2008). On operation of the ultra-fine water-based CPC TSI 3786 and comparison with other TSI models (TSI 3776, TSI 3772, TSI 3025, TSI 3010, TSI 3007). Aerosol Sci. and Technol., 42, 152-158.

Ntziachristos, L., Amanatidis, S., Samaras, Z., Rostedt, A., Janka, K., & Tikkanen, J. (2012). Pegasor particle sensor PPS–M: Mass and number calibration, 22nd CRC Real World Emissions Workshop, San Diego, March 25-28, 2012

Ntziachristos, L., & Samaras, Z. (2006). Combination of aerosol instrument data into reduced variables to study the consistency of vehicle exhaust particle measurements. Atmospheric Environment, 40, 6032–6042.

Ntziachristos, L., Amanatidis, S., Samaras, Z., Janka, K., & Tikkanen, J. (2013). Application of the Pegasor particle sensor for the measurement of mass and particle number emissions. SAE, 2013-01-1561.

Ntziachristos, L., Fragkiadoulakis, P., Samaras, Z., Janka, K., & Tikkanen, J. (2011). Exhaust particle sensor for OBD application. SAE, 2011-01-0626.

Ntziachristos, L., Giechaskiel, B., Ristimäki, J., & Keskinen, J. (2004). Use of a corona charger for the characterisation of automotive exhaust aerosol. J. Aerosol Sci., 35, 943-963.

Ntziachristos, L., Polidori, A., Phuleria, H., Geller, M., & Sioutas, C. (2007). Application of a diffusion charger for the measurement of particle surface concentration in different environments. Aerosol Sci. Technol., 41, 571-580.

Ouf, F., & Sillon, P. (2009). Charging efficiency of the electrical low pressure impactor's corona charger: influence of the fractal morphology of nanoparticle aggregates and uncertainty analysis of experimental results. Aerosol Sci. Technol., 43, 685-698.

Qi, C. & Kulkarni, P. (2012). Unipolar charging based, hand-held mobility spectrometer for aerosol size distribution measurement. J. Aerosol Sci., 49, 32-47.

Qi, C., Asbach, C., Shin, W., Fissan, H., & Pui, D. (2009). The effect of particle pre-existing charge on unipolar charging and its implication on electrical aerosol measurements. Aerosol Sci. Technol., 43, 232-240.

Ranjan, M., & Dhaniyala, S. (2007) Theory and design of a new miniature electrical-mobility aerosol spectrometer. J. Aerosol Sci. 38, 950-963.

Riccobono, F., Giechaskiel, B., Weiss, M., Bonnel, P. (2014). How to extend the real drive emission test procedure to particle number. Presentation at the 18th ETH Conference on Combustion Generated Nanoparticles, 25th June 2014, Zurich, Switzerland

Rostedt, A., Marjamäki, M., Yli-Ojanperä, J., Keskinen, J., Janka, K., Niemelä, V., & Ukkonen, A. (2009). Non-collecting electrical sensor for particle concentration measurement. Aerosol and Air Quality Research, 9, 470-477.

Schlatter, J. (2012). New Swiss legislation on portable particle counters for construction machinery. 16th ETH conference on combustion generated nanoparticles, June 24-27, 2012.

Shin, W., Pui, D., Fissan, H., Neumann, S., Trampe, A., (2007). Calibration and numerical simulation of Nanoparticle Surface Area Monitor (TSI model 3550 NSAM). J. Nanopart. Res., 9, 61-69.

Shin, W., Wang, J, Mertler, M., Sachweh, B., Fissan, H., Pui, D. (2009). The effect of particle morphology on unipolar diffusion charging of nanoparticle agglomerates in the transition regime. J. Aerosol Sci., 41, 975-986.

Siegmann, K., & Siegmann, H. (2000). Fast and reliable “in-situ” evaluation of particles and their surface with special reference to diesel exhaust. SAE, 2000-01-1995.

Wang, J., Shin, W., Mertler, M., Sachweh, B., Fissan, H., Pui D. (2010). Measurement of nanoparticle agglomerates by combined measurement of electrical mobility and unipolar charging properties. Aerosol Sci. Technol., 44, 97-108.

Wilson, W., Stanek, J., Han, H., Johnson, T., Sakurai, H, Pui, D., Turner, J., Chen, D., Duthle, S. (2007). Use of the Electrical Aerosol Detector as an Indicator of the Surface Area of Fine Particles Deposited in the Lung. Journal of the Air & Waste Management Association, 57, 211-220.

Woo, K., Chen, D., Pui, D., & Wilson, W. (2001). Use of continuous measurements of integral aerosol parameters to estimate particle surface area. Aerosol Sci. Technol., 34, 57-65.

Park, D., Kim, S., An, M., & Hwang, J. (2007). Real-time measurement of submicron aerosol particles having a log-normal size distribution by simultaneously using unipolar diffusion charger and unipolar field charger. J. Aerosol Sci., 38, 1240–1245.

Liu, B., & Pui, D. (1975). On the performance of the electrical aerosol analyzer. J. Aerosol Sci., 6, 249–264.

Annex: Correction for doubly charged particles

The aerosol downstream of the DMA contains mainly singly charged particles of the diameter s(size) selected. However bigger particles with more charges can also enter. These particles will result in higher signal of the DC and this has to be taken into account.

To estimate the effect of doubly charged particles the following equations were used (see also Bau et al. 2009):

$$PN_{meas} = PN_1 + PN_2 \quad \text{(A1a)}$$

$$R_{meas} = R + R_2 = PN_1 ad_1^x + PN_2 ad_2^x \quad \text{(A2a)}$$

$$E_{meas} = R_{meas}/PN_{meas} \quad \text{(A3)}$$

$$f = PN_2/PN_1 \quad \text{(A4)}$$

Where *PN* is Number Concentration, *R* reading of instrument (surface area or lung deposited area) given by the instrument and *E* is the normalized response of the instrument or efficiency. The index *meas* refers to the measurement result, 1 refers to singly charged particles and 2 to doubly charged particles. It is assumed that the response of the instrument is a power function of the particle size, but the calculations are valid for any function of size. *f* is the fraction of doubly charged particles. Triply charged particles were not taken into account, because their contributions should be small.

$$PN_{meas} = PN_1 + fPN_1 = (1+f)PN_1 \quad \text{(A1b)}$$

$$PN_{meas} = PN_2/f + PN_2 = PN_2(1+f)/f \quad \text{(A1c)}$$

$$R_1 = R_{meas} - R_2 = R_{meas} - PN_2 ad_2^x = R_{meas} - PN_{meas} f/(1+f) ad_2^x \quad \text{(A2b)}$$

$$E_1 = R_1/PN_1 = [E_{meas} - ad_2^x f/(1+f)](1+f) \quad \text{(A4)}$$

The *f* for sizes at and above 100 nm was 10-15%. This resulted in 5% correction (E_1 / E_{meas} =95%).

European Commission

EUR 26997 EN – Joint Research Centre – Institute for Energy and Transport

Title: **Feasibility study on the extension of the Real Driving Emissions (RDE) procedure to Particle Number (PN): Experimental evaluation of portable emission measurement systems (PEMS) with diffusion chargers (DCs) to measure particle number (PN) concentration**

Author(s): Barouch Giechaskiel, Francesco Riccobono, Pierre Bonnel

Luxembourg: Publications Office of the European Union

2014 – 83 pp. – 21.0 x 29.7 cm

EUR – Scientific and Technical Research series - ISSN 1831-9424 (online), ISSN 1018-5593 (print)

ISBN 978-92-79-44651-1 (PDF)

ISBN 978-92-79-44650-4 (print)

doi:10.2790/326943 (online)

LD-NA-26997-EN-N

JRC Mission

As the Commission's in-house science service, the Joint Research Centre's mission is to provide EU policies with independent, evidence-based scientific and technical support throughout the whole policy cycle.

Working in close cooperation with policy Directorates-General, the JRC addresses key societal challenges while stimulating innovation through developing new methods, tools and standards, and sharing its know-how with the Member States, the scientific community and international partners.

Serving society
Stimulating innovation
Supporting legislation

Publications Office

doi : 10.2790/326943
ISBN 978-92-79-44651-1